354
4-16-80

DR. 1126

FE-15529-4

MASTER

FOSSIL ENERGY

MHD ELECTRODE DEVELOPMENT

Quarterly Report for the Period July—September 30, 1979

October 1979

Work Performed Under Contract No. AC01-79ET15529

Westinghouse Electric Corporation
Advanced Energy Systems Division
Pittsburgh, Pennsylvania

DEPARTMENT OF ENERGY · UNITED STATES OF AMERICA

U. S. DEPARTMENT OF ENERGY

Available from the National Technical Information Service, U. S. Department of Commerce, Springfield, Virginia 22161.

Price: Paper Copy $9.00
Microfiche $3.50

FE-15529-4
Distribution Categories UC-90g and UC-93

MHD ELECTRODE DEVELOPMENT

Quarterly Report for the Period

JULY - SEPTEMBER 30, 1979

John W. Sadler
Jeff Bein
David L. Black
Laurence H. Cadoff*
H. Dean Coe, Jr.
James A. Dilmore*
Edsel W. Frantti
Edgar L. Kochka
Jack A. Kuszyk
S. K. Lau
Joseph Lempert**
Bill L. Pierce
Barry R. Rossing*
Stephen J. Schneider*
Eugene E. Smeltzer*

*Westinghouse Research & Development Center
**Consultant

WESTINGHOUSE ELECTRIC CORPORATION
Advanced Energy Systems Division
P. O. Box 10864
Pittsburgh, Pa. 15236

OCTOBER 1979

PREPARED FOR THE
UNITED STATES DEPARTMENT OF ENERGY

Under Contract No. DE-AC-01-79-ET-15529

APPROVED:

J. W. Sadler, Project Manager
Advanced Energy Systems Division

TABLE OF CONTENTS

TABLE OF CONTENTS (Continued)

LIST OF TABLES

LIST OF TABLES (Continued)

LIST OF FIGURES

LIST OF FIGURES (Continued)

LIST OF FIGURES (Continued)

I. ABSTRACT

Technical progress under DOE Contract DE-AC-01-79-ET-15529 during the July to September 1979 quarter is reported.

A fused cast spinel, $MgAl_2O_4$, has been evaluated for its corrosion resistance in western slag. The spinel appears to be insignificantly affected by the corrosive nature of the slag and based on this performance will be subjected to further testing. Results of thermal conductivity measurements of a number of hafnia and zirconia based electrode materials, to be run in the upcoming WESTF Test 42, are reported.

Laboratory electrochemical screening tests have continued. Results are presented for iron cathodes and platinum anodes in western slag. Further results are presented on the evaluation of single crystal and polycrystalline zirconia samples which were tested previously. Results from additional electrochemical polarization tests have shown the desirability of modifying the test cell to improve test reproducibility.

A summary of available data covering electrode durability has been prepared covering laboratory electrochemical and generator tests for various MHD environments. This summary establishes the general framework for viewing activities within this program. Emphasis has been placed in refractory electrode materials. The status of various design activities, including design of the Materials Test Section (MTS), the modified WESTF test section, and various WESTF test design activities, are presented. Results of post-test analysis activities for WESTF Test 41 - Run 2 and WESTF Test D-9 are presented.

During this period significant WESTF operations included completion of WESTF Test 41 - Run 2 and WESTF Test D-9. Total operating time, combustor on to combustor off, was 69 hours under slagging conditions for these tests.

Status of design, procurement and modification activities in support of the installation of a conventional 3 Tesla magnet is presented. Installation is currently projected for February 1980.

II. OBJECTIVE AND SCOPE OF WORK

In continuation of the program to develop MHD power generation to commercial feasibility, Westinghouse is conducting a program to develop improved electrode designs for open-cycle coal-fired MHD generator applications. The program includes the link between basic and supportive materials development and testing in an engineering test rig that offers an adverse MHD environment for extended periods of time.

Specific development activities of this program are as follows:

(a) Laboratory screening tests to provide preliminary electrochemical stability data on selected advanced or modified ceramic candidate electrode and insulation materials.

(b) Laboratory screening tests to evaluate the resistance of selected candidate anode materials to simulated arc impingements under a representative range of chemical and thermal conditions.

(c) Engineering rig tests of preferred electrode designs, selected on the basis of the screening test results and/or pertinent outside data, under simulated open-cycle coal-fired MHD operating conditions.

(d) Preparation and fabrication of experimental electrode materials, as warranted by favorable laboratory screening test results, to provide samples for engineering rig tests.

In addition to these four main development activities, this project includes providing such laboratory, design, test and analytical support as necessary to characterize test materials, and to determine such essential physical and chemical properties as are required to properly design the test specimens and to interpret and analyze test data. Dependent on development results, preferred electrode materials will be prepared for advanced testing in other DOE contractor facilities.

These objectives are being pursued in accordance with a statement of work which is consistent with the National Plan for MHD development formulated by DOE.

The major elements of the program are presented in a Work Breakdown Structure which is presented in Table 1. The Level I effort is the MHD Electrode Development Contract, and Level II consists of the following four tasks.

- WBS 1.1 ELECTRODE AND INSULATOR MATERIALS
- WBS 1.2 ENGINEERING TESTS
- WBS 1.3 WESTF MODIFICATION
- WBS 1.4 PROJECT MANAGEMENT AND DOCUMENTATION

WBS 1.1 - ELECTRODE AND INSULATOR MATERIALS

The objective of this task is to provide for the development, laboratory evaluation and fabrication of electrode and insulator materials. All necessary experimental material preparation, as well as fabrication of test samples for laboratory screening tests, engineering rig tests in the Westinghouse Electrode System Test Facility, WESTF (WBS 1.2), or other tests will be completed under this task. This task also includes supporting pre-test material characterization and laboratory screening tests used to evaluate the relative performance of candidate materials. These screening tests include electrochemical and anode arc impingement tests.

WBS 1.2 - ENGINEERING TESTS

The objective of this task is to provide for the engineering tests of promising electrode/insulator materials resulting from the WBS 1.1 activity. In particular, this task provides for the supporting design, test and post-test analysis effort as well as maintenance and operation of the engineering test rig, WESTF. Table 2 summarizes WESTF test capabilities.

This task incorporates the elements of planning, experiment design, test operations and post-test analysis and provides the close engineering design and test discipline necessary to effect successful electrode/insulating wall system development. In addition, final fabrication and assembly operations necessary to incorporate electrode and interelectrode insulating elements fabricated under WBS 1.1 into a complete assembly ready for testing in WESTF

TABLE 1

WORK BREAKDOWN STRUCTURE

(SUBELEMENTS TO DOE WBS 2.2.2)

WBS 1.0 MHD ELECTRODE DEVELOPMENT

- WBS 1.1 ELECTRODE AND INSULATOR MATERIALS
  - WBS 1.1.1 EXPERIMENTAL MATERIALS FABRICATION
    - MATERIAL DEVELOPMENT
    - MATERIAL CHARACTERIZATION
    - MATERIAL FABRICATION
  - WBS 1.1.2 LABORATORY SCREENING TESTS
    - ELECTROCHEMICAL TESTS
    - ANODE ARC TESTS
- WBS 1.2 ENGINEERING TESTS
  - WBS 1.2.1 TEST ENGINEERING
    - DEVELOPMENT REQUIREMENTS
    - EXPERIMENT DESIGN
    - POST-TEST ANALYSIS
  - WBS 1.2.2 TEST ASSEMBLY FABRICATION
  - WBS 1.2.3 WESTF OPERATIONS
    - PRE-TEST ACTIVITY
    - TEST OPERATIONS
- WBS 1.3 WESTF MODIFICATION
- WBS 1.4 PROJECT MANAGEMENT AND DOCUMENTATION

I II III - SYSTEMS LEVEL

TABLE 2

WESTF TEST CAPABILITIES

Mass Flow	To 0.5 lb/sec
Combustion Temperature	To 2850^{o}K
Combustor Pressure	1 to 5 atm
Channel Velocity	Subsonic, 500 to 800 m/sec
Seeding	K_2CO_3 or K_2SO_4 wet with ash or char additions (Rosebud)
B Field	3 Tesla, nominal - 3.3 Tesla, objective
Fuel	Toluene/#2 Fuel Oil
Oxidant	Preheated air with oxygen enrichment
Data Collection	240 channels coupled with minicomputer
Test Duration	Up to 100 hours
Test Frequency	Up to 2 per month
Channel Configuration	12.5 cm^2 flow cross section
Startup Ramp, Minimum	$\approx$25^{o}K/min

will be provided under this task. Required test documentation and facility opeating procedures will also be prepared.

WBS 1.3 - WESTF MODIFICATION

This task has been established to provide for the planned modification of WESTF. The primary element of this task is the addition of a conventional 3.0 Tesla magnet.

WBS 1.4 - PROJECT MANAGEMENT AND DOCUMENTATION

This centralized management task provides the focal point for directing the activities which comprise the full project effort. The Project Manager is responsible for the proper definition, integration and implementation of the technical, schedule, contractual, and financial aspects of the program. Coordination of the preparation of required documentation will also be completed under this task.

III. SUMMARY OF PROGRESS TO DATE

Figure 1 summarizes the overall program schedule and status based on the approved Project Management Summary Baseline Report dated April 1979.

During the July to September 1979 quarter, the principal areas of activity were as follows:

- Continuation of electrode and insulator material development activities.
- Continuation of electrochemical corrosion tests with emphasis on anode/slag interface polarization.
- Completion of WESTF Test 41 - Run 2.
- Design, fabrication and operation of the Materials Test Section (WESTF D-9).
- Continuation of the design of the modified WESTF Test Section for use with the magnet.
- Review of overall planning activities with emphasis on redefining the content and sequence of near term WESTF tests.
- Initiation of magnet modification and procurement of long lead supporting hardware.

1.0 WBS 1.1 - ELECTRODE AND INSULATOR MATERIALS

The corrosion resistance of a fused cast spinel insulator from Carborundum was determined in a twenty hour test in western slag. As reported in Section IV - 1.1.1, this material shows promise and will be subjected to further testing. Results of thermal conductivity measurements, by Battelle PNL, are presented in Section IV - 1.1.2 for the zirconia and hafnia based materials to be included in WESTF Test 42.

Electrochemical corrosion tests of Pt/Fe have been completed in a western slag as reported in Section IV - 1.2. Results of the post-test analysis of

U.S. DEPARTMENT OF ENERGY

DOE Form CR-535 (1-78)

MILESTONE SCHEDULE AND STATUS REPORT

1. Contract Identification: MHD ELECTRODE DEVELOPMENT PROGRAM	2. Reporting Period: through 9/30/79	3. Contract Number: DE-AC-01-79-ET-15529
4. Contractor (name, address): WESTINGHOUSE ELECTRIC CORPORATION, ADVANCED ENERFY SYSTEMS DIVISION, P. O. Box 10864, Pittsburgh, Pa. 15236		5. Contract Start Date: April 23, 1979
		6. Contract Completion Date: September 30, 1980

7. Identification Number (WBS)	8. Reporting Category (e.g., contract line item or work breakdown structure element)	9. Fiscal Years and Months (79: O N D J F M A M J J A S; 80: 1Q 2Q 3Q 4Q)	10. Percent Complete (a) Planned	(b) Actual
1.1	ELECTRODE AND INSULATOR MATERIALS			
1.1.1	EXPERIMENTAL MATERIALS FABRICATION			
1.1.2	LABORATORY SCREENING TESTS			
1.2	ENGINEERING TESTS			
1.2.1	TEST ENGINEERING			
1.2.2	TEST ASSEMBLY FABRICATION			
1.2.3	WESTF OPERATIONS			
1.3	WESTF MODIFICATION			
1.4	PROJECT MANAGEMENT AND DOCUMENTATION			

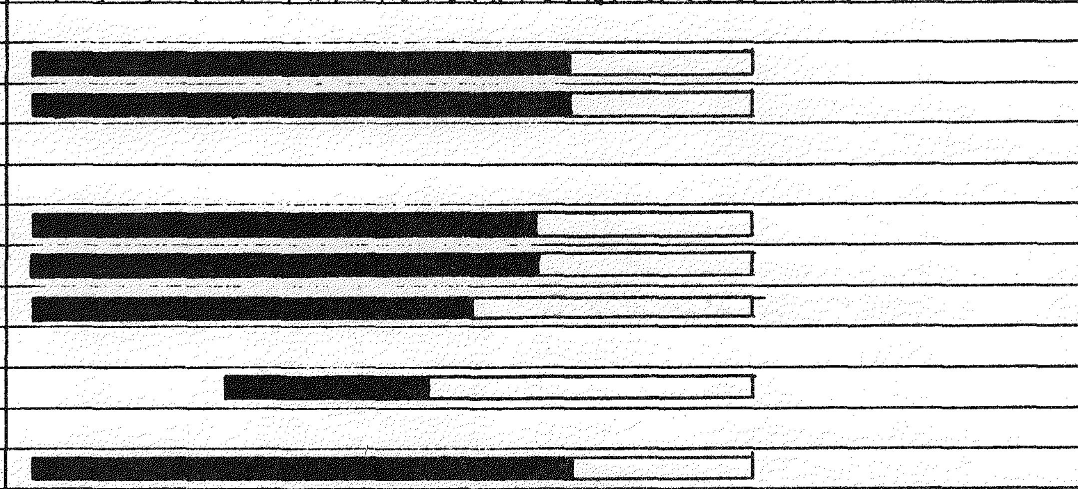

11. Remarks

12. Signature of Contractor's Project Manager and Date: John W. Sadler

13. Signature of Government Technical Representative and Date

Figure 1. Program Schedule and Status

prior $ZrO_2(Y_2O_3)$ electrochemical tests are also presented. A series of electrochemical polarization tests with zirconia and platinum electrodes has been completed. In order to overcome a lack of reproducibility in the data, future tests will be run a revised electrochemical cell configuration.

2.0 WBS 1.2 - ENGINEERING TESTS

A general review of available electrode durability data was completed to guide future program activities. Results of this review, with emphasis on refractory electrode systems, are discussed in Section IV - 2.0. WESTF Test Specifications/Revisions have been issued for WESTF Test 42, 44, D-9, D-10 and D-11. These tests are summarized in Section IV - 2.1.1.

As presented in Section IV - 2.1.2 the design of the initial Materials Test Section (MTS) has been completed. In addition, the design concept has been established for the modified WESTF test section for use with the magnet. This modular concept will be employed in both the Mini-WESTF test section and the WESTF II test section. Results of supporting thermal analyses for WESTF tests 42 and 43 are similarly presented. Section IV - 2.1.3 reports the results of the post-test analysis of WESTF Test 41 - Run 2 and WESTF Test D-9.

Table 3 provides a summary of WESTF tests completed to date. During this quarter WESTF Test 41 - Run 2 and WESTF Test D-9 were completed (see Section IV - 2.3).

WESTF operating time during this quarter was 58 hours. As of the end of this quarter the total operating time of WESTF, defined as the cumulative time interval from combustor on to combustor off, is 355 hours. This total time covers WESTF Test 35 through WESTF Test D-9. Of this total time 187.4 hours were accumulated under clean firing conditions while 166 hours were accumulated under slagging conditions.

3.0 WBS 1.3 - WESTF MODIFICATION

As presented in Section IV - 3.0, significant progress has been made in support of the magnet addition to WESTF including:

TABLE 3

WESTF TEST HISTORY

OPERATING MODE	CLEAN	CLEAN COLD	CLEAN SH	CLEAN SH	CLEAN SH	CLEAN SH	SLAG COLD
Test ID	D-7	W-35	W-36	W-37(2)	W-38(2)	W-39(2)	D-8
Test Section	Dummy	WESTF	WESTF	WESTF	WESTF	WESTF	Dummy
Date	5/77-6/77	7/77-9/77	9/77	10/77	11/77	1/78	6/78-9/78
Electrode Material(1)	NA	Cu	$LaCrO_3$	MAFF 31 MAFF 41 HfO_2 Comp.	$LaCrO_3$(3) $LaCrO_3$-ZrO_2 $LaCrO_3$	$LaCrO_3$-$LaAlO_3$ $LaCrO_3$-$SrZrO_3$ $LaCrO_3$ MAFF 31	NA
Insulator Material	NA	$MgAl_2O_4$	$MgAl_2O_4$ MgO	$MgAl_2O_4$	$MgAl_2O_4$ MgO	$MgAl_2O_4$ - MgO	NA
T_E, °C	NA	400-100	1700	1700+	1700+	1700+	NA
J, amp/cm^2	NA	To 1.0	1.0	1.0	1.0	1.0	NA
$\dot{Q}$, w/cm^2	NA	~90	~30	~30	~30	~30	NA
B, Tesla	NA	NA	NA	NA	NA	NA	NA
Axial Field, Kv/m	NA	No	No	No	No	No	NA
Ash Type	NA	NA	NA	NA	NA	NA	Rosebud
Seed	K_2CO_3	K_2CO_3	K_2CO_3	K_2CO_3	K_2CO_3	K_2CO_3	K_2CO_3
SO_2 Level, m/o	--	--	--	--	--	--	--
Duration-Hrs.	NA	22	20	20	20	20	NA

OPERATING MODE	SLAG COLD	SLAG COLD	NON-SLAG SH
Test ID	W-40	W-41	D-9
Test Section	WESTF	WESTF	MTS(6)
Date	10/78-1/79	1/79-6/79	9/79
Electrode Material(1)	Cu	Cu-Pt (+) Cu-W/Cu (-)	$LaCrO_3$
Insulator Material	$MgAl_2O_4$	BN	MgO
T_E, °C	150/275	150	To 1900
J, amp/cm^2	To 1.25	0.9	NA
$\dot{Q}$, w/cm^2	~125	~125	--
B, Tesla	NA	NA	NA
Axial Field, Kv/m	Yes	Yes	No
Ash Type	Eastern	Eastern	Rosebud
Seed	K_2CO_3	K_2CO_3	K_2CO_3
SO_2 Level, m/o	0.01	0.01	0.01
Duration-Hrs.	14(4)	63(5)	5(7)

(1) Anode and Cathode Unless Otherwise Noted
(2) U-02 Phase III Proof Test
(3) With ZrO_2 Caps.
(4) Four Runs
(5) Two Runs
(6) Materials Test Section
(7) Two Runs

- placement of a number of long-lead procurements
- completion of coil rework fixture design and initiation of fabrication
- receipt of magnet modification drawings
- magnet disassembly

The current projection for magnet installation is during the month of February 1980.

4.0 WBS 1.4 - PROJECT MANAGEMENT AND DOCUMENTATION

Significant project documentation issued included the following:

- Quarterly Report, April - June 1979
- Project Management Summary Baseline Report, FY80 Revision (DRAFT)

The Project Management Summary Baseline Report, FY80 Revision, was approved by DOE with comments. This document has been revised and will be issued shortly reflecting actual FY70 financial data.

IV. DETAILED DESCRIPTION OF TECHNICAL PROGRESS

1.0 WBS 1.1 ELECTRODE AND INSULATOR MATERIALS

1.1 WBS 1.1.1 - Experimental Materials Fabrication

1.1.1 Material Development

Hafnia-Based Electrodes

WESTF Test 42 will consist of 'coupons' of ZrO_2 and HfO_2-based electrode compositions to be evaluated under non-slagging super-hot conditions. The HfO_2-based electrodes have been processed and fabricated by Battelle Pacific Northwest Laboratories (BPNL). Three HfO_2 compositions have been identified for the test and will be positioned in the channel walls to achieve various surface temperatures. Specifically, the compositions are:

	Composition	Identity	Sintered Density (g/cc)
•	$Er_{0.82}Hf_{0.18}O_2$	(HO-BN0401)	8.69
•	$Pr_{0.27}Yb_{0.09}Hf_{0.64}O_2$	(HO-BN0302)	8.78
•	$Tb_{0.20}Y_{0.10}Hf_{0.70}O_2$	(HO-BN0102)	8.81

The materials were fabricated from powders which were processed by a coprecipitation technique, Reference 1. This technique consists of dissolving the respective oxides in a nitric or hydrocholoric acid solution. The solutions are then mixed and coprecipitated with ammonium hydroxide. The resulting powder is washed with toluene and acetone prior to calcination at 1273K to produce the oxide powder. The average grain size is usually less than 0.5μm. The powders are then cold pressed and sintered at 2273K for 2-4 hours resulting in densities up to 98% of theoretical. This fabrication technique has the advantage of producing these hafnia-based oxides with uniform composition and with reproducible controlled miscrostructures.

The resulting three hafnia electrode materials were homogeneous in composition as determined by metallography and energy dispersive x-ray analysis technique (EDAX) on the scanning electron microscope (SEM). The crystal structure was also determined by x-ray diffraction. Several of the sample compositions were not single phase, but the phases identified were reasonable to those areas predicted by phase equilibrium. For these compositions, the phase equilibria data are non-existent; therefore, equilibria must be estimated by extrapolation from known compositions of analogous compounds with similar chemical properties.

Two of the hafnia compositions, $Pr_{0.27}Yb_{0.09}Hf_{0.64}O_2$ and $Tb_{0.20}Y_{0.10}Hf_{0.70}O_2$ were additionally hot-pressed at Westinghouse from coprecipitated powders supplied by Battelle. The intent was to have small quantities of each composition available for inclusion in WESTF Test 42 in the event the sintered electrode materials were low in density. The powders were hot-pressed in a graphite die at 1600°C and 4000 psi. for several hours. The final densities of hot pressed $Pr_{0.27}Yb_{0.09}Hf_{0.64}O_2$ and $Tb_{0.20}Yb_{0.10}Hf_{0.70}O_2$ were 8.82 and 8.88 g/cc, respectively.

WESTF Test 44 is being designed to include hafnium rare-earth oxide electrodes with the capacity to accept an electrical current. It is planned to use $Tb_{0.20}Y_{0.10}Hf_{0.70}O_2$ as the electrode material, however, this electrode material will be graded to an oxide current leadout of 0.161 $Y_2O_3 \cdot 0.55\ In_2O_3 \cdot 0.29\ HfO_2$. This material has been fabricated in small quantity by BPNL by sintering in air at 1775K for four hours. The density achieved was 5.92 g/cc. The electrical conductivity (>10 $ohm\text{-}cm^{-1}$) at room temperature was sufficiently high enough that it could be attached to cold copper.

General Insulating Materials

A fused cast spinel ($MgAl_2O_4$) insulator from Carborundum was evaluated for its corrosion resistance in Western coal slag. A simple static immersion test was used to assess and compare its performance with a previously run fused cast spinel from Corhart. Photographs of the sectioned insulator are shown in Figure 2. A macro-photograph of the sectioned 'mini-crucible' is shown on the left side of the page along with a higher magnification photo of the insulator/slag interface on the right-hand side.

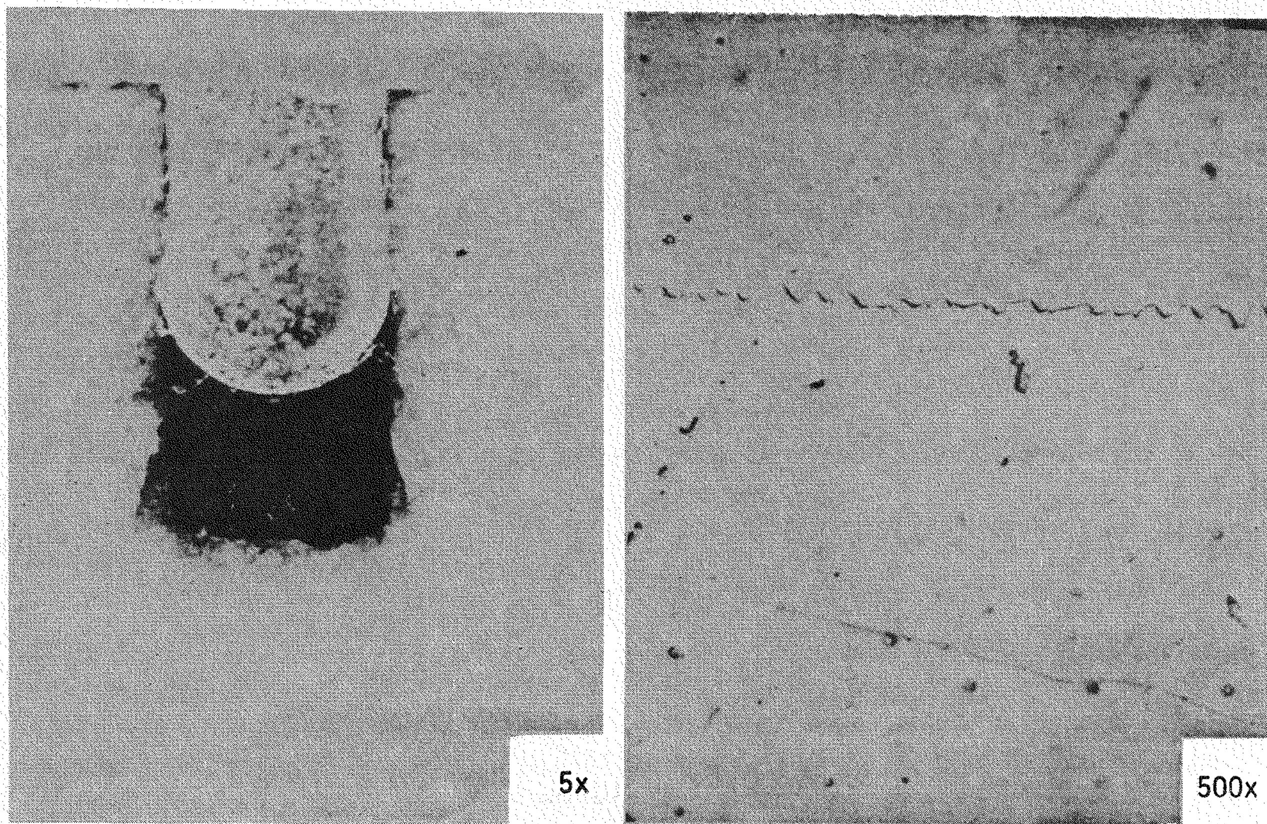

Figure 2. Appearance of $MgAl_2O_4$ (Fused Cast) from Carborundum

The spinel appears to be insignificantly affected by the corrosive nature of the slag. Little penetration through the surface of the spinel is noted and no detectable reaction boundary layer is observed. The microphotograph of the insulator/slag interface shows a very distinct separation between the slag and ceramic and no apparent interaction between the two. From a slag penetration standpoint this spinel is much superior to the more porous spinel from Corhart. The material definitely shows promise and will be subject to further testing in a future WESTF test.

To date, eighteen insulators of varying compositions, densities, and microstructures have been tested for their corrosion resistance in Western slag at 1400°C.

Table 4 lists the refractories according to their performance for the 20 hour test. The top six insulators (in the excellent catagory) will subsequently be subjected to another slag compatibility test at a higher temperature (1500-1600°C) to simulate surface temperatures of insulators found in actual generator tests. The insulators will then be re-evaluated metallographically at these more severe conditions. In addition, a number of these insulators are being positioned in the downstream transition section of WESTF Test 42 to evaluate its slag corrosion resistance along with its thermal shock suceptibility.

Attachment Techniques

The anode electrodes in WESTF Test 43 will consist of 0.25 cm platinum foil which will be attached to high density alumina blocks by diffusion bonding. Previous work, Reference 2, has shown that a bond can be obtained between these two materials using a hot press. Currently, the platinum and alumina components are being degreased and cleaned for the bonding operation. The foils are blocks will then be aligned and positioned in a graphite lined hot press. The initial bonding conditions will be a temperature of 1500°C under a pressure of 300 psi for 30 minutes. Forty-eight Pt/Al_2O_3 assemblies will be bonded together in this manner if the technique is proven successful.

An oxide current leadout of 72.5 w/o In_2O_3 - 8.55 w/o HfO_2 - 5.09 w/o Y_2O_3 is proposed for the electodes in WESTF Test 44. This material has a high enough

TABLE 4

RANKING OF CANDIDATE INSULATORS FOR USE IN SLAGGING HOT OR NON-SLAGGING SUPER-HOT GENERATORS*

Excellent

Recommended for use in higher temperature (1500°C) slag compatibility test.

Al_2O_3	Fused Cast	Carborundum
$Al_2O_3 - Cr_2O_3$	Fused Cast	Carborundum
$MgAl_2O_4 - Cr_2O_3$	Fused Cast	Carborundum
$MgAl_2O_4$	Fused Cast	Carborundum
$MgAl_2O_4$	High Sintered	Trans-Tech
MgO	Fused Grain	Norton

Acceptable

Satisfactory for use in WESTF test of short duration (<20 hrs).

MgO	High Sintered	Trans-Tech
Al_2O_3	High Sintered	Trans-Tech
$MgAl_2O_4$	Fused Cast	Corhart

Unsatisfactory

Not recommended for use in future WESTF channels.

MgO	Exp. High Sintered	Harbison-Walker
MgO	Commercial Sintered	Harbison-Walker
MgO	Commercial Sintered	Kaiser
MgO	Hi Purity, High Sintered	North Am. Refractories
MgO	Hi Purity, High Sintered, Pitch Impregnated	North Am. Refractories
$MgAl_2O_4$	Commercial Sintered	Norton
ZrO_2	Castable	Zircoa
ZrO_2	Fused Cast	Carborundum
SiC/Si_3N_4	Sintered, Reaction Bonded	Carborundum

*Ranking is based on slag compatibility test.

electrical conductivity at room temperature for it to be bonded directly to copper. Compounds which contain In_2O_3 are difficult to attach to any type of metal. Attempts to braze In_2O_3 doped compounds in a reducing atmosphere have failed, most likely due to the vaporization of In_2O at the lower temperatures. Samples of the oxide current leadout will be supplied to Westinghouse by BPNL for studying this attachment problem.

1.1.2 Material Characterization

Thermal Conductivity

WESTF Test 42 will consist of "coupons" of zirconia- and hafnia-based electrodes that will be designed to run under super hot non-slagging conditions. The thermal conductivity of each of the electrode materials, along with the insulators, has been determined to support detail design of the test section. The conductivity (λ) of each electrode composition was calculated from the thermal diffusivity (α), room temperature density (ρ), thermal expansion ($\Delta \ell / \ell$) and the specific heat (Cp) by the equation

$$\lambda = \alpha \rho C_p$$

The thermal diffusivities were measured by BPNL using a laser pulse technique from near room temperature to temperatures up to 1750°C.

The thermal conductivities of the five electrode materials are shown in Figures 3 through 7. The raw data points (noted by the open circles) represent the measured values by Battelle; the curves represent the curve fit used for the computer code input.

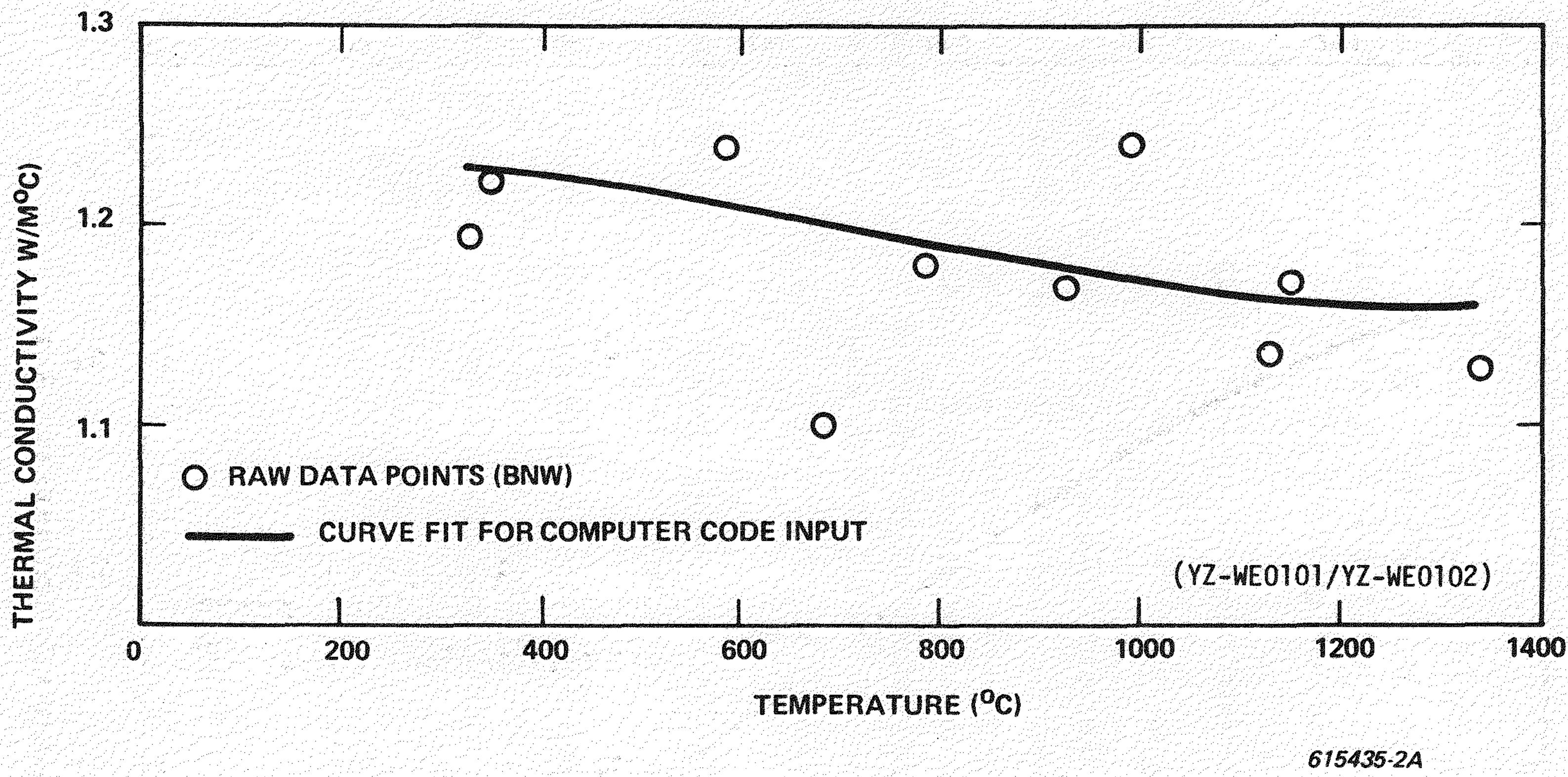

Figure 3. Thermal Conductivity of 12 Y_2O_3-$88ZrO_2$

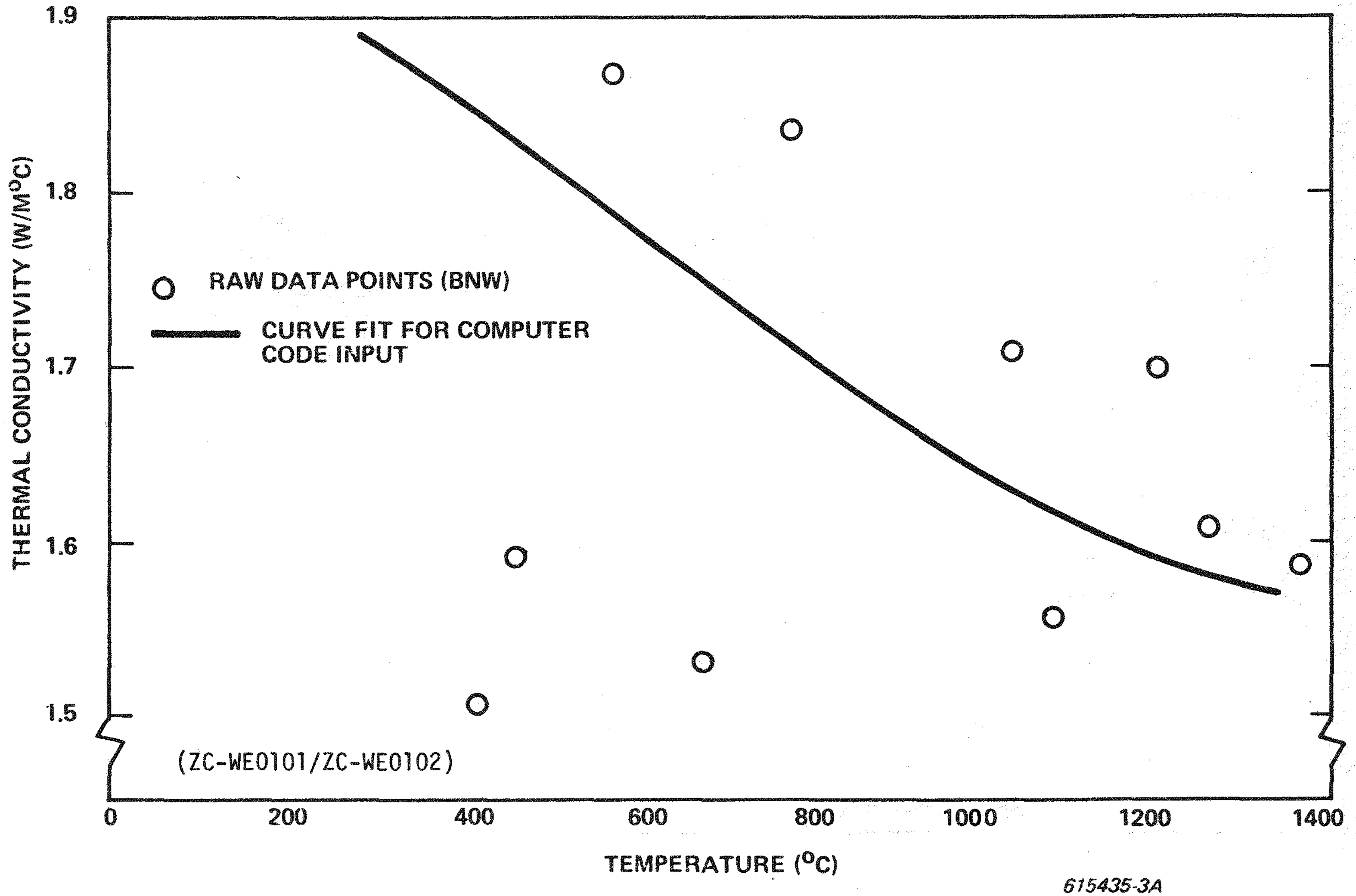

Figure 4. Thermal Conductivity of 15 $(Mg_{0.625}Ca_{0.375})$ - $85ZrO_2$

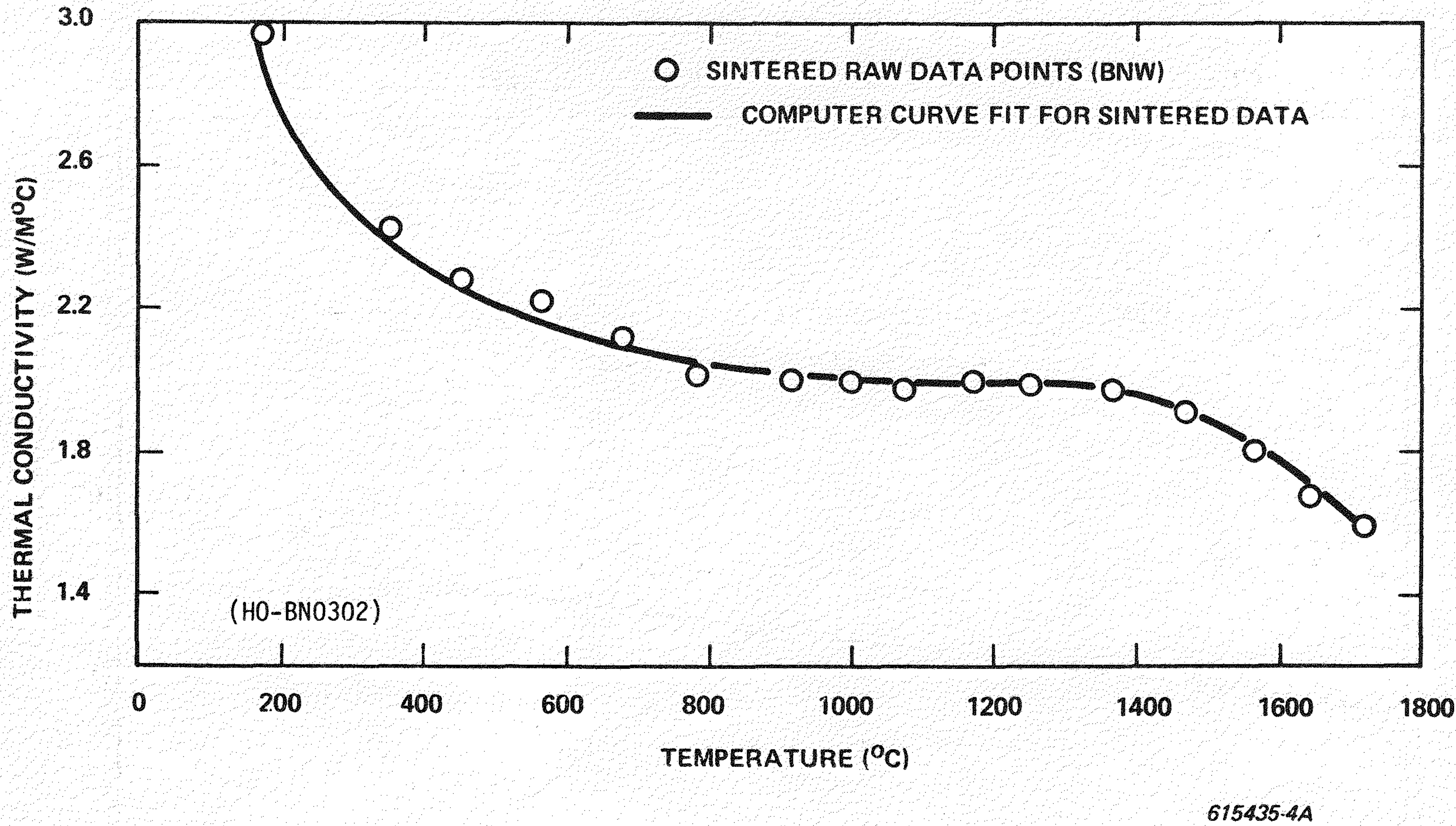

Figure 5. Thermal Conductivity of $Pr_{0.27}Yb_{0.09}Hf_{0.64}O_2$

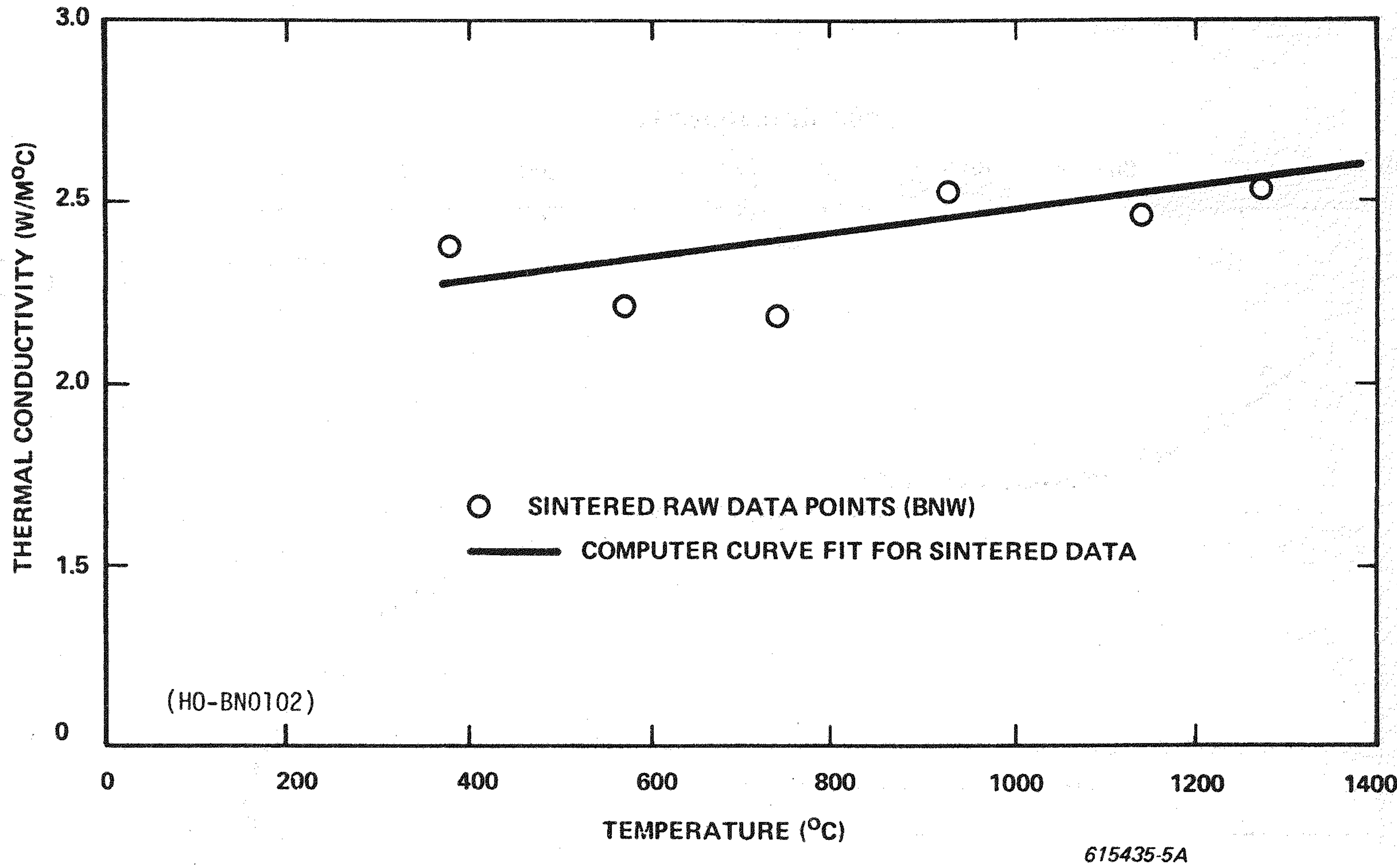

Figure 6. Thermal Conductivity of $Tb_{0.20}Y_{0.10}Hf_{0.70}O_2$

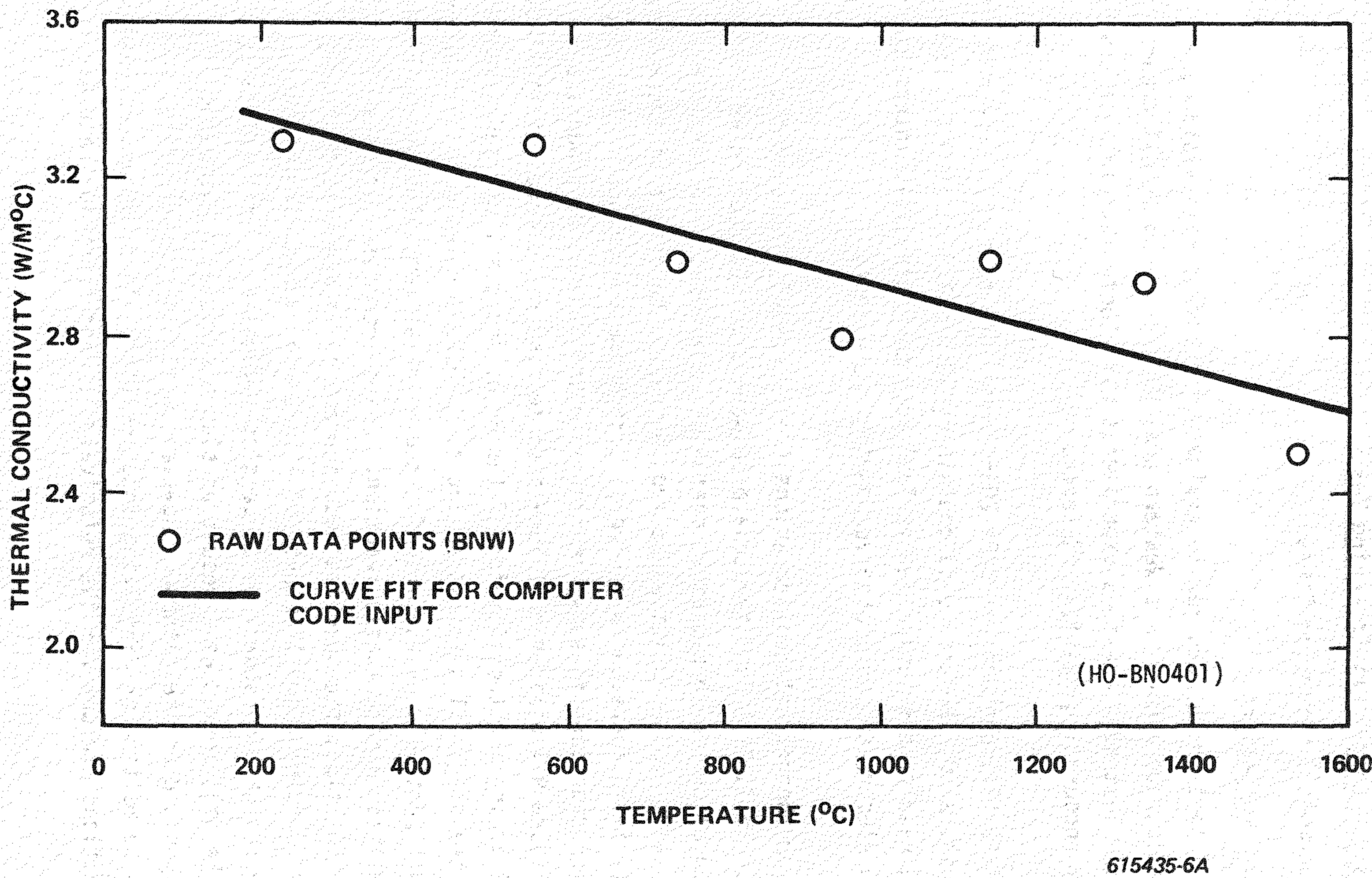

Figure 7. Thermal Conductivity of $0.7Er_2O_3$-$0.3\ HfO_2$

1.2 WBS 1.1.2 - Laboratory Screening Tests

1.2.1 Electrochemical Corrosion Tests

Platinum Anode/Iron Cathode

Electrochemical tests have been run to evaluate the corrosion resistance of iron cathodes/platinum anodes in a Western coal slag prior to actual channel testing in WESTF Test 43. Previous experiments with these materials in eastern slag gave very encouraging results, (Reference 3).

A mild steel AISI 1018 cathode and 80Pt-20Rh anode were tested in molten Montana Rosebud coal ash, W-50, (Reference 4) containing 10 w/o K_2O at 1400°C. Experimental conditions and results are summarized in Table 5. Low intensity, intermittent arcing at both electrodes, were observed during these tests.

As expected from theoretical considerations (Reference 4), the extent of corrosion given in Table 5 is intermediate between that obtained in an eastern slag (Reference 3) and in an extremely corrosive experimental western slag, W-50, (Reference 5) which contained no iron oxides. The effect of increasing current density is to increase corrosion at both anode and cathode. The nature of the corrosion reactions is shown in Figures 8 and 9. The Pt anode/slag interface in Figure 8 indicates that localized melting has occured, most likely as a result of arcing and the alloying of the Pt by iron, silicon and aluminum components of the slag. Slag agitation due to O_2 bubble release at this interface is at least partially responsible for the material removal shown in Figure 8. The cathode exhibits a more subtle reaction. Aside from some globules of Fe-Si alloy in the slag, the outer cathode surface in Figure 9 is basically an Fe-Si alloy containing small amounts of Ti. Close examination of the dark regions inside the cathode show them to be slag inclusions. This indicates that metallic Fe(Si), formed as a result of slag electrolysis, is being epytaxially deposited on the cathode. However, while this is occuring, some iron must also be melting or dissolving into the slag. These dynamic solution-deposition reactions account for the relatively low net corrosion rate of the iron cathode.

TABLE 5

ELECTROCHEMICAL CORROSION TEST

Tests on 80 Pt - 20 Rh Anode, AISI 1020 Steel Cathode

Test I.D.	159	160
Slag I.D.	W-50	W-50
Temperature, °C	1395	1400
Duration, min.	26	13
Current Density, A/cm^2	1.1	1.5
Corrosion, ΔW, μg/Coulomb		
Cathode ΔW_C	20.0	40.6
Anode ΔW_A	16.6	25.4
$\Delta W_C/\Delta W_A$	1.2	1.6
Test Cell	D2	D2

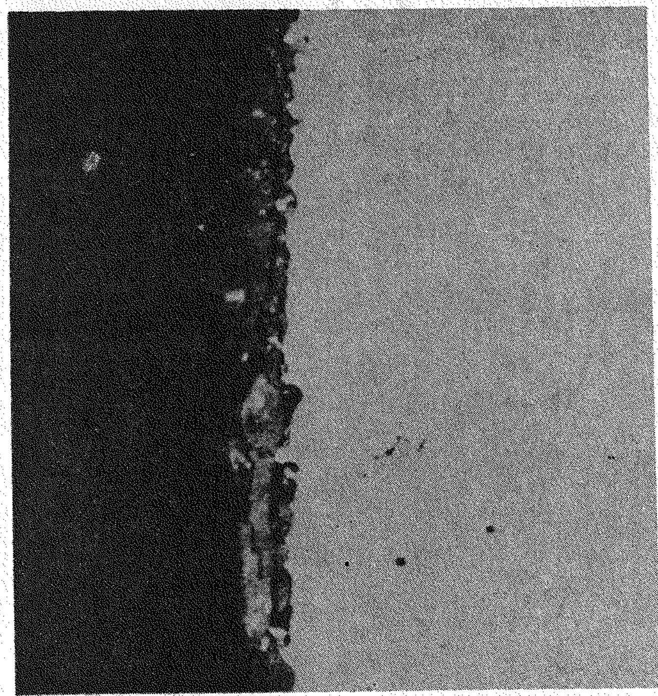

Figure 8. Slag/80Pt-20Rh Anode Interface from Test 159.

800x

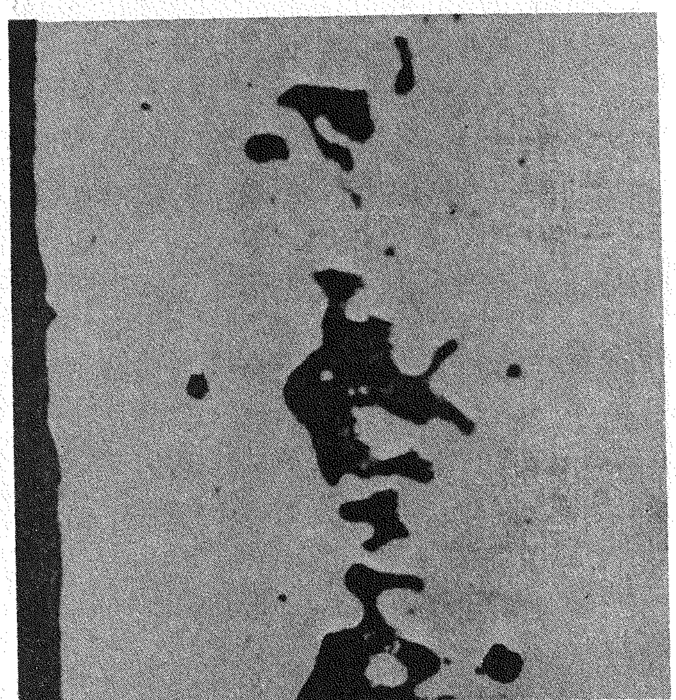

Figure 9. Slag/AlSi 1020 Steel Cathode Interface from Test 160.

500x

The above results confirm that even in western coal slag, iron cathodes/ platinum anodes are relatively corrosion resistant, and are strong candidate electrode materials for testing under dynamic MHD Channel conditions. Extreme care is necessary, however, to ensure that the iron cathode is totally covered by slag, in order to prevent its oxidation to the plasma atmosphere.

$ZrO_2(Y_2O_3)$ Electrodes

X-ray and SEM-EDAX analysis on electrochemically tested samples of single crystal ZrO_2-10 m/o Y_2O_3 (Tests 154, 155) and polycrystalline ZrO_2-8 w/o Y_2O_3 (Test 157) described in the previous quarterly report, Reference 6, have been obtained. In agreement with results from other ZrO_2 tests, there is some solutioning of Zr and Y into the slag at both anode/slag and cathode/slag interfaces. Metallic globules which form at the cathode/slag interfaces, after the ZrO_2 cathodes have completely blackened and become electronically conducting, have been identified as iron alloyed with silicon and containing small amounts of titanium. In general, the ZrO_2 at slag interfaces became enriched in Si, Fe, Mg and Ca with corresponding decreases of those elements in the neighboring slag. At the anode/slag interface, there is some particle fluxing (see for example Figure 10, Test 155). These particles are predominately silicates of zirconia.

The partially stabilized polycrystalline ZrO_2-8 w/o Y_2O_3 electrodes experienced much more corrosion than the single crystal material slag tended to intrude at cracks in ZrO_2-8 w/o Y_2O_3, and flux off the partially reacted grains. This is readily seen at slag/cathode interface shown in Figure 11. These fluxed grains are zirconium silicates and zirconium silicides alloyed with some Mg and Ca. Intermixed with the fluxed grains are metallic iron particles alloyed mainly with Si.

Electrochemical Polarization

The desirability of using ionically conducting electodes (ie: ZrO_2 based materials) under hot slagging MHD conditions has been demonstrated and reviewed in earlier reports (References 2, 4 and 7). A major advantage of ionic electrodes

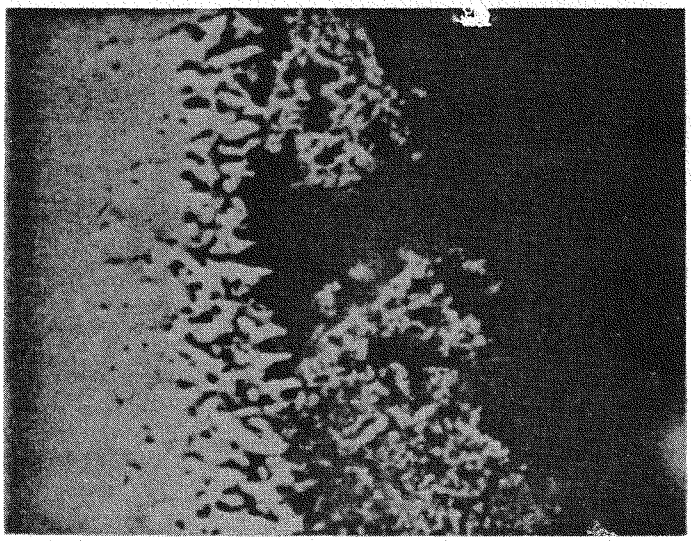

Anode Slag 2000x

Figure 10. SEM Photomicrograph of Particles Fluxing Off Single Crystal ZrO_2(10 w/o Y_2O_3) Anode, Test 155.

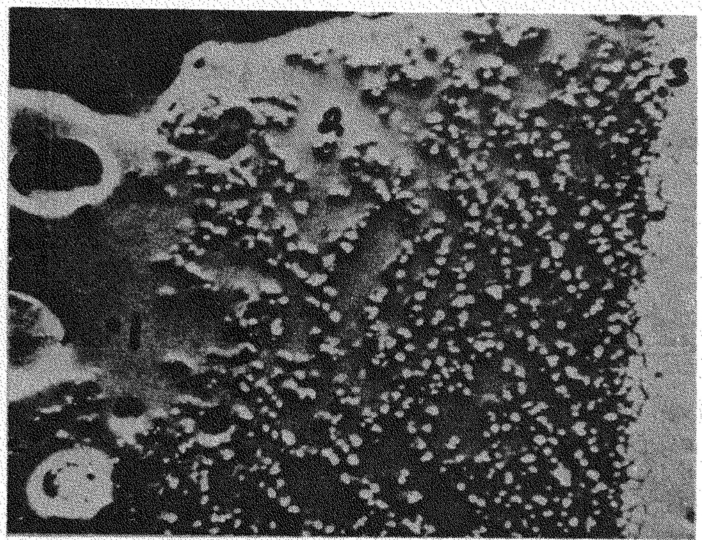

Slag Cathode 500x

Figure 11. SEM Photomicrograph of Corrosion of ZrO_2(8 w/o Y_2O_3) Cathode from Test 157.

is that they can minimize electrochemical stresses (ECS) and hence lead to reduced corrosion. A concomittant benefit is that the extent of polarization (overvoltage) at electrode/slag interfaces should also be reduced by using ion reversible electrodes. Lower polarization translates into reduced power loss in MHD generators and to smaller probabilities for destructive arc mode current transfer across the slag layer. In the future, selection guidelines for electrode materials will most likely include a minimum polarization criteria.

Recently, experiments have been initiated to measure polarization in molten western slags. The experimental setup utilitizes the D2 electrochemical cell configuration (Reference 3) but includes an additional .040" diameter Pt wire probe positioned midway in the slag between the two electrodes. The Pt probe functions as a reference electrode. In operation, a constant external voltage is impressed across the cell while current and the voltage drops (polarization voltages) between the central probe and the two electrodes are continuously read. In general, about a 10 minute hold at a given applied voltage is required to obtain stable voltammetry readings.

To date, polarization measurements have been run in W-50 slag (Reference 5) containing 10 w/o K_2O at 1400°C for the following combinations of cathode/anode materials:

- Run E-60 Fe(-)/Pt(+)
- Run E-62, E-65, ZrO_2(-)/Pt(+)
- Run E-61, E-66 ZrO_2(-)/ZrO_2(+)
- Run E-63, E-64 Pt(-)/ZrO_2(+)

The results are plotted as anode and cathode polarization voltages (referenced to the central Pt probe) versus log current density and are given in Figures 12 to 15.

It can be seen that the results are not reproducible making comparison between polarization voltages for different anode and cathode materials at this time a fruitless exercise. There is some evidence that the scatter in the data is due to short circuiting of the electrical leads through the slag and/or to gas bubbles that become entrapped between the electrodes. Future efforts will be directed at developing new cell configurations to overcome these problems.

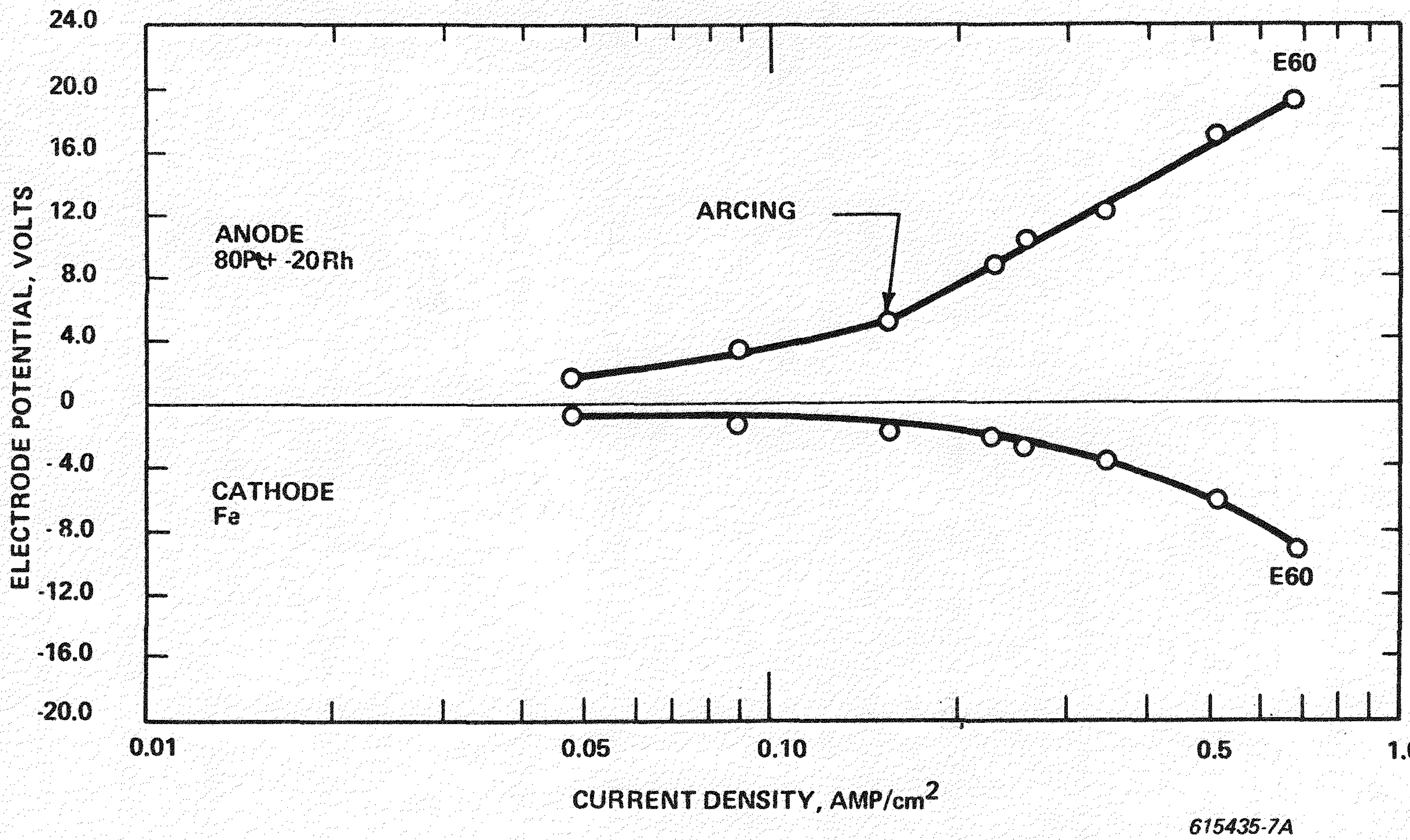

Figure 12. Electrode Polarization with 80Pt-20Rh Anode and AISI 1020 Steel Cathode. Run E-60

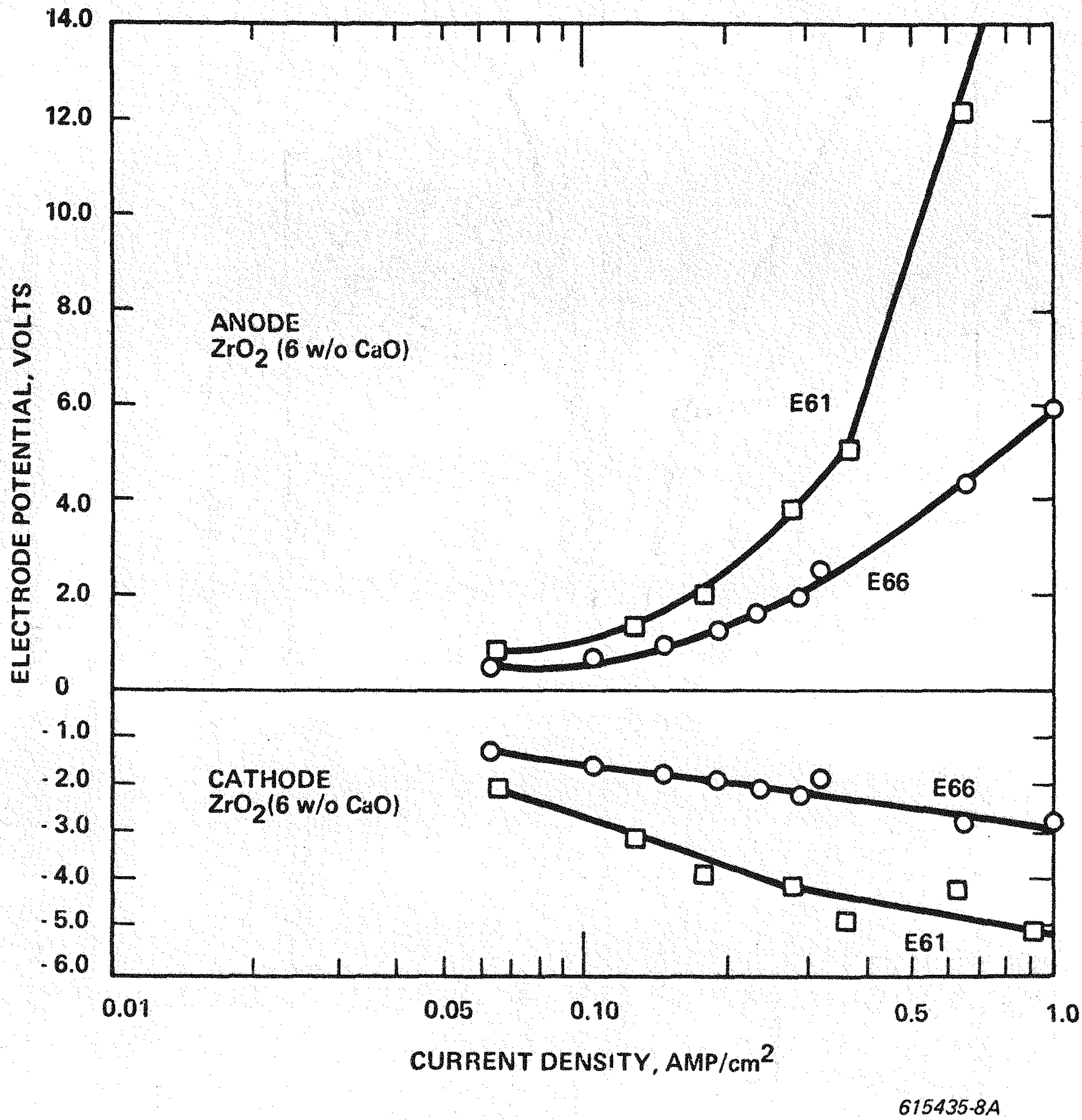

Figure 13. Electrode Polarization with ZrO_2(6 w/o CaO) Anode and Cathode. Run E-61, E-66.

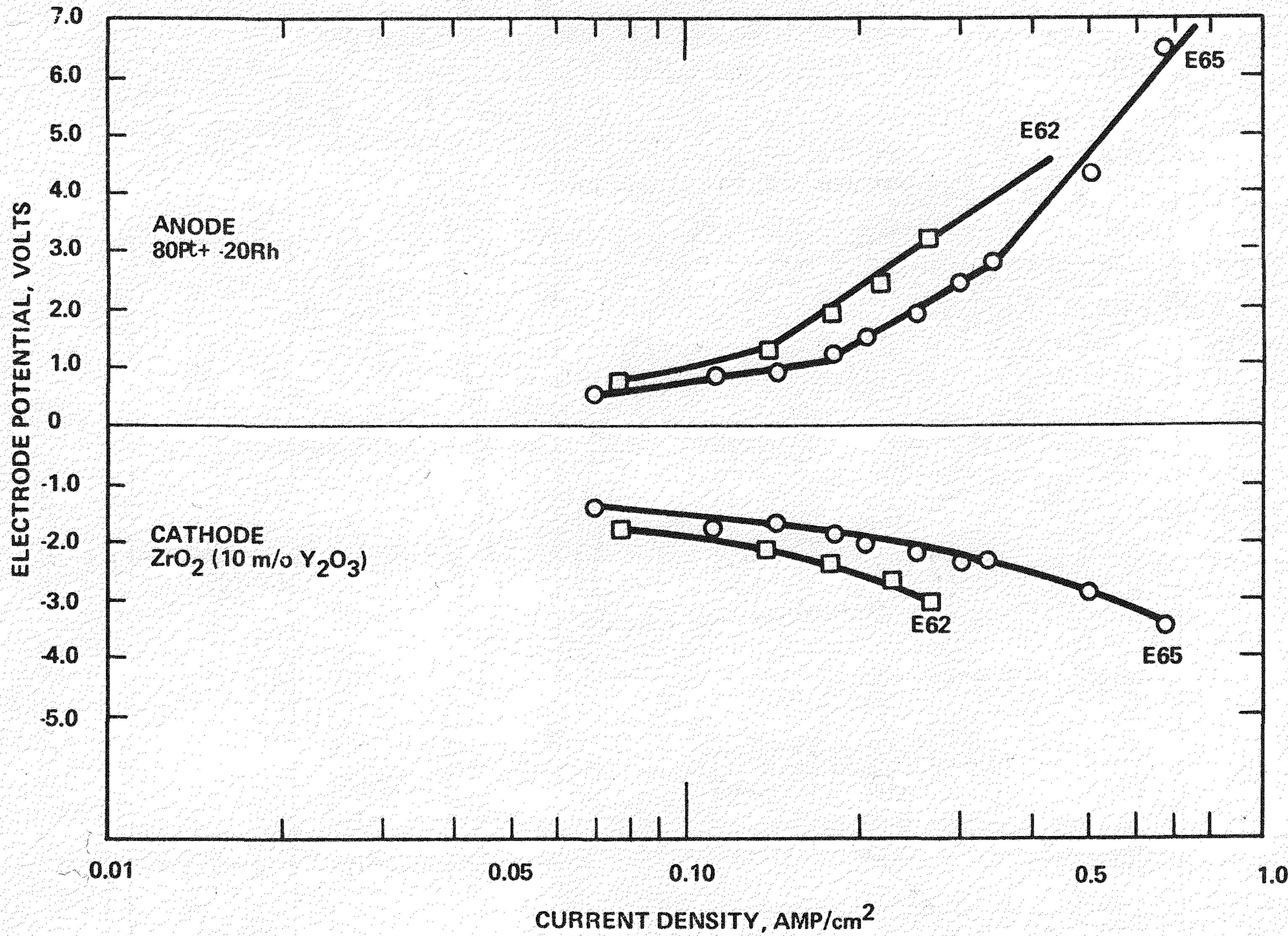

615435-9A

Figure 14. Electrode Polarization with 80Pt-20Rh Anode and Single Crystal ZrO_2 (10 m/o Y_2O_3) Cathode. Run E-62, E-65.

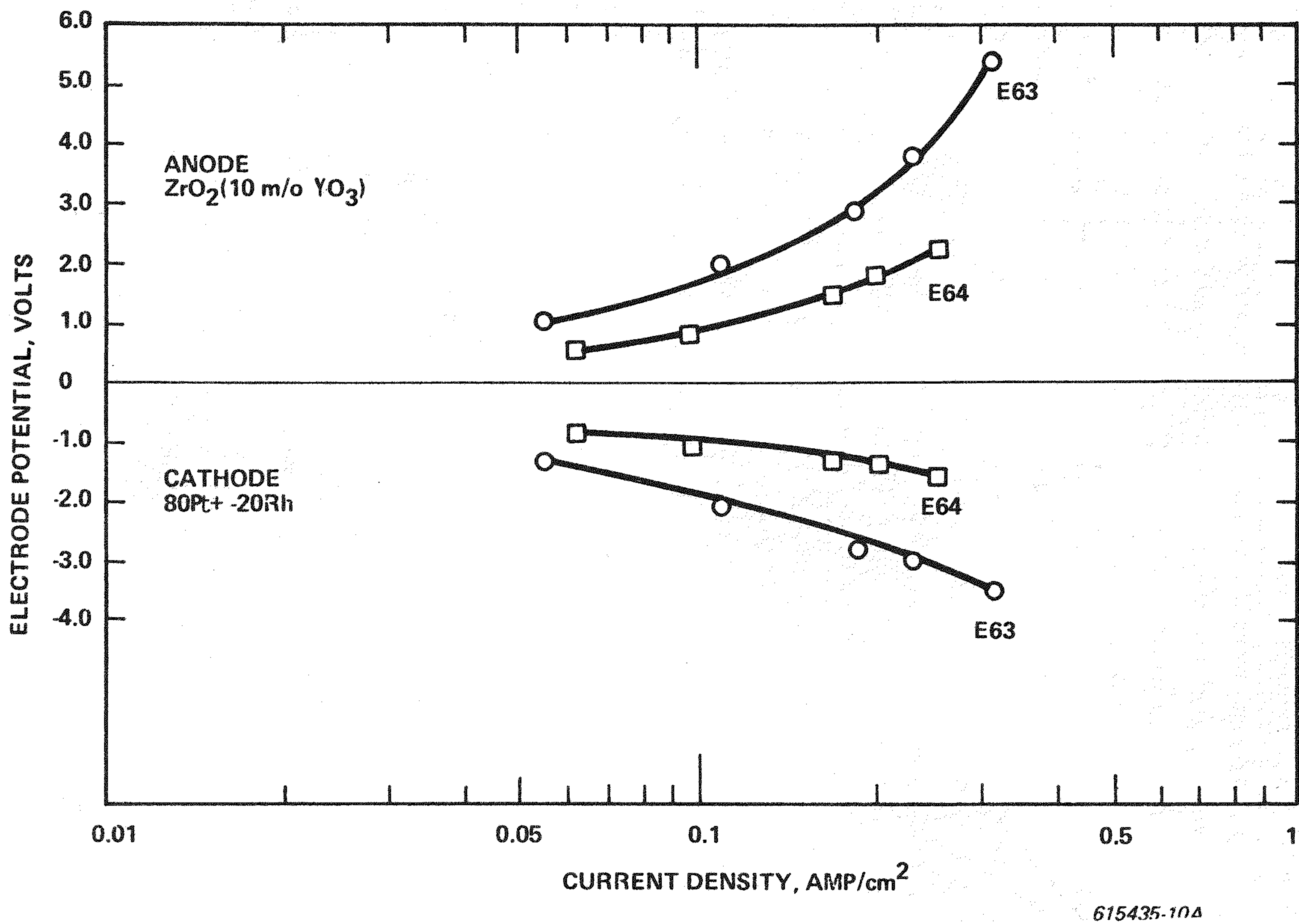

Figure 15. Electrode Polarization with Single Crystal ZrO_2(10 m/o Y_2O_3) Anode and 80Pt-20Rh Cathode, Runs E-63, E-64.

2.0 WBS 1.2 - ENGINEERING TESTS

In order to provide some overall perspective to the activity in this program, a review of previous studies of electrode durability was made. This review included studies in various MHD environments and included both generator tests and electrochemical laboratory tests. This review is summarized in Table 6 for a variety of materials which were tested over a range of temperatures and MHD environments. Data is reported in terms of material loss in μg per coulomb of current. Any comparisons made using this table must be made with the understanding that the effect of other test parameters such as current density, magnetic field, plasma velocity, heat flux, etc., varied between studies and could have significant effects on loss rates. Secondly, these loss rates are calculated assuming uniform erosion or corrosion and uniform current distribution. Recognizing these limitations, this table can be used to make qualitative comparisons between materials and to show the effect of temperature and MHD environment on material loss. Future WESTF test activity is directed towards providing more quantitative data for operation in a western slag/K_2CO_3-K_2SO_4 test environment.

Future WESTF tests will include operation at much higher and more realistic sulfur levels than in past generator or laboratory electrochemical tests. Table 7 shows the calculated gaseous species anticipated in a future base load plant burning Illinois #6 or Montana Rosebud coals and those calculated for WESTF Test #41. The latter conditions approach those of the AVCO Mark VI generator. Table 7 shows that sulfur levels for WESTF Test 41, which reflected AVCO conditions are an order of magnitude lower than those anticipated for commercial plants. This is based on the assumption that a maximum amount of K_2SO_4 will be recycled as seed to reduce seed regeneration costs while satisfying EPA SO_2 requirements. Beginning with WESTF Test #42, sulfur levels approximating that to be found in future base load plants will be used in WESTF.

2.1 WBS 1.2.1 - Test Engineering

Test planning activities have been reviewed in order to more fully satisfy the engineering data needs associated with electrode development. This review has resulted in test plans and test section designs that will increase the

TABLE 6

MATERIAL LOSS RATES OF ELECTRODE MATERIALS IN VARIOUS MHD ENVIRONMENTS(1) (MATERIAL LOSS RATES ARE GIVEN IN μg/COULOMB)

			PRESENT TEST ENVIRONMENT								FUTURE TEST ENVIRONMENT			
		TEMP.	K_2CO_3		K_2SO_4		EASTERN SLAG K_2CO_3		WESTERN SLAG K_2CO_3		EASTERN SLAG K_2CO_3-K_2SO_4		WESTERN SLAG K_2CO_3-K_2SO_4	
MATERIAL	TEST	K	ANODE	CATHODE	ANODE	CATHODE	ANODE	CATHODE	ANODE	CATHODE	ANODE	CATHODE	ANODE	CATHODE
COPPER	G	~400	10.0[8*]	0.07[8]	100.0[8]	0.2[8]	8.0[11]	<0.2[12]	ND	ND	E	C	E	C
PLATINUM	G EC	>400 1670	0.03[8]	0.10[3]	0.3[8] 36.0	0.4[8] 79.0[8]	<0.5[12] >1.0	ND >5.0[13]	ND 105.0[17]	ND 502.0[17]	C C	E E	C E	E E
IRON	G EC	<1200 1670	5.0 ND	40.0 ND	ND ND	ND ND	ND 254[12]	ND 25[17]	ND ND	ND ND	E E	E C	E E	E C
INCONEL	G	<1200	ND	ND	ND	ND	7.0[16]	ND	ND	ND	E	E	E	E
$MoSi_2$	EC	1670	ND	ND	ND	ND	8.0[13]	27.0[13]	ND	ND	P	P	P	P
SiC	EC	1670	ND	ND	ND	ND	ND	ND	49.0[17]	65.0[17]	P	P	P	P
$MgCr_2O_4$	EC	1670	ND	ND	ND	ND	1.0[13]	22.0[13]	39.0[17]	59.0[17]	C	E	E	E
$YCrO_3$	EC	1700	ND	ND	10.0[14]	5-10[14]	7-29[14]	14-127[14]	42-190[14]	75-369[14]	C*	C*	E	E
Cr_2O_3	EC	1670	ND	ND	ND	ND	ND	ND	41.0[17]	52.0[17]	P	E	E	E
$Fe_3O_4 \cdot 3MgAl_2O_4$	EC	1700	ND	ND	ND	ND	10.0[10]	64.0[10]	74.0[10]	180.0[10]	E	E	E	E
STABILIZED ZrO_2	EC G	1700 2000	ND <0.5[9]	ND >1.5[9]	ND ND	ND ND	ND ND	ND ND	21-165[17] ND	32-165[17] ND	P C	P C	E C	E C
STABILIZED ZrO_2(2)	EC	1700	ND	ND	ND	ND	ND	ND	1-3[15]	20-26[15]	P	P	C*	C*
RARE EARTH OXIDE-HAFNIA	EC	1700	ND	ND	1-5[15]	1-5[15]	ND	ND	3-4[15]	3-400[15]	P	P	C*	C*
$LaFeO_3$-$SrFeO_3$-$SrZrO_3$	TR	2000	<1.0[10]	ND	ND	ND	ND	ND	ND	ND	C	C	C	C

*Unbracketed superscripts refer to References at end of this section.

(1) NOMENCLATURE:

G - GENERATOR TEST
EC - LABORATORY ELECTROCHEMICAL TEST
TR - TEST RIG TEST
ND - NOT DETERMINED

C - CANDIDATE MATERIAL FOR FURTHER TEST
C* - CANDIDATE, BOTH HOT AND SUPER HOT
E - ELIMINATED AS CANDIDATE MATERIAL
P - POSSIBLE CANDIDATE MATERIAL

(2) SINGLE CRYSTAL

TABLE 7

CALCULATED GASEOUS SPECIES†

Facility Temperature Pressure	Illinois #6 Future Baseload Plant* 2600 K, 5 atm	Montana Rosebud Future Baseload Plant* 2600 K, 5 atm	#2 Fuel Oil + Eastern Flyash WESTF Test 41 2600 K, 2 atm
N_2	70.8 m/o	69.7 m/o	45.9 m/o
CO_2	13.3	13.8	16.7
H_2O	7.34	8.17	17.8
CO	3.68	3.88	2.17
O_2	1.02	0.976	11.1
Ar	0.909	0.893	0.576
NO	0.598	0.581	1.58
OH	0.521	0.544	1.84
KOH	0.453	0.312	0.883
SO_2	0.433	0.324	0.0138
H_2	0.317	0.360	0.363
K	0.299	0.197	0.405
O	0.104	0.101	0.535
H	0.095	0.101	0.159
SO	0.018	0.0144	0.0003
SiO	0.018	0.0144	
KO	0.0084	0.0054	
SiO_2	0.0068	0.0052	
FeO	0.0063	0.0014	
Fe	0.0041	0.0009	
CaOH	0.0030	0.0040	
MgO	0.0012	0.0027	
Mg	0.0003	0.0008	
AlO_2	0.0001	<0.0001	

*Assumes 10% ash carryover, maximum use of K_2SO_4 as seed also meeting EPA SO_2 requirements.

†Calculated using Westinghouse CHEM EQ Program.

the level of testing to provide a basis for the sections of electrode/insulator systems and designs to be tested in WESTF after the magnet is installed and operating. Three distinct levels of testing are planned:

- Materials Test Section
- Mini-WESTF Test Section
- WESTF Test Section

The WESTF test section is being redesigned to be compatible with the magnet pole spacing of 5-3/8 inch and pole piece length of 16 in (40 cm). This test section will consist of a stack of "window frame" modules, each consisting of an electrode pair and insulating elements. The modular design will permit the assembly of a variety of test section configurations with considerable flexibility. Two basic versions of this modular test section will be used; first a "Mini-WESTF" test section, consisting of 3 or 4 electrode pairs and secondly; a full WESTF-II test section consisting of 8 to 12 electrode pairs. In addition screening tests of materials under dynamic MHD test conditions will be conducted in the Materials Test Section (MTS). The MTS consists of 1 to 3 small electrode pairs and will be used to expedite the generation of data on the durability and performance of materials.

Current test planning activities have been reflected in Table 8 which provides a revised summary of future WESTF Tests. The general format of the table has been modified to incorporate a number of additional data items applicable to the particular test, including, magnetic field, seed type, sulfur level, etc. In addition the table identifies the particular test section to be used for the specific WESTF test.

2.1.1 Development Requirements

Preliminary test specifications are issued to initiate design activity on the channel for each test. Materials development/procurement and electrode systems development activities are initiated based on the Preliminary Test Specification. Final Test Specifications are issued after completion of all development activities and provide the basis for detail design of the channel and WESTF testing.

TABLE 8

FUTURE WESTF TESTS

OPERATING MODE	NON-SLAG SH	CLEAN SH	NON-SLAG SH	SLAG HOT	SLAG HOT	SLAG COLD	NON-SLAG SH
Test ID	D-10	D-11 (5)	W-42	W-45	W-43	W-46	W-44
Test Section	Transition	Transition	WESTF	MTS	WESTF	MTS	WESTF II
Approx. Date	10/79	10/79	11/79	11/79	12/79	12/79	TBD
Electrode Material (1)	NA	NA	ZrO_2 Based HfO_2 Based Perovskite	Zirconia	Pt (+) Fe (-)	NA	HfO_2 Based (2)
Insulator Material	MgO	NA	Various	TBD	$MgAl_2O_4$ Al_2O_3	Various	Various
T_E, °C	NA	NA	1700-1900	~1450	1000-1300	NA	1700-1900
J, amp/cm^2	NA	NA	NA	~1	To 1.25	NA	TBD
$\dot{Q}$, w/cm^2	NA	NA	60	~30	~80	NA	~80
B, Tesla	NA	NA	NA	NA	NA	NA	NA
Axial Field, Kv/m	NA	NA	NA	NA	Yes	NA	TBD
Ash Type	Rosebud	None	Rosebud	Rosebud	Rosebud	Rosebud	Rosebud
Seed	K_2CO_3	None	K_2CO_3	K_2CO_3	K_2CO_3	K_2CO_3	K_2CO_3
SO_2 Level, m/o	TBD	TBD	0.3	0.3	0.3	0.3	0.3
Duration-Hrs.	~4	~10	8/Increm.	~10	~20	~10	~20

OPERATING MODE	SLAG HOT	SLAG HOT	NON-SLAG SH	SLAG HOT	SLAG COLD		
Test ID	TBD	TBD	TBD	TBD	TBD		
Test Section	TBD	TBD	TBD	TBD	TBD		
Approx. Date	TBD	TBD	TBD	TBD	TBD		
Electrode Material (1)	SiC	$LaFeO_3$- (3) $SrZrO_3$- $SrFeO_3$	ZrO_2 Based HfO_2 Based Perovskite	$MgCr_2O_4$	TiB_2 (+) Cu-Pt (+) Cu-W/Cu (-)		
Insulator Material	Si_3N_4	TBD	TBD	$MgAl_2O_4$ Al_2O_3	BN		
T_E, °C	1000-1300	1700-1900	1700-1900	1000-1400	~150		
J, amp/cm^2	To 1.25	To 1.25	To 1.25	To 1.25	0.9		
$\dot{Q}$, w/cm^2	~80	TBD	<60	~80	~125		
B, Tesla	NA	NA	TBD	TBD	TBD		
Axial Field, Kv/m	Yes	TBD	TBD	Yes	Yes		
Ash Type	Rosebud	Rosebud	Rosebud	Rosebud	Rosebud		
Seed	K_2CO_3	K_2CO_3	K_2CO_3	K_2CO_3	K_2CO_3		
SO_2 Level, m/o	0.3	0.3	0.3	0.3	0.3		
Duration-Hrs.	~20	~20	~8/Increm.	~20	~10		

(1) Anode and Cathode Unless Otherise Noted
(2) With Indium Current Leadout
(3) MIT Material
(4) Materials Test Section
(5) Thermal Test

During this quarter, a revision was issued to complete the Final Test Specification for WESTF Test 42, and a Preliminary Test Specification was issued for WESTF Test 44. Also, Specifications were issued for Tests D-9, D-10, and D-11, tests that were added to the original program. Each of these tests will be discussed in the following sections of this report.

WESTF Test D-9

WESTF Test D-9 was added to the testing sequence to check out the design of the Materials Test Section at selected thermal conditions in several short runs. It is to provide, in addition, an evaluation of lanthanum chromite as an electrode operating under super-hot non-slagging conditions in the presence of Western slag. In the D-9 run series, data correlations are to be made for mass flow rates ranging from 0.07 Kg/sec to 0.33 Kg/sec.

WESTF Test D-10

WESTF Test D-10 was added to the testing sequence to evaluate alternate thermal designs for the WESTF Test 42 inlet transition section. The designs, based on thermal analysis, consist of three different thicknesses of 85% dense high purity MgO and four different attachments. The test article is composed of inlet and outlet transition sections joined together to provide a configuration suitable for testing bulk materials such as commercial refractories in the MHD environment.

WESTF Test D-11

WESTF Test D-11 was added to the testing sequence to investigate the facility and test section thermal response to operation over a range of fuel equivalence ratios and mass flow rates. As in WESTF Test D-10, the test article will be composed of inlet and outlet transition sections. The upstream section is the primary test article and will be lined with high density MgO brazed to nickel mesh brazed to copper. Five indium rhodium thermocouples will measure the gas stream temperatures and four Type R thermocouples will measure the ceramic temperatures. A sight port will be provided for optical pyrommetry.

WESTF Test 42

The primary objective of WESTF Test 42 is to compare the relative performance of selected materials over a range of temperatures in a super-hot MHD channel environment in the absence of electrical or magnetic fields. There are two walls for electrode materials with six coupon holders on each wall. One wall will test mostly zirconia based coupons, and the other wall will test hafnia based coupons. The zirconia based materials are furnished by Westinghouse, and the hafnia based compositions and the thermal conductivities for all materials are furnished by Battelle PNL. The electrode coupon materials are identified in Table 9. A schematic diagram showing the final layout of the channel for WESTF Test 42 is given in Figure 16.

The insulator walls each have five copper cooling blocks lined with magnesia. Surface temperatures are to range from 1650°C at the inlet to 1750°C at the exit of the channel. The materials selected for the insulating walls and their sizes are shown below: (brazed attachments with nickel mesh interface material)

Surface Temp. Max. (°C)	Material	I.D.	Thickness (in.)	
			MgO	Mesh
1650	Norton MgO	MG-NT0501	0.97	0.1
1650	Norton MgO	MG-NT0501	0.56	0.2
1750	Narco MgO	MG-NA0101	0.40	0.2
1750	Narco MgO	MG-NA0101	0.40	0.2
1750	Norton MgO	MA-NT0501	0.48	0.2

The inlet transition section is lined with high purity MgO (Norton 85% dense - MG-NTOX01) and designed to run below 1650°C. Several competing designs are to be compared in a transition section test (WESTF D-10, discussed above) to be run prior to WESTF Test 42. Thus, the actual design of the inlet transition section will be determined based on an evaluation of the different designs tested in WESTF D-10. The exit transition section design remains as originally presented in the previous quarterly report.

With the exception of the inlet transition section, all of the parts required for the assembly of WESTF Test 42 have been machined. The insulating and coupon walls are in different stages of assembly.

TABLE 9

ELECTRODE COUPON MATERIALS AND CHANNEL LOCATIONS

Coupon Location	Surface Temp., °C	Materials Identification[1]	MATERIAL THICKNESS, IN.[2] Coupon	MATERIAL THICKNESS, IN.[2] MgO Beneath Coupon
A1 (inlet)	1650	YZ-WE0101/YZ-WE0102	.230	.050
A2	1650	ZC-WE0101/ZC-WE0102	.200	.000
A3	1750	YZ-WE0101/YZ-WE0102	.265	.100
A4	1750	ZC-WE0102/ZC-WE0102	.300	.100
A5	1850	YZ-WE0102/YZ-WE0102	.270	.050
A6	1850	HO-BN0401 (D3, D4, D5)	.300	.950
C1 (inlet)	1650	HO-BN0302 (A11, A12, A13)	.200	.100
C2	1650	HO-BN0102 (B3, D7, B5)	.300	.150
C3	1750	HO-BN0302 (A15, A18, A19)	.300	.100
C4	1750	HO-BN0102 (B26, B27, B28)	.300	.450
C5	1850	HO-BN0302 (A23, A24, A25)	.300	.200
C6	1850	HO-BN0102 (B29, B30, B31)	.300	1.050

(1) YZ-WE0101/YZ-WE0102 = 12 Y_2O_3 - 88 ZrO_2
ZC-WE0101/ZC-WE0102 = 15 ($Mg_{.625}$ $Ca_{.375}$) - 85 ZrO_2
HO-BN0401 = $Er_{.82}$ $Hf_{.18}O_2$
HO-BN0302 = $Pr_{.27}$ $Yb_{.09}$ $Hf_{.64}$ O_2
HO-BN0102 = $Tb_{.20}$ $Y_{.10}$ $Hf_{.70}$ O_2
"A11, etc." = Battelle PNL Sample Number

(2) At a plasma flow rate of .075 kg/sec and 0.1 inch of nickel interface material.

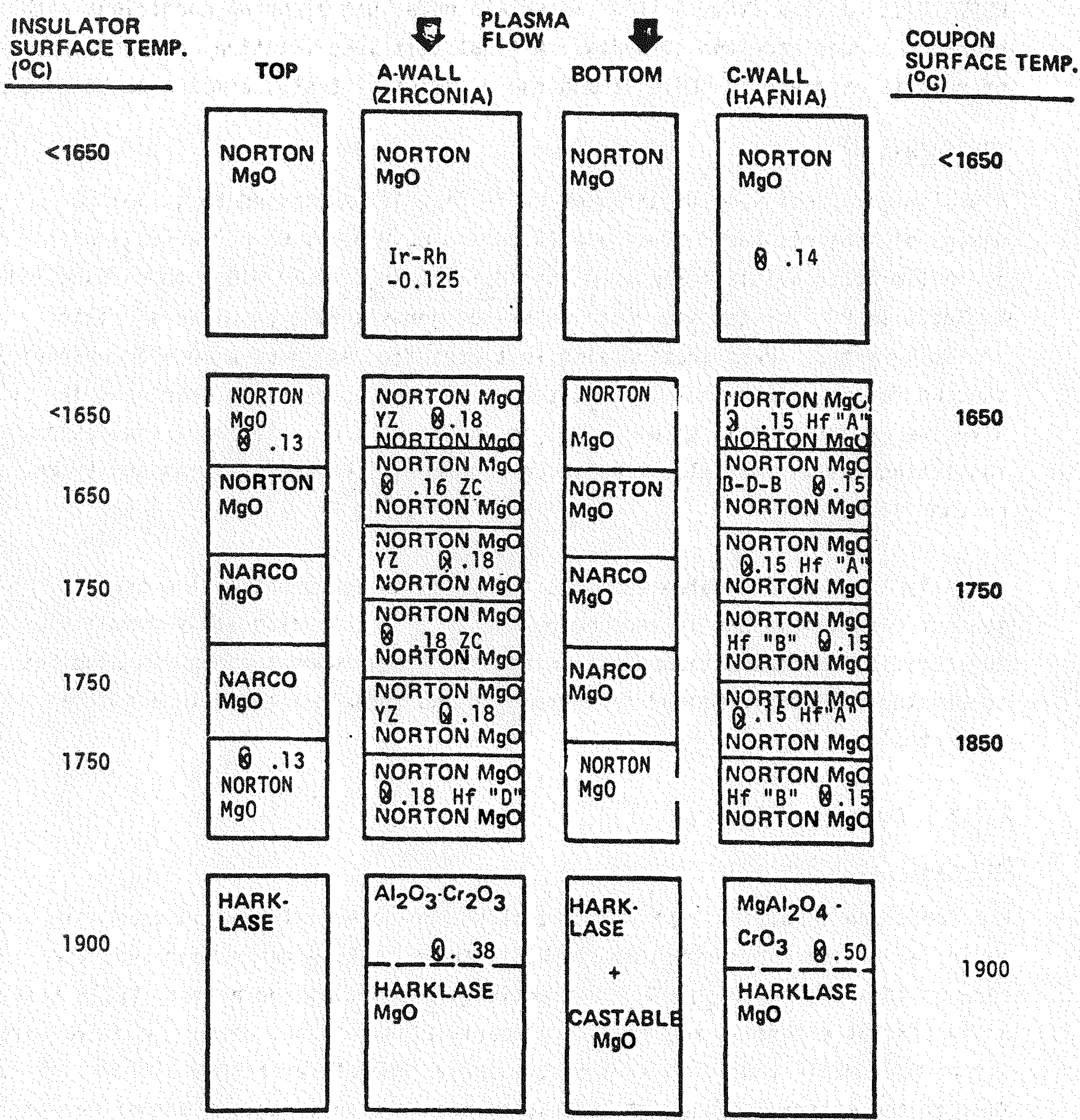

⊗ Type "B" Thermocouple Locations (adjacent number is distance from surface in inches)

Figure 16. WESTF Test 42 Channel Schematic

WESTF Test 43

WESTF Test 43 is a first test of materials under hot slagging conditions with platinum anodes and iron cathodes. A final test specification, delayed because of priorities given to WESTF 42 and the D-series of tests, remains to be issued.

WESTF Test 44

A preliminary test specification on WESTF Test 44 was issued to guide the design of a hafnia-based electrode ($0.063 \cdot Tb_4O_7 \cdot 0.063\ Y_2O_3 \cdot 0.874\ HfO_2$) with an indium doped hafnia leadout ($0.16\ Y_2O_3 \cdot 0.55\ In_2O_3 \cdot 0.29\ HfO_2$) to be supplied by Battelle PNL for testing under super-hot non-slagging conditions. This preliminary test specification also initiates the design of a modular channel section for this test that is a prototype of the design to be developed for use with the magnet that is to be installed in WESTF. Interelectrode insulation, insulating walls, and inlet transition region will have dense high purity MgO on the plasma side.

An early test has indicated that the indium oxide component of the ceramic leadout material is easily reduced by the Ti Cu Sil brazing alloy normally used for ceramic to metal attachment. Therefore, a development effort is required to provide a suitable method for attaching the ceramic leadout to a nickel mesh compliant layer.

2.1.2 Experiment Design

Materials Test Section

Electrode and insulator materials and structures are evaluated on the basis of their durability and performance in WESTF tests. These tests represent the core of this program with all other activity supporting the primary WESTF tests. A significant effort is required to properly plan, design, conduct and evaluate the primary WESTF tests; this is particularly true of refractory systems. Since many of the materials under consideration are in a very early stage of development and further, the list of candidate materials is a relatively long one, there is need for meaningful tests reflecting the availability of limited volumes of electrode/insulator materials and the desire for quick turn-around time. The

Materials Test Section (MTS) serves as the vehicle for tests of this type. With limited design and fabrication effort, many materials-related questions can be investigated in a test of this type. The MTS tests will not impose full electrical nor thermomechanical stresses on materials, but will provide for tests of these materials under realistic MHD conditions and will eliminate much uncertainty and the inclusion of high risk materials in the primary WESTF tests. An initial version of the MTS has been designed for WESTF Test D-9.

The test section is composed of an upstream square steel pipe which is lined with refractory material and incorporates the test materials. The balance of the total length required to mate with WESTF is made up by a round steel pipe section which is lined with a castable refractory. As shown in Figure 17, the external surfaces of the test section are cooled by means of a water cooled copper tubing wrap.

For WESTF D-9, two $La_{.95}Mg_{0.5}CrO_3$ electrode pairs were imbedded in the brick of the upstream square section. Each of the electrodes had a thickness of 1.27 cm with face dimensions of 1.27 x 1.27 cm (1.61 cm^2) exposed to the plasma. Type S thermocouples were positioned 2 mm from the surface in the downstream electrode pair. A platinum wire electrical leadout was employed with 0.040 in Pt wire attached to the back face of the electrode with platinum paste and mesh. A sight port was included to view the surface of one of the downstream electrodes. The nominal flow cross section at the electrodes was 2.54 cm x 5.08 cm (12.9 cm^2). Table 10 summarizes the thermal design conditions for WESTF Test D-9. The specific intent was to monitor the surface temperatures of the lanthanum chromite electrodes while varying the mass flow rate through the channel at a constant plasma temperature of 2550 K. No seed or slag was to be injected into the channel during the run. A one dimensional thermal analysis was used to predict the surface heat fluxes and electrode surface temperatures at the selected mass flow rates.

Modified WESTF Test Section

Design work is underway on a modified test section structure suitable for use with the 3 Tesla conventional magnet which is to be installed in the WESTF

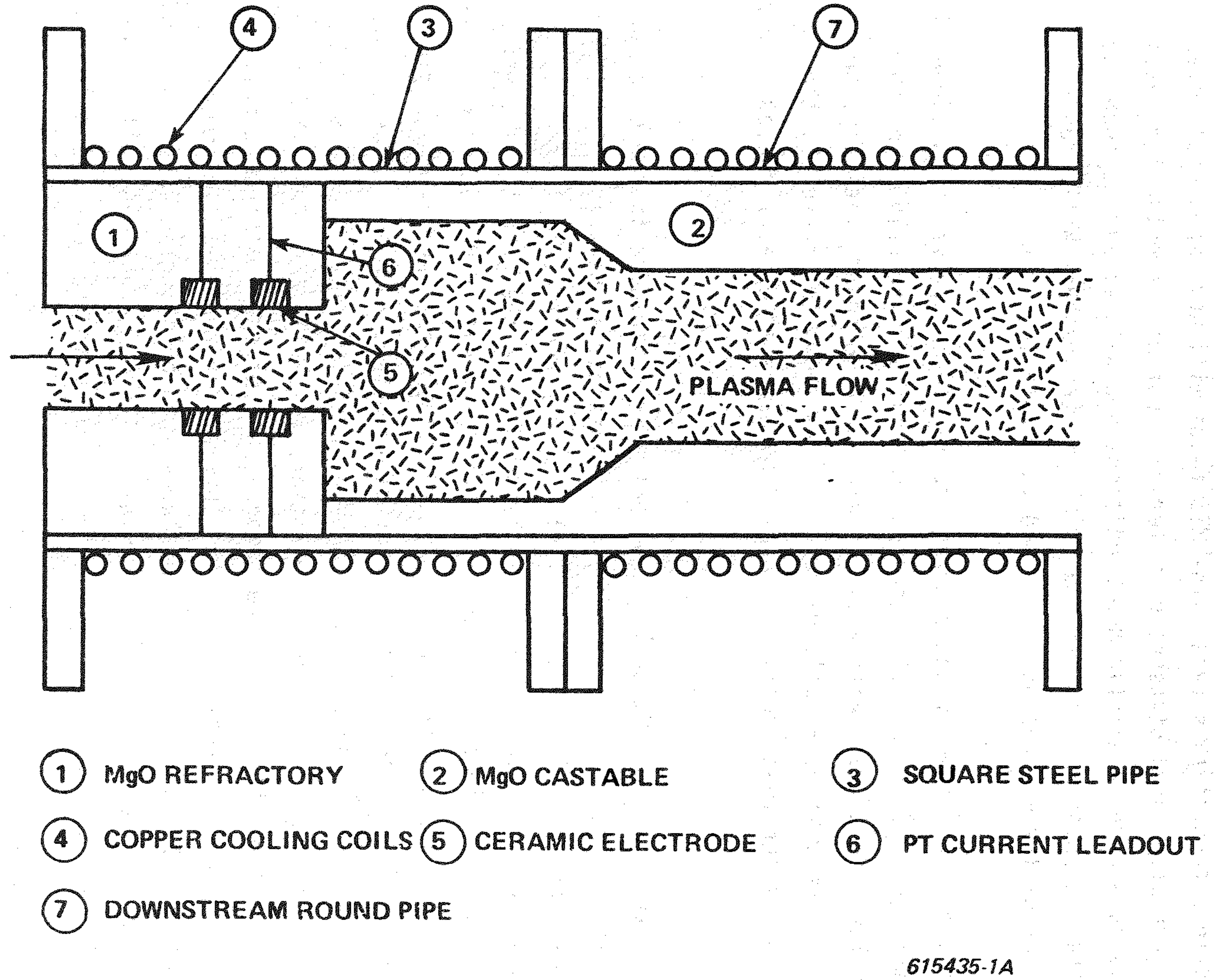

Figure 17. Cross Section of Materials Test Section (MTS)

TABLE 10

MTS THERMAL DESIGN CONDITIONS, WESTF TEST D-9

Plasma Temp K	Mass Flow Rates (Kg/s) Fuel	Air	Oxygen	Total	(Btu/hr-ft^2-°F)	Surface Heat Flux W/cm^2	Predicted Surface Temp °C	Electrode ($LaCrO_3$) Thickness (in.)
2500	0.0076	0.0663	0.0254	0.099	125	44.7	1640	0.5
2550	0.0107	0.0928	0.0356	0.139	163	47.9	1750	0.5
2550	0.0153	0.1326	0.0509	0.199	220	50.9	1870	0.5

facility. The primary constraint on the design of this modified test section is the available space within the magnet. Specifically, the entire test section, including cooling water connections, electrical leads and instrumentation, must fit within a 5.25 in. x 10 in. cross section. In particular all cooling water and other penetrations must be in the electrode wall, that is in the 10 in. dimension.

A different configuration is being considered than that used with the present test section design. In particular, the present WESTF test section has: an inlet transition section, the test section proper which is formed by four slab walls (two electrode walls and two insulating walls) and an exit transition section. A notable characteristic of the existing test section configuration is that it incorporates intersecting gaskets which is a poor design practice.

The primary structure will consist of solid fiberglass reinforced "window frames", one to two inches thick, held together by axial bolts. Each frame may contain from one to three electrode pair, depending on the pitch, and the associated insulating wall elements. The active portion of the test section will consist of a stack of "window frame" modules. The entrance and exit regions will be similarly constructed. However, these sections will use insulating materials on all walls. The faces of these frames are the primary surfaces to be sealed at assembly and will use a form-in-place type of gasket which will result in a more reliable seal and generally more rigid structure.

The modular design, see Figure 18, will permit the assembly of a variety of test section configurations with considerable flexibility. It is anticipated that two basic versions of this modular test section will be used; first a "Mini-WESTF" test section and a full WESTF II test section. In the case of the Mini-WESTF test section, the number of electrode pairs will be approximately four, while a WESTF II test section will include 8 to 12 electrode pairs. The number of frames in a given test section is dependent on electrode pitch. This modular configuration will also permit varying electrode pitch within a given test section.

Mechanical and leakage properties of the various reinforced fiberglass materials are being determined to supplement available data.

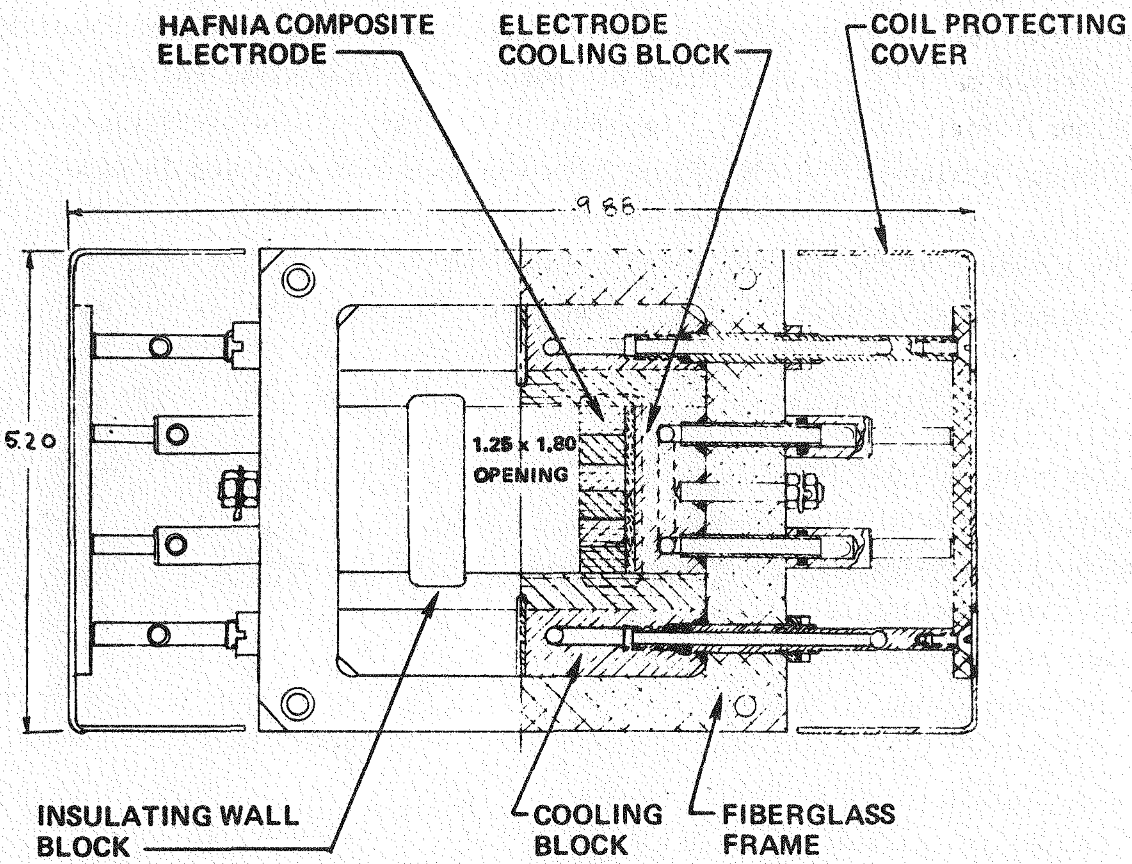

Figure 18. Modified WESTF Test Section Schematic

Detail design has been initiated for the first specific application of this test section for a WESTF test. WESTF Test 44, hafnia electrodes with oxide current leadout, will use this new test section.

WESTF Test 42

WESTF Test 42 is a test of hafnia and zirconia based "coupons" under super hot slagging/seed conditions (>1900 K temperature regime). The primary objective of this test is to compare and to evaluate the relative performance of the selected materials over a range of temperatures in a super hot MHD channel environment in the absence of electrical or magnetic fields. The thermal design of the electrode channel coupons was detailed in Reference 6.

As a result of the materials and thermal post-test analysis efforts for the preceeding WESTF Test 41, the design of the test section was reviewed.

Insulating Walls/Transition Sections

The major changes pertain to the design constructions, material selection and temperature requirements associated with the channel top and bottom insulating walls and the outlet transition section components. The design of these components, reflecting the post-test analysis of WESTF Test 41 series, requires the use of equilibrium rather than frozen properties for the computation of bulk gas to electrode surface heat transfer. This method will ensure that the maximum material surface temperature limits are not exceeded.

The design candidates and their associated geometries for the insulating walls and the outlet transition section components for WESTF Test 42 are presented in Table 11. These constructions reflect both the revised design procedure and the revised surface temperature constraints.

Three candidate constructions are presented for each coupon insulating wall position (top and bottom) for each of two material candidates. These three constructions correspond to those ceramic tiles whose underlying thermal nickel mesh compliant layer has a thickness of 0.200, 0.100 inches

TABLE 11

DESIGN CANDIDATES AND THEIR ASSOCIATED CONSTRUCTION FOR INSULATING WALLS AND OUTLET TRANSITION SECTION COMPONENTS FOR MHD WESTF TEST 42

COMPONENT/LOCATION	FUNCTION	MATERIAL/CONSTRUCTION	SURFACE TEMPERATURE REQUIREMENT(maximum)(°C)	DIMENSION PERPENDICULAR TO PLASMA FLOW (in.)
Channel Insulating Walls (Top & Bottom - 10 components total)	1) Electrical Insulation for Faraday Mode WESTF Channel 2) Thermal Insulation 3) Interior Channel Envelope (Structural/Thermal)			
Coupon Position 1-2		Norton MgO/Nickel Mesh (.2,.1,0) Narco MgO/Nickel Mesh (.2,.1,0)	1650	(0.562,0.902,1.24) (0.355,0.570,0.785)
Coupon Position 2-3		" " " " " "	 1650	(0.562,0.902,1.24) (0.355,0.570,0.785)
Coupon Position 3-4		" " " " " "	1750	(0.483,0.775,1.07) (0.341,0.548,0.755)
Coupon Position 4-5		" " " " " "	1750	(0.483,0.775,1.07) (0.341,0.548,0.755)
Coupon Position 5-6		" " " " " "	1750	(0.483,0.775,1.07) (0.341,0.548,0.755)
Outlet Transition Section - 4 components total	1) Cool Test Gas (spray flange) Prior to Entry In Exhaust System Complex	Al_2O_3 - Cr_2O_3	1900	0.756
	2) Length Requirements Influence Flow Characteristics Through Duct Aspect Ratio	$MgAl_2O_4$ - CrO_3 (E,K-3)	1900	1.21,0.756
	L/D	Harklase MgO	1900	1.43
Bottom Insulating Tiles Outlet Transition Section		Harklase MgO/w Castable MgO plug insert	1900	1.43/1.46

respectively. This matrix of possibilities permits material choice and incorporation of existing hardware to minimize fabrication difficulty while still preserving the design intent. In a similar manner, several constructions are presented for the outlet transition section (material component) designs.

The inlet transition section for WESTF Test 42 has been redesigned based upon the WESTF Test 41 results, see Section 2.1.3, in a more conservative manner. In order to properly screen the most appropriate design configuration for use in WESTF Test 42, a transition section proof test, WESTF Test D-10, with the appropriate simulated thermal environment will be conducted prior to WESTF Test 42. Several competing designs based upon high purity 85% Norton MgO ceramic tiles are to be compared and evaluated. These include a 0.677 in. thick MgO tile bonded to copper using silastic RTV, a 0.918 in. thick MgO tile bonded to copper using stainless steel and copper filled ceramic adhesives and 0.325 in. thick MgO tile brazed to a 0.1 in. thick nickel mesh thermal compliant layer which is in turn soldered to copper.

The first design (0.918 in. MgO) is based upon the original analysis, the other two reflect the new designs. All designs will be independently monitored with respect to calorimetry and with respect to the ceramic temperatures as measured by type B thermocouples. Thus, the actual configuration of the inlet transition section for WESTF Test 42 will be determined by the outcome of this transition section test run.

The algorithms for the on-line computation of surface temperature and heat flux for the WESTF Test 42 MHD electrode coupon designs have been developed. These linear sets of equations may be easily programmed into the existing data acquisition system to provide for the required thermal monitoring for this testing series.

Figure 19 illustrates the general conceptual coupon electrode wall design for WESTF Test 42. The general material and temperature requirements evolved for each wall based upon the test plan are shown in Table 12. The detailed design of these coupon electrode walls (Reference 6) was based upon converted

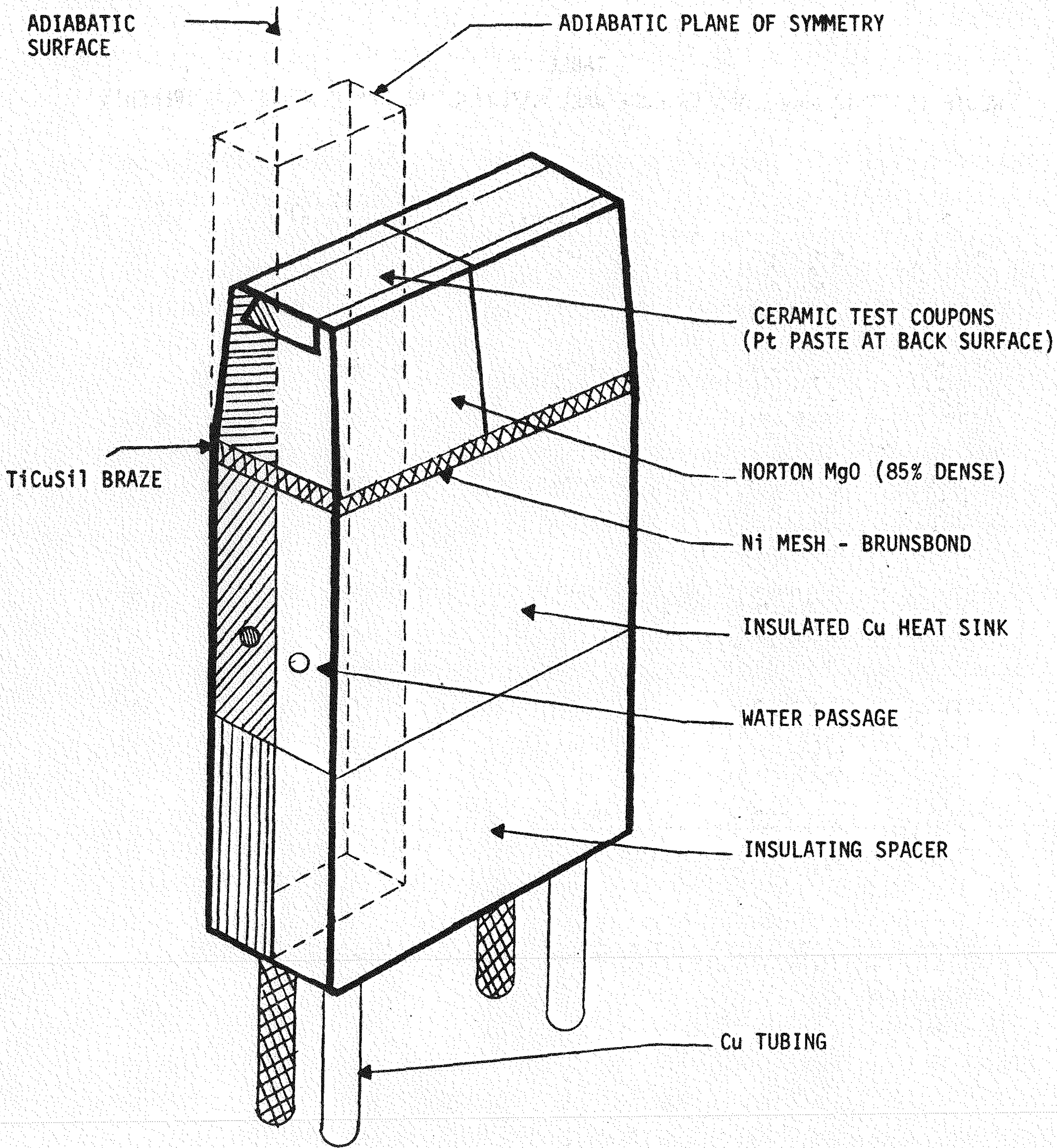

Figure 19. General Coupon Electrode for WESTF Test 42 Electrode Walls

TABLE 12

WESTF TESTS 42 ANODE AND CATHODE WALL MATERIAL AND TEMPERATURE REQUIREMENTS

Material	(Molar) Composition	Coupon Surface Temperature (°C)	Guideline[2] Maximum Insulator (MgO) Surface Temperature (°C)	Generator Axial Location ($\frac{x}{D_h}$)[1]
Norton MgO	85-90% dense MgO	1600-1650	1475-1550	3.93
YZ (M-155)[3]	12 Y_2O_3 - 88 ZrO_2			
YZ (M-154)[3]	12 Y_2O_3 - 88 ZrO_2			
Hafnia A	$Pr_{0.27}Yb_{0.09}Hf_{0.64}O_2$			
Hafnia B	$Tb_{0.20}Y_{0.10}Hf_{0.70}O_2$			
Norton MgO	85-90% dense MgO	1650-1700	1550-1600	4.77
ZC (M-156)[3]	15 $(Mg_{0.625}Ca_{0.375})$ O-85 ZrO_2			
YZ (M-154)[3]	12 Y_2O_3 - 88 ZrO_2			
Hafnia A	$Pr_{0.27}Yb_{0.09}Hf_{0.64}O_2$			
Hafnia B	$Tb_{0.20}Y_{0.10}Hf_{0.70}O_2$			
Norton MgO	85-90% dense MgO	1700-1750	1575-1625	5.61
YZ (M-155)[3]	12 Y_2O_3 - 88 ZrO_2			
YZ (M-154)[3]	12 Y_2O_3 - 88 ZrO_2			
Hafnia A	$Pr_{0.27}Yb_{0.09}Hf_{0.64}O_2$			
Hafnia B	$Tb_{0.20}Y_{0.10}Hf_{0.70}O_2$			
Norton MgO	85-90% dense MgO	1750-1800	1600-1650	6.45
ZC (M-156)[3]	15 $(Mg_{0.625}Ca_{0.375})$ O-85 ZrO_2			
YZ (M-154)[3]	12 Y_2O_3 - 88 ZrO_2			
Hafnia A	$Pr_{0.27}Yb_{0.09}Hf_{0.64}O_2$			
Hafnia B	$Tb_{0.20}Y_{0.10}Hf_{0.70}O_2$			
Norton MgO	85-90% dense MgO	1800-1850	1625-1675	7.28
YZ (M-155)[3]	12 Y_2O_3 - 88 ZrO_2			
YZ (M-154)[3]	12 Y_2O_3 - 88 ZrO_2			
Hafnia A	$Pr_{0.27}Yb_{0.09}Hf_{0.64}O_2$			
Hafnia B	$Tb_{0.20}Y_{0.10}Hf_{0.70}O_2$			
Norton MgO	85-90% dense MgO	1850-1900	1650-1700	8.12
ZC (M-156)[3]	15 $(Mg_{0.625}Ca_{0.375})$ O-85 ZrO_2			
YZ (M-154)[3]	12 Y_2O_3 - 88 ZrO_2			
Hafnia A	$Pr_{0.27}Yb_{0.09}Hf_{0.64}O_2$			
Hafnia B	$Tb_{0.20}Y_{0.10}Hf_{0.70}O_2$			

[1] Axial location relative to area of constant cross section. That is x = 0 corresponds to the entrance of the transition section, while x = 4 11/16" corresponds to the entrance of the generator channel. The above is based upon the sum of the lengths of the WESTF channel components of identical cross sectional area.

[2] Not a requirement.

[3] U-02 Phase I material

finite difference three dimensional modeling such as that illustrated in Figure 20. The results of that detailed design are presented in summary form via Table 13 and 14 for the "cathode" and "anode" wall respectively.

The algorithms for the on-line monitoring of electrode coupon surface temperature and heat flux are based upon these detailed electrode coupon designs, temperature distributions (see Figure 21) for each respective position and the as-specified instrumentation package as is presented in Table 15.

The electrode heat sinks will be connected in a completely parallel configuration to facilitate independent monitoring of the calorimetry. That is, the bulk water rise or heat input will reflect the individual electrode coupon surface heat input as each axial channel location (six per wall). In this matter, the axial heat flux gradient may be characterized with a minimum of measurement error. It is anticipated that the present facility arrangement (pump and booster pump addition) can provide the required design coolant flow rates of 85 $\pm$ 10 gph to each electrode coupon heat sink. Verification and facility check-out of this item will be conducted prior to the test date to ensure that these flow rates are indeed achievable.

The resultant algorithms for the computation of the projected electrode coupon ceramic surface temperature are shown in Table 16 for the "cathode" or "C" wall (typical representation).

The calorimetric expressions for surface flux has been prepared for use via two methods. These are shown in Table 17. Method 1 provides independent direct computation of surface heat flux as a function of channel location. Method 2 provides a normalized comparison (for the other coupons) to the high conductivity (minimal lateral heat loss) MgO ceramic coupon calorimeter. Both methods are recommended for use during the test to provide additional comparative data for thermal monitoring and both methods are interchangeable.

Reference 6 details the instrumentation sepcification and the algorithms for the on-line monitoring of the dependent thermal parameters for WESTF Test

Dimensions in inches

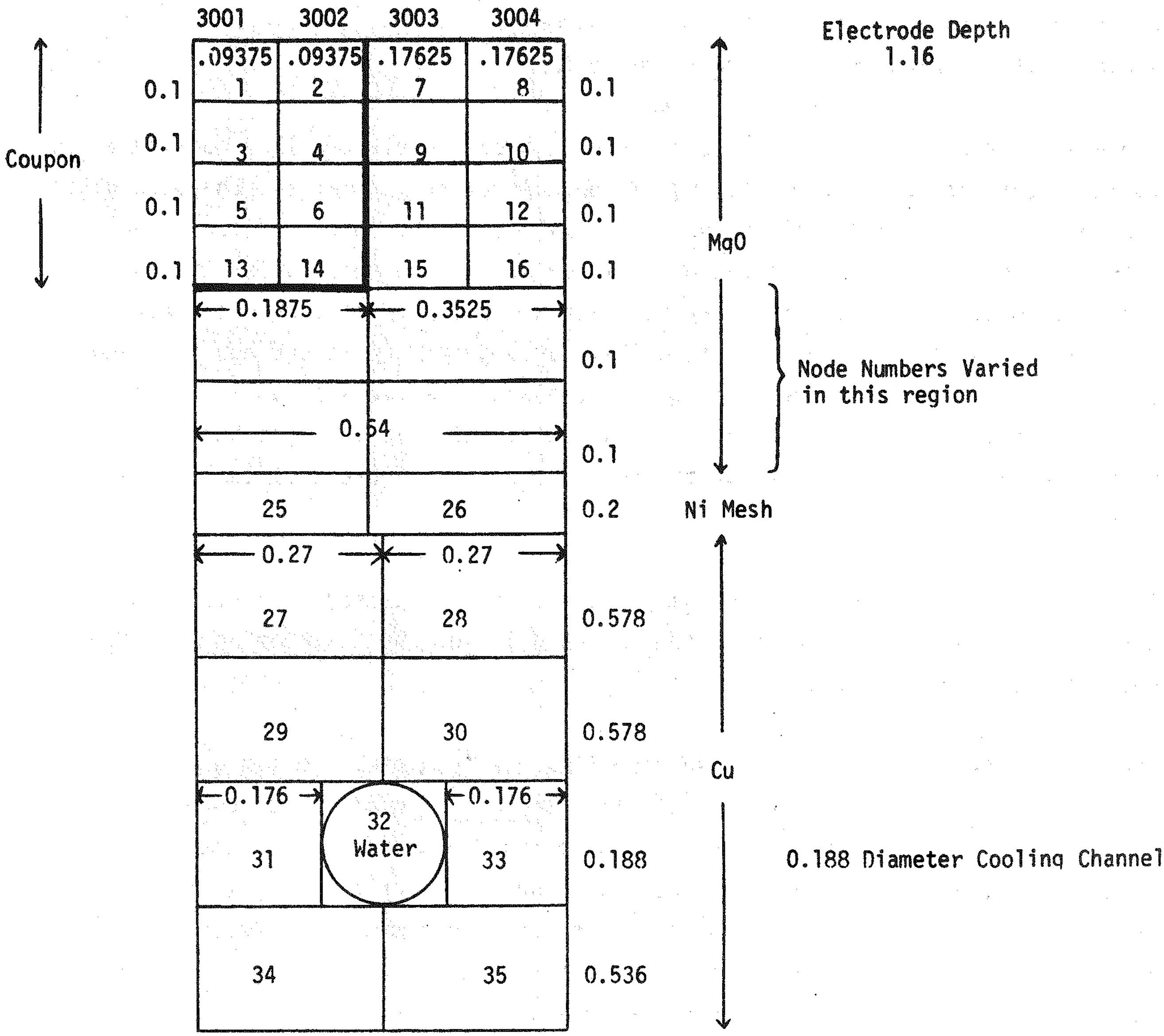

Figure 20. Coupon Electrode Model

TABLE 13

SELECTED CATHODE WALL DESIGN COUPON CONSTRUCTIONS AND RECOMMENDED FACILITY OPERATING POINTS BASED UPON THE SURFACE TEMPERATURE & THE SINGLE THICKNESS NICKEL MESH (Thermal Compliant Layer) REQUIREMENTS[1]

Coupon Position		1	2	3	4	5	6
Batelle Designation	1)	Norton MgO[2]	Norton MgO[2]	Norton MgO[2]	Norton MgO[2]	Norton MgO[2]	Norton MgO[2]
	2)	Hafnia Comp. A	Hafnia Comp. A	Hafnia Comp. A	Hafnia Comp. A	Hafnia Comp. A	Hafnia Comp. A
	3)	Hafnia Comp. B	Hafnia Comp. B	Hafnia Comp. B	Hafnia Comp. B	Hafnia Comp. B	Hafnia Comp. B
Temperature Requirement (°C)		1600-1650	1650-1700	1700-1750	1750-1800	1800-1850	1850-1900
Coupon Thickness[3] (in.)	1)	0.30	0.40	0.45	0.47	0.51	0.55
	2)	0.20	0.25	0.30	0.30	0.30	0.30
	3)	0.30	0.30	0.30	0.30	0.30	0.30
MgO Thickness Adjacent to Coupon (in.)	1)	0.30	0.40	0.45	0.47	0.51	0.55
	2)	0.20	0.25	0.30	0.30	0.30	0.30
	3)	0.30	0.30	0.30	0.30	0.30	0.30
MgO Thickness Below Coupon (in.)	1)	0.10	0.10	0.10	0.47	0.10	0.10
	2)	0.10	0.10	0.10	0.15	0.20	0.25
	3)	0.06	0.15	0.25	0.45	0.80	1.05
Surface to Nickel Mesh (in.)	1)	0.40	0.50	0.55	0.94	0.61	0.65
	2)	0.30	0.35	0.40	0.45	0.50	0.55
	3)	0.36	0.45	0.55	0.75	1.10	1.35
Nickel Mesh Thickness (in.)	1)	0.20	0.20	0.20	0.20	0.20	0.20
	2)	0.10	0.10	0.10	0.10	0.10	0.10
	3)	0.10	0.10	0.10	0.10	0.10	0.10
h(Btu/hr/ft^2 °F)	1)	110	107	105	103	100	95
	2)	100	100	100	100	100	100
	3)	105	104	103	102	100	100
Average Coupon Surface Flux (W/cm^2)	1)	44.6	39.3	42.0	34.0	34.0	31.4
	2)	43.3	40.4	37.5	34.9	32.4	29.8
	3)	42.4	41.0	38.0	35.3	31.5	29.7
Average Coupon Surface Temperature (°C)	1)	1611	1704	1751	1765	1825	1875
	2)	1634	1685	1736	1781	1826	1871
	3)	1650	1675	1725	1775	1842	1875

Notes:

1 - Distance Nickel Mesh Interface to Cooling Channel Center (in.) - 1.25.

2 - Hydraulic Diameter of Cooling Channel (in.) - 0.188.

3 - Coolant Flow Rate (gph) - 75-95.

4 - Recommended Facility Total Mass Flow Rate of Combustion Products (kg/sec) - 0.073-0.075.

TABLE 14

SELECTED ANODE WALL DESIGN COUPON CONSTRUCTIONS AND RECOMMENDED FACILITY OPERATING POINTS BASED UPON THE SURFACE TEMPERATURE AND THE SINGLE THICKNESS NICKEL MESH (Thermal Compliant Layer) REQUIREMENTS[1]

Coupon Position	1	2	3	4	5	6
Coupon Material (Batelle Designation)	1) Norton MgO[3,4] 2) YZ-155[2] 3) YZ-154[2]	Norton MgO[3,4] ZC-156[2] YZ-154[2]	Norton MgO[3,4] YZ-155[2] YZ-154[2]	Norton MgO[3,4] ZC-156[2] YZ-154[2]	Norton MgO[3,4] YZ-155[2] YZ-154[2]	Norton MgO[3,4] ZC-156[2] YZ-154[2]
Surface Temperature Requirement (°C)	1600-1650	1650-1700	1700-1750	1750-1800	1800-1850	1850-1900
Coupon Thickness (in.)	1) 0.30 2) 0.25 3) 0.20	0.40 0.20 0.20	0.45 0.29 0.24	0.47 0.30 0.30	0.51 0.25 0.35	0.55 0.36 0.40
MgO Thickness Adjacent to Coupon (in.)	1) 0.30 2) 0.25 3) 0.20	0.40 0.20 0.20	0.45 0.29 0.24	0.47 0.30 0.30	0.51 0.25 0.35	0.55 0.36 0.40
MgO Thickness Below Coupon (in.)	1) 0.10 2) 0.05 3) 0.20	0.10 0.00 0.10	0.10 0.10 0.10	0.47 0.10 0.10	0.10 0.05 0.10	0.10 0.10 0.10
Surface to Nickel Mesh (in.)	1) 0.40 2) 0.30 3) 0.40	0.50 0.20 0.30	0.55 0.39 0.34	0.94 0.40 0.40	0.61 0.30 0.45	0.65 0.46 0.50
Nickel Mesh Thickness (in.)	1) 0.20 2) 0.10 3) 0.10	0.20 0.10 0.10	0.20 0.10 0.10	0.20 0.10 0.10	0.20 0.10 0.10	0.20 0.10 0.10
h(Btu/hr/ft^2 °F)	1) ≈110 2) ≈ 87.5 3) ≈110	≈107 ≈105 ≈100	≈105 ≈103 ≈103	≈103 ≈102 ≈100	≈100 ≈100 ≈100	≈ 95 ≈105 ≈100
Average Coupon Surface Flux (W/cm^2)	1) 44.6 2) 29.8 3) 42.6	39.3 41.8 39.8	42.0 28.6 37.8	34.0 34.0 34.7	34.0 32.6 32.2	31.4 31.0 29.6
Average Coupon Surface Temperature (°C)	1) 1611 2) 1650 3) 1645	1704 1659 1696	1751 1725 1725	1765 1797 1786	1825 1825 1825	1875 1875 1875

[1]All coupon copper block and nickel mesh layers for the YZ-154, YZ-155 and ZC-156 materials have been previously machined to accommodate the 0.1" (single thickness) nickel mesh. The Norton MgO coupon will be used only if enough materials are not available at the time of fabrication or it will be used as a control coupon of uniform (MgO) material to facilitate calorimetry measurements. Accordingly, its dimensions are given above for each position if any or all of the positions are to be occupied by the Norton MgO.

[2]U-02 Phase I material whose position has yet to be specified by W R&D. Accordingly, dimensions are supplied to satisfy the thermal requirements at each coupon station.

[3]Highest conductivity material.

[4]Cathode wall as required, see footnote 1 above.

Notes: (applicable for all coupon designs)

1. Distance Nickel Mesh Interface to Cooling Channel Center (in.) - 1.25
2. Hydraulic Diameter of Cooling Channel (in.) - 0.188
3. Coolant Flow Rate (gph) - 75-95
4. Recommended Facility Total Mass Flow Rate of Combustion Products (kg/sec) - 0.073-0.075

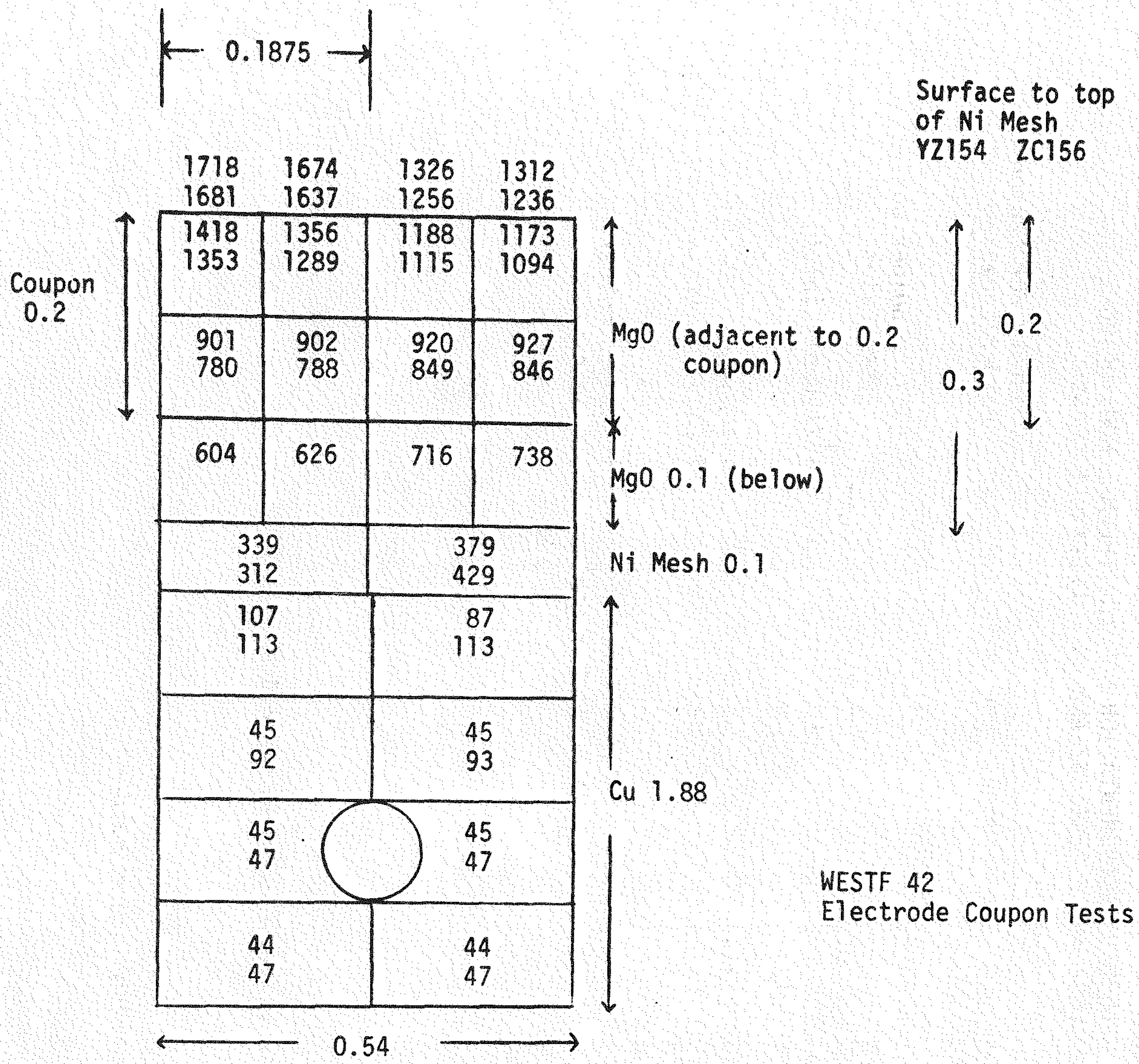

[1]Top number in nodes is representative of material YZ154, bottom number is representative of material ZC156.

Figure 21. Electrode Temperature Distribution
Coupon Position 2 - WESTF Test 42

TABLE 15

REQUIRED INSTRUMENTATION FOR THE THERMAL MONITORING
OF WESTF TESTS 42 AND 44 - ELECTRODE CHANNEL

Item	Purpose	Type	Quantity Per Coupon Holder/Location	Total Quantity
1. Thermocouple	Water calorimetry (outlet)	E	1/(Coupon holder outlet) heat sink	12[3]
2. Thermocouple	Water calorimetry (inlet supply)	E	1[1]/(Supply inlet)	1
3. Thermocouple	Bulk solid surface Temperature Extrapolation	B,S, or R B,S, or R	1 (Coupon) 1 (MgO substrate)	12[3] 12[3]
4. Flow meter	Water calorimetry	In-line water rated at 2.2 gpm[2]	1 (Coupon holder) heat sink	12[3]

[1] Total required quantity for entire electrode channel.

[2] Gallons per minute.

[3] 6 per electrode wall (1 each per coupon holder).

TABLE 16

INSTRUMENTATION SPECIFICATIONS AND ANALYTICAL EXPRESSIONS FOR THE ON-LINE MONITORING OF COUPON SURFACE TEMPERATURE -WESTF TESTS 42 & 44

Coupon Position		1	2	3	5	5
General Material Description		Hafnia Comp. A	Calorimetric Coupon[5] Norton MgO	Hafnia Comp. A	Hafnia Comp. A	Hafnia Comp. B
Specimen Coupon Thickness[1]		0.20	0.40	0.30	0.30	0.30
Average Coupon Surface Temperature at Design Pt[2] (°C)		1630	1700	1740	1830	1840
Coupon Centerline Thermocouple Location	1)	0.15" (3.81 mm) - coupon	0.15" (3.81 mm) - MgO	0.15" (3.81 mm) - Coupon	0.15" (3.81 mm) - Coupon	0.15" (3.81 mm) - Coupon
	2)	0.25 (6.35 mm) - MgO	0.25" (6.35 mm) - MgO	0.25" (6.35 mm) - Coupon	0.25" (6.35 mm) - Coupon	0.25" (6.35 mm) - Coupon
Relative Importance for Surface Monitoring[3]	1)	Primary	Primary	Primary	Primary	Primary
	2)	Secondary	Secondary	Secondary	Secondary	Secondary
ANSI Type[4]	1)	B, S or R*	B, S or R*	B, S or R*	B, S or R*	B, S or R*
	2)	B* E or K	B, S or R*	B*, E or K	B, S or R*	B, S or R*
Analytical Expression for Surface Temp. (°C)[6]	1)	$T_s = T_t + 800$	$T_s = T_t + 400$	$T_s = T_t + 710$	$T_s = T_t + 730$	$T_s = T_t + 510$
	2)	$T_s = T_t + 1070$	$T_s = T_t + 570$	$T_s = T_t + 1040$	$T_s = T_t + 1060$	$T_s = T_t + 770$
Approximate Limits of Error (°C)	1)	± 75	± 80	± 85	± 95	± 95
	2)	± 95	± 100	± 105	± 115	± 115

[1] MgO substrate thickness and MgO thicknesses adjacent to coupon vary according to position. See also Tables 10 and 11 DRM-0681.

[2] Design total mass flow and seed/ash conditions.

[3] Two thermocouples are preferred in the event of surface erosion and/or corrosion. If only one be employed the first or primary thermcouple should be selected.

[4] *denotes the preferred type although availability may determine alternate choice since temperature ranges indicated for operation and responses are roughly equivalent. Criteria for selection include survivability, cost, response and availability.

[5] Homogeneous construction to facilitate calorimetric monitoring as described in DRM 0681.

[6] T_s denotes surface temperature, T_t denotes indicated thermocouple temperature.

TABLE 17

INSTRUMENTATION SPECIFICATIONS AND ANALYTICAL EXPRESSIONS FOR THE ON-LINE MONITORING OF COUPON SURFACE HEAT FLUX - WESTF TESTS 42 & 44[3]

Coupon Position	1	2	3	5	5
General Material Description	Hafnia Comp. A	Calorimetric coupon[2] Norton MgO	Hafnia Comp. A	Hafnia Comp. A	Hafnia Comp. B
Average Coupon Surface Heat Flux at Design Pt[1]	43.3	39.9	37.5	32.4	31.5
Analytical Expression for Coupon Average Surface Heat Flux Computation (W/cm²)[4] Method 1: $\left(\frac{q}{A}\right) = 29.194 \cdot K_1 \cdot \dot{m} \cdot (T_{outlet} - T_{inlet})$	$K_1 = 0.581$	$K_1 = 0.757$	$K_1 = 0.566$	$K_1 = 0.578$	$K_1 = 0.726$
Analytical Expression for Coupon Average Surface Heat Flux Computation (W/cm²) Method 2: $\left(\frac{q}{A}\right) = \left(\frac{q}{A}\right)_{\text{Position 2, Method 1}} \cdot K_2$	$K_2 = 1.10$	$K_2 = 1.00$	$K_2 = 0.954$	$K_2 = 0.824$	$K_2 = 0.802$
Approximate Limits of Error %	± 30	± 27	± 25	± 25	± 25

[1]Design total mass flow and seed/ash conditions. (0.075 - 0.073 kg/s).

[2]Homogeneous construction to facilitate calorimetric monitoring as described in DRM 0681.

[3]One common Type E in-line thermocouple for the inlet water supply will be sufficient if all coolant circuits are independently monitored and/or controlled, i.e., parallel configuration. [T_{inlet} (°C)].

[4]All electrode coupon holders are assumed to be connected in the parallel (independent) path configuration for cooling.

Notes: (applicable for all coupon designs above)

1. Design Coolant Mass Flow Rate (gph) - 75-95.
2. Thermocouple[3] Instrumentation and Location - TYPE E, in-line water exit. [(T_{outlet} (°C)]
3. Flow Meter - 1 In-line Water Rated at 2.2 gpm. [$\dot{m}$ (gpm)]
4. Variables Monitored & Corresponding Units - $\dot{m}$ (gpm), T_{inlet} (°C), T_{outlet} (°C).

42 for the "C" wall. Since the final "A" wall construction has been selected based upon and subsequent supporting analyses, the instrumentation specification for that wall has also been completed. This is presented in Table 18.

WESTF 44

WESTF Test 44 is to be an initial test of the channel design that is to be a prototype of the design to be developed for use with the 3 tesla magnet. Specific test objectives include the following:

1) Evaluate the ease of assembly and disassembly of the "mini"-WESTF.

2) Evaluate the performance of the mini-WESTF design under actual MHD operating conditions and

3) Evaluate the integrity and the performance of the electrode/leadout/attachment design in the MHD operating environment.

The general as-specified test conditions are presented in Table 19.

The general conceptual design as is illustrated in Figure 22, has been established to conservatively meet the general test objectives and the particular thermal, structural, and electrical objectives of WESTF 44.

The detailed design of the electrode walls for WESTF 44 will be completed during the next quarter. The design and analyses efforts associated with the transition sections and the electrical/insulating wall sections will also be undertaken during the next quarter. Subsequent efforts in the following quarter will include the development of algorithms for the on-line monitoring of surface heat flux and surface temperatures of the respective electrode assembly components.

2.1.3 Post-Test Analysis

WESTF Test 41 - Run 2

Results of the post-test analysis of WESTF Test 41 - Run 2 are presented in the following secitons and include electrode wall/transition section/insulating

TABLE 18

INSTRUMENTATION SPECIFICATION FOR THE WESTF 42 "A" WALL COUPON ELECTRODE COMPONENTS

Coupon Location	A1	A2	A3	A4	A5	A6
Design Surface Temperature	1600-1650	1650-1700	1700-1750	1750-1800	1800-1850	1850-1900
Materials Identification[1]	YZ-WE0101/ YZ-WE0102	ZC-WE0101/ ZC-WE0102	YZ-WE0101/ YZ-WE0102	ZC-WE0102/ ZC-WE0102	YZ-WE0102/ YZ-WE0102	HO-BN0401 (D3,D4,D5)
Material Thickness[2],in. Coupon	0.230	0.200	0.265	0.300	0.270	0.300
MgO Substrate Thickness	0.050	0.000	0.100	0.100	0.050	0.950
Centerline Location of Imbedded Thermocouple Bead (Depth) Perpendicular to Plasma Flow Direction	0.16-0.20" (4.06-5.08 mm)	0.15-0.16" (3.81-4.06 mm)	0.16-0.20" (4.06-5.08 mm)	0.16-0.20" (4.06-5.08 mm)	0.16-0.20" (4.06-5.08 mm)	0.16-0.20" (4.06-5.08 mm)

Footnotes:

[1] YZ-WE0101/YZ-WE0102 = 12 Y_2O_3 - 88ZrO_2

ZC-WE0101/ZC-WE0102 = 15 $(Mg_{0.625}Ca_{0.375})$ - 85ZrO_2

HO-BN0401 = $Er_{0.82}Hf_{0.18}O_2$

HO-BN0302 = $Pr_{0.27}Yb_{0.09}Hf_{0.64}O_2$

HO-BN0102 = $Tb_{0.20}Y_{0.10}Hf_{0.70}O_2$

All are designated Batelle Sample Numbers

[2] At a design plasma or total combustion products flow rate of 0.073-0.075 kg/s and with a coupon construction including 0.10 inch of nickel mesh interface (thermal compliant layer) material.

Notes:

1. Thermocouple Type and Function - B or R/Indicated Ceramic Temperature.
2. Purpose - Surface Temperature Extrapolation
3. Thermocouple Configuration - Radial Mode Parallel to Electrode Hot Surface

TABLE 19

GENERAL CONDITIONS FOR WESTF TEST 44

Operating Mode	Super Hot
Plasma Temperature, K	2600-2700
Electrode Surface Temerature, K (°C)	2023 (1750) ± 100
Electrode/Leadout Interface Temperature, K (°C)	1523 (1250) ± 100
Leadout/Attachment Interface Temperature, K (°C)	<773 (<500)
Interelectrode Insulator Surface Temperature, K (°C)	1923 (1650) max 1723 (1450) min
Insulating Wall Surface Temperature, K (°C)	1923 (1650) max 1723 (1450) min
Sulfur (m/o SO_2)	0.3
Expected Heat Flux (W/cm^2)	~60
Current Density (A/cm^2)	To 1.25
Axial Field, kv/m	None
Duration, hrs	~20
Fuel Type	No. 2 Oil
Ash/Seed Slurry	Rosebud/K_2CO_3

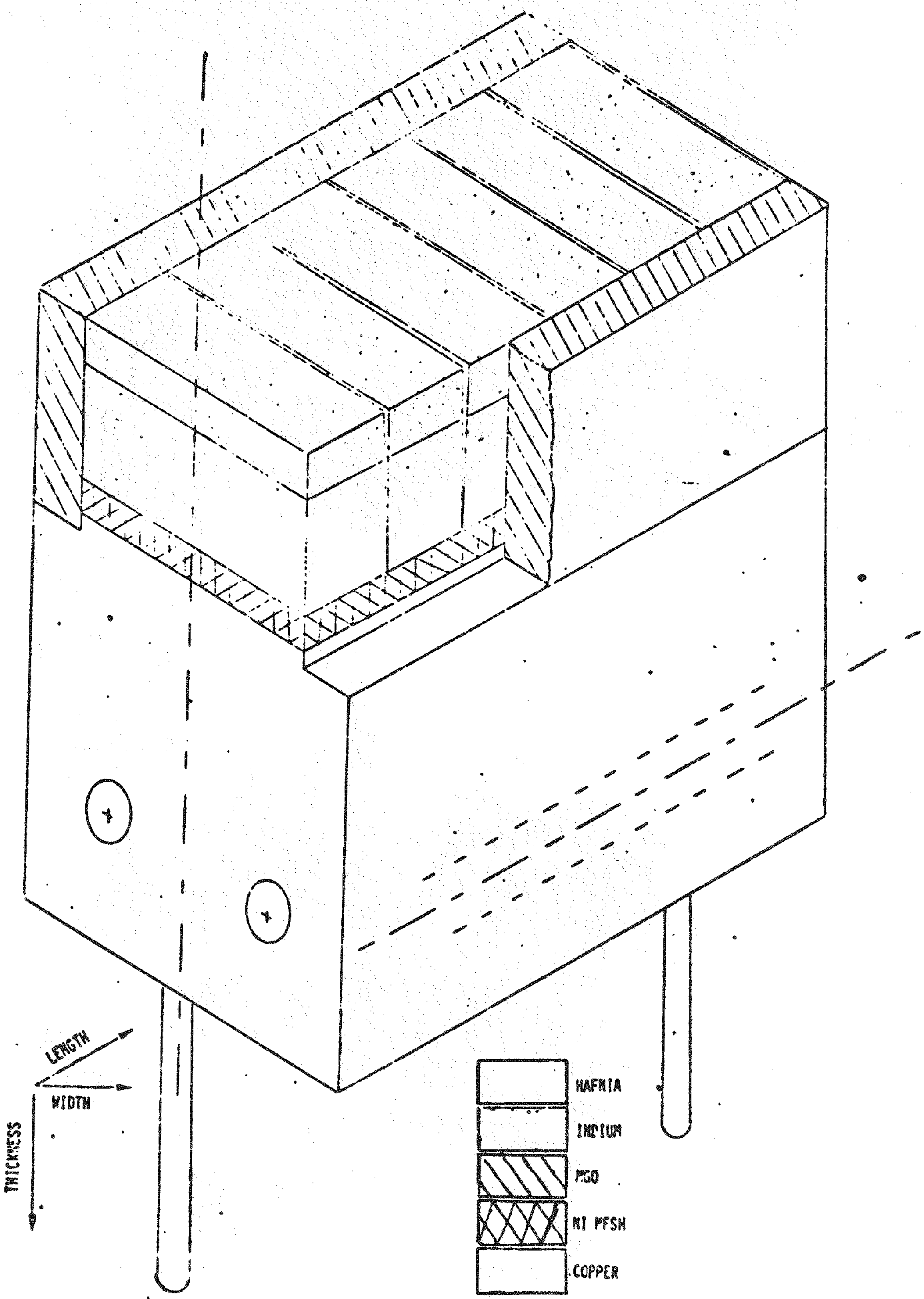

Figure 22. WESTF Test 44 Design Schematic

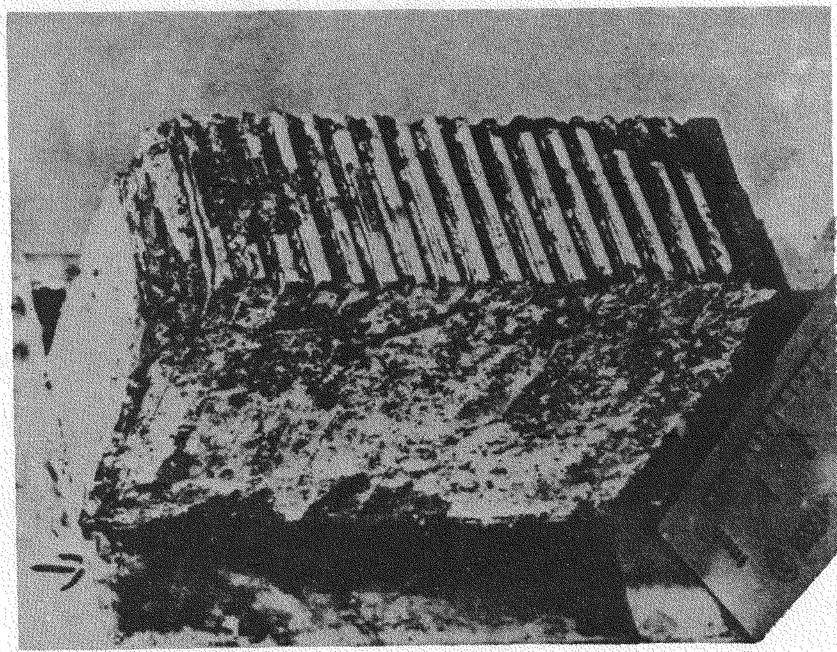

→ FLOW DIRECTION

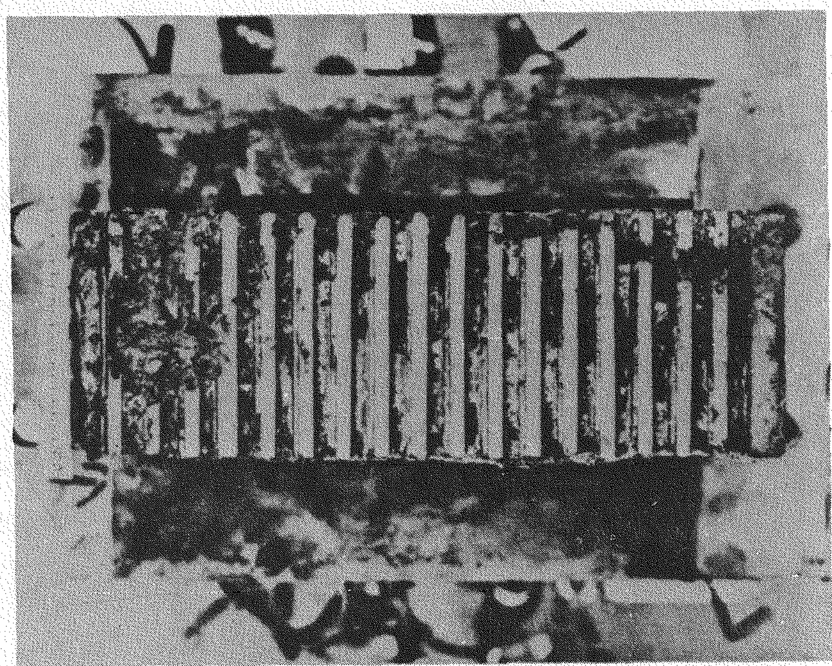

Figure 23. WESTF Test 41-Run 2 - Anode Wall, Post-Test

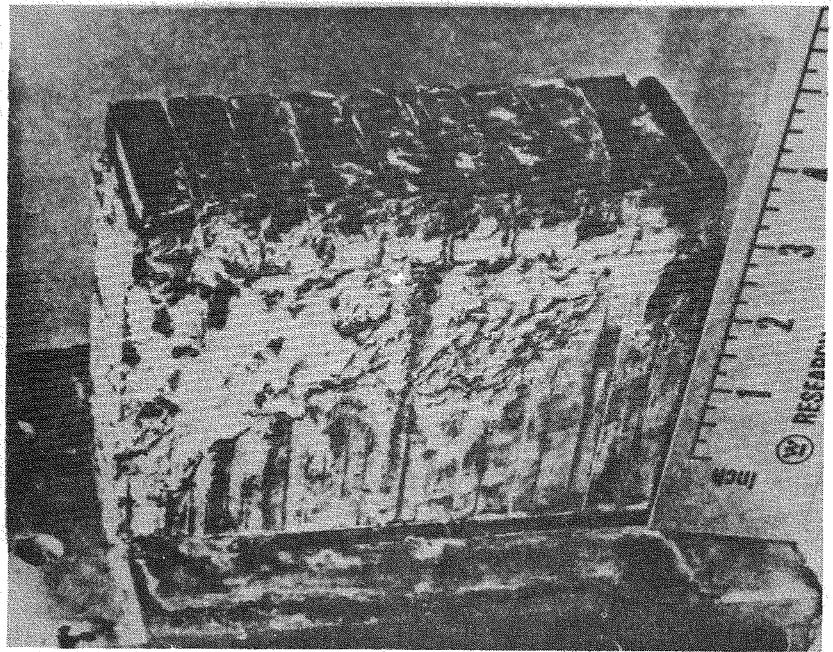

→ FLOW DIRECTION

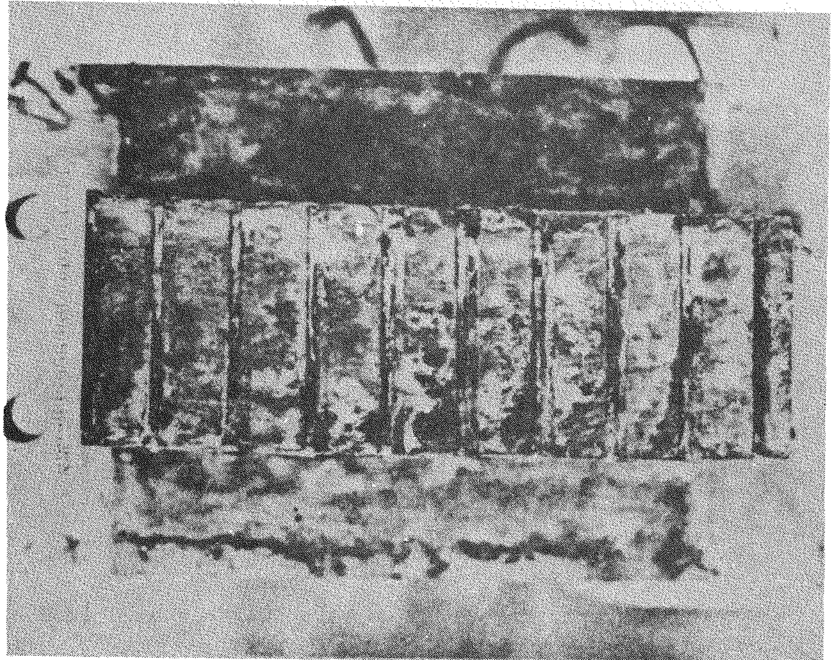

Figure 24. WESTF Test 41-Run 2 Cathode Wall, Post-Test

wall materials evaluations as well as electrical anlayses. The chronology and pertinent facility data are summarized in Section 2.3.2.

Following discussions with AVCO personnel, a portion of the upstream anode wall will be forwarded to Battelle PNL for detailed post-test characterization studies Results of this effort will be reported when completed. The balance of the electrode walls will be retained so that they may be included in a subsequent test if desirable. No firm plans have been established at this time to use the residual electrode wall elements in a subsequent WESTF test.

Electrode Walls

The data reduction and thermal analyses efforts associated with WESTF Test 41 - Run 2 have been completed. Electrode channel heat fluxes during steady state facility operation at the design point ranged from 75-175 w/cm^2 with the anode wall electrode components exhibiting slightly higher heat fluxes than the corresponding cathode wall electrode components. Surface temperature extrapolations of the indicated bulk material thermocouple measurements range from 100-275°C. The nominal test predictions for the above parameters were 125 w/cm^2 and 150°C for the electrode wall heat flux and the mean electrode surface temperature respectively. The channel thermal environment objectives for the testing series were therefore, successfully met.

The general condition of the anode and cathode walls after WESTF Test 41 (~55 power hours) was judged to be very good to excellent. Figures 23 and 24 generally show the relative post-test condition of both electrode walls. The exception to the favorable condition of electrodes was the first anode which had lost its protective platinum cap and had been severly eroded or corroded by the impinging hot plasma to the point that copper had been eroded away and ultimately breached the water cooling passage. As previously reported, this water leak was the cause for shutdown of the test. This situation had been created by the severe erosion of the Harklase magnesia refractories in the inlet transition section (see subsequent discussions). Erosion of the first cathode by the hot plasma, on the other hand, was very slight - although there was much more severe thermal degradation of the G-10 spacers under the copper cathodes. These features point to the powerful effect of cathodic conditions in preventing oxidation and erosion of copper based electrodes while anodic conditions promote these reactions. It should also be noted that the copper spacer on the downstream end of the cathode wall which was electrically floating and passing no current shows significant oxidation and wear.

Although the anode wall is generally in very good condition, there has been significant degradation of various materials. Table 20 summarizes post-test observations. First the .062 deep grooves in the copper have been enlarged considerably. In two anodes (#10 and #18) the increase in depth exceeded 40 mils. The feature is similar to that observed in the AVCO Mark VI 250 hour test. Figure 25 makes a comparison of the condition of anodes after Test 41 and the AVCO test. This degradation has been ascribed to electrochemical corrosion by electrolytic slag. Calculation of erosion rates in WESTF Test 41 for various electrodes is estimated to be between 3 and 20 μg/coulomb. This assumes uniform current distribution across the electrode and compares with 41 μg/coulomb for WESTF Test 40 and 8 μg/coulomb for an AVCO Mark VI test. Comparisons were made between the ampere-hours of loading for individual anodes and copper recession depths (see Table 20). No correlation could be made between copper recession depth and any electrical parameter.

A second degradation feature on the anode wall was recession of the boron nitride insulator. Most of the loss in insulator material is most probably associated with the wearing away of the coppor around the groove. However, in several anodes, large pieces of insulator appear to have been lost due to thermal fracture. Since BN does have a relatively high resistance to thermal shock, it is most probable that loss of this material was due to large electric arcs - either from axial interelectrode breakdown early in the test or from transverse plasma to electrode arcs.

The third degradation feature noted on the anode wall was arc tracks and even localized melting of platinum near the upstream corner. Anodes 9 and 11 demonstrated the most severe damage of this type. This type of degradation is similar to that observed in the AVCO Mark VI 250 hour test. Arcing, as evidenced by localized melting of platinum, was also observed on edges adjacent to the insulating walls.

TABLE 20

VISUAL OBSERVATIONS OF ANODE WALL,
WESTF TEST 41-RUN 2

Anode #	Ampere Hours	Electrode Groove Recession (mils)	Insulator Recession (mils)	Remarks
1				Platinum Cap Gone, Badly Eroded
2-4		Could Not Be Determined		Slag Covered
5	74	10-18	75-86	Slight Arc Damage to Pt
6	76	22-24	43-54	Moderate Arc Damage to Pt
7	112	0-8	12-28	Slight Arc Damage to Pt
8	68	10-15	20-30	Very Slight Arc Damage to Pt
9	123	7-17	3-24	Severe Arc Damage to Pt
10	117	18-43	38-58	Moderate Insulator Thermal Fracture
11	118	18-30	18-38	Severe Arc Damage to Pt Moderate Insulator Thermal Fracture
12	120	20-23	42-47	Slight Arc Damage to Pt Slight Insulator Thermal Fracture
13	121	2-11	4-8	Very Good Condition
14	119	2-9	18	Very Good Condition
15	38	0-11	26-36	Moderate Insulator Thermal Fracture
16	36	19-27	60-65	Moderate Insulator Thermal Fracture
17	116	10-15	40-60	Slight Insulator Thermal Fracture
18		18-48	110-170	Severe Insulator Thermal Fracture

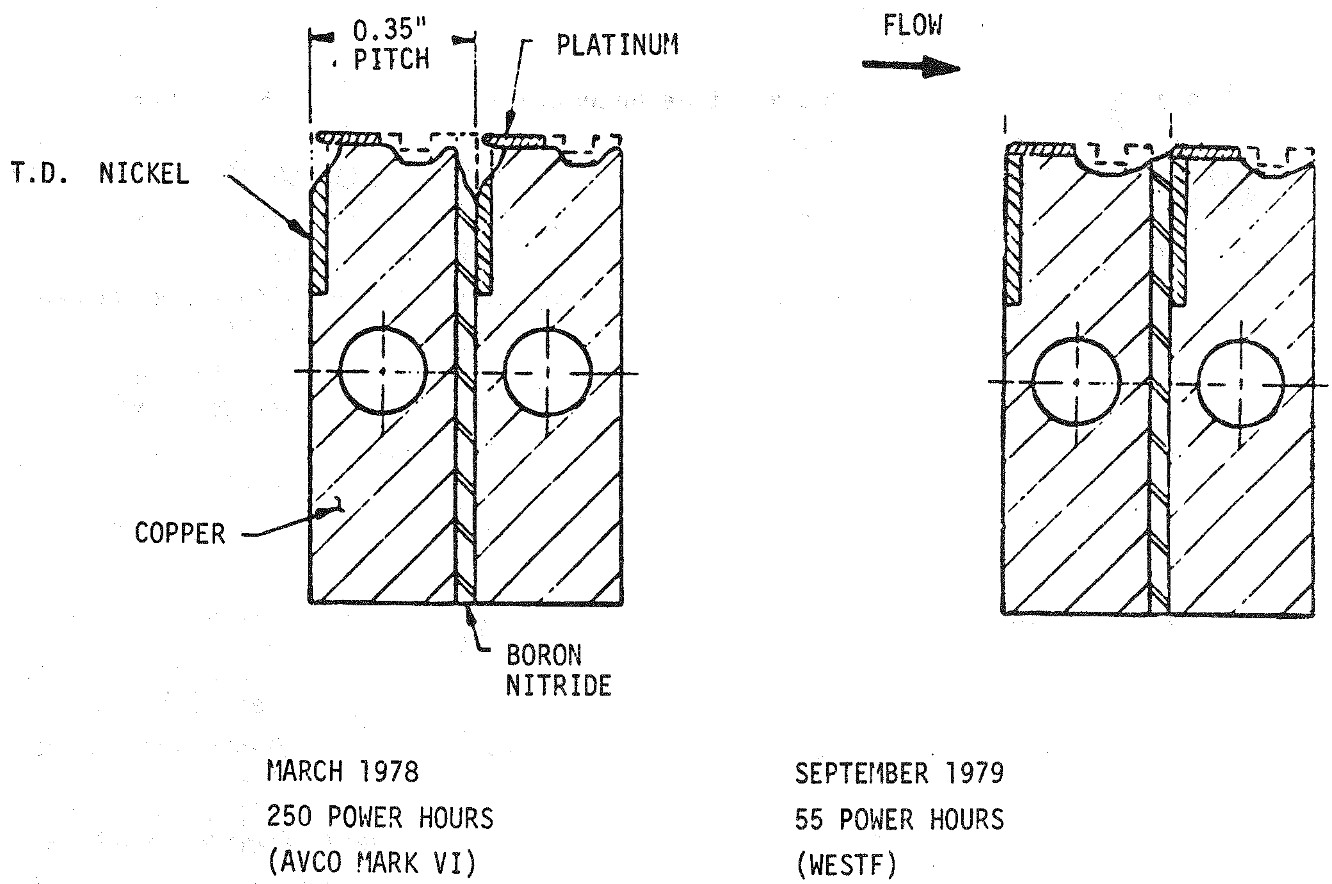

Figure 25. Mark VI Anodes - Comparison of Erosion after Tests in Mark VI and WESTF Facilities

In general, the degradation observed after WESTF Test 41 was similar to that of the AVCO Mark VI 250 hour test, see Figure 25. However, there was one notable degradation feature of the AVCO test that was not observed; i.e., the electro-chemical corrosion of anodic upstream surfaces, particularly the TD nickel. Since the strong axial fields present in the Mark VI could not be established during this test, it is reasonable that this type of degradation was not observed.

In summary, WESTF Test 41 closely simulated the degradation experienced in the Mark VI that was related to transverse fields and currents, but it did not simulate that damage which was due to axial fields and currents.

The damage to cathodes was minimal and they appeared in excellent condition after the test. Since axial fields had not been imposed during Test 41 and since the major degradation in the Mark VI was shown to be electro-chemical anodic corrosion resulting from axial fields, it again is reasonable that since these fields and currents were not simulated in WESTF Test 41 this damage was not observed. While the cathodes themselves were virtually untouched, there was some damage (or loss) of inter-electrode BN insulators.

Transition Sections

Following the completion of WESTF Test 41 - Run 2 (AVCO cold wall electrodes), data reduction and thermal analysis efforts were completed to assess the performance of the inlet transition section. The inlet transition section had been subjected to a significant degree of insulating tile erosion and corrosion. The post test condition of the transition section has been attributed to the thermal loading and the minimal slag resistance of the Harklase magnesia to the eastern (Bow New Hampshire) flyash/seed slurry at high temperatures. Transition section surface heat fluxes and surface temperatures based upon the calorimetric (test) measurements were computed to be 52-111 w/cm^2 and well in excess of 2000°C respectively. An exact determination of surface temperature was difficult due to the progressive loss of surface material which was not necessarily reflected in the Kaye channel instrument printouts of the temperature-time and the heat flow-time characteristics.

The higher than anticipated thermal loading, in turn, has been partially attributed to the original design procedure used which was based on frozen plasma property extrapolations to compute the bulk gas to electrode surface heat transfer. Concurrent analysis of the U.S.-U.S.S.R. U-02 Phase III test data and the Phase III WESTF proof test data had indicated that the use of equilibrium properties for the computation of the gas side heat transfer coefficient was more appropriate. In order to prevent overtemperaturing of that portion of the WESTF test section that is subjected to the highest heat loading, i.e., the inlet transition section, a conservative design must be based upon the maximum anticipated gas-surface heat transfer coefficient. Material dimensions established in this manner would ensure that the maximum service ceiling temperature requirements for a particular class of materials will not be exceeded. Design of the outlet transition section, which is a configuration identical to the inlet transition section, would be assured of a lower maximum operating temperature than the inlet section owing to the gas enthalpy extraction.

The inlet transition section lining of Harklase MgO was severely eroded/corroded by the slag during the test. On the upstream end, the sidewall linings were greatly reduced in thickness and within the first 1.5 inches tapered down to the bare copper walls. Top and bottom walls, however, were eroded, but intact. This is, apparently, due to the flow and temperature profiles within the channel and the fact that the inlet transition section wall materials ran hotter than predicted.

Figure 26 shows photographs of samples taken from the inlet transition section approximately 1.5 in. in from the inlet end. The thickness differences are clearly seen in this figure. Microscopic examination of these samples showed that slag had completely penetrated the material to the extent that each grain was completely surrounded by slag.

Figure 27 shows photographs of samples taken from the supstream end of the exit transition section. Material loss is much less here than it was on the inlet

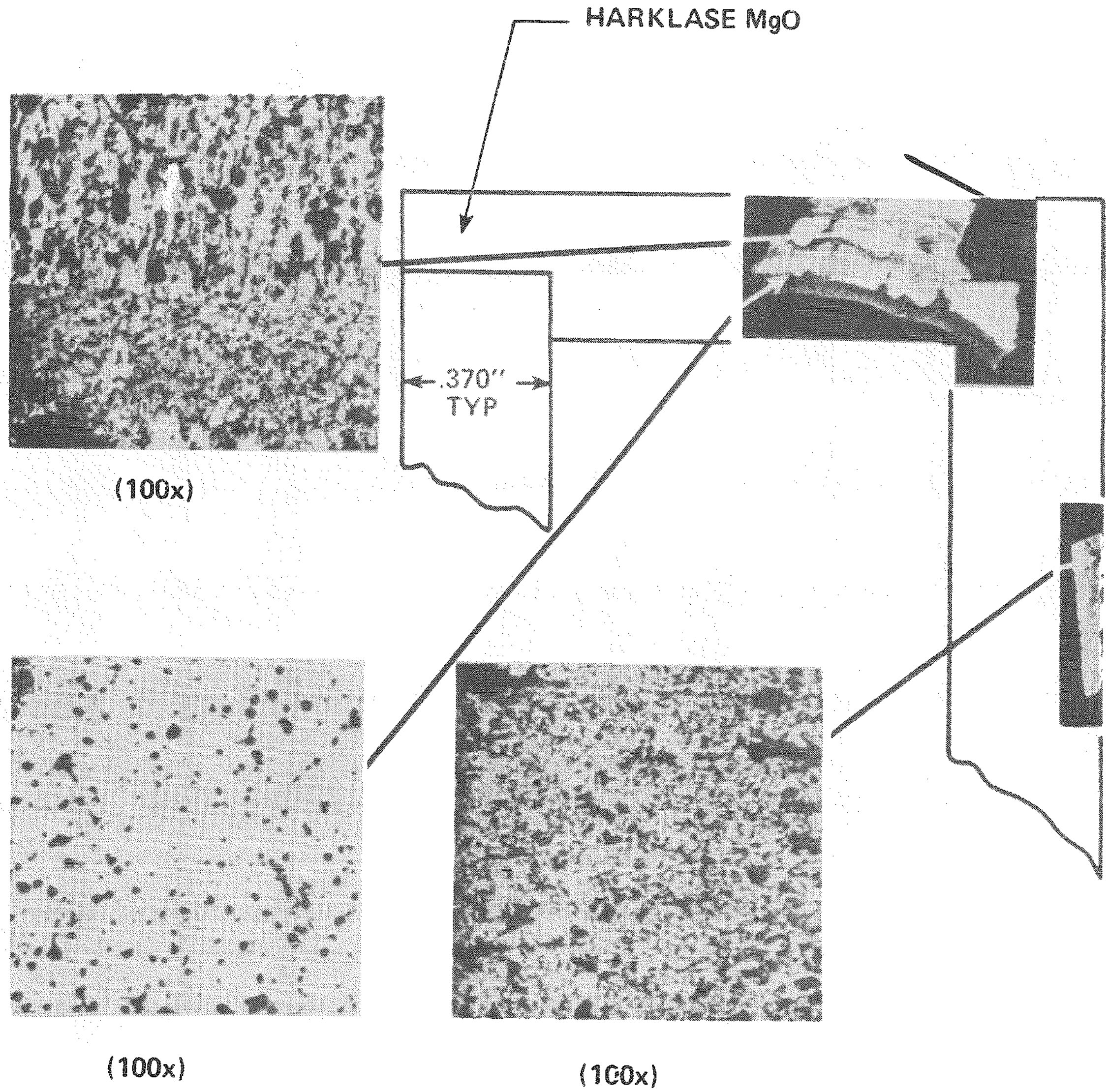

Figure 26. Downstream 1.5 Inch from WESTF Test 41-2 Inlet Transition Section Comparing Thickness Difference Pre-and Post-Test and Top and Side Wall

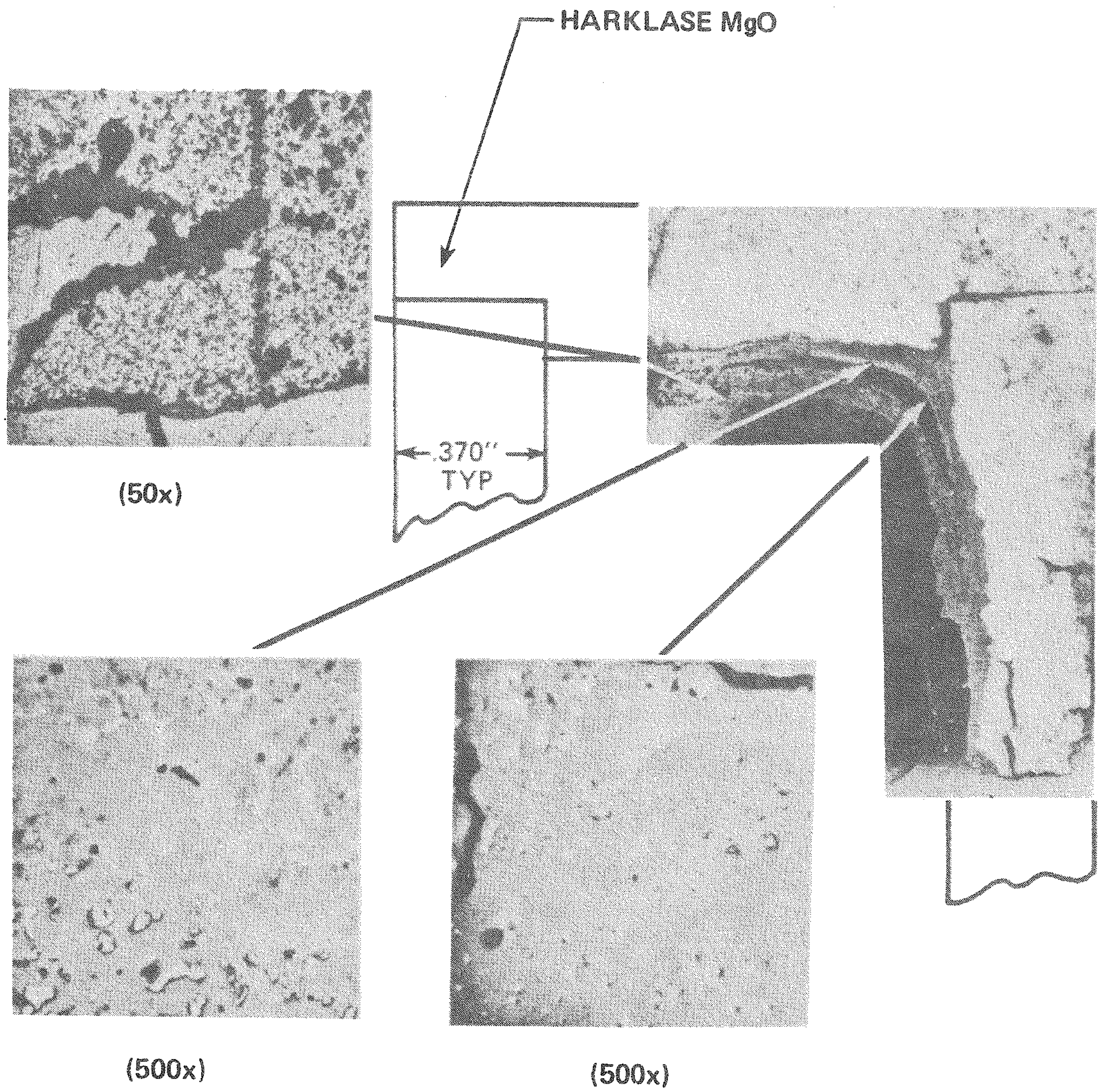

Figure 27. Upstream End of WESTF Test 41-2 Exit Transition Section Comparing Pre-and Post-Test Thickness of Ceramic Lining

section and is probably indicative of the drop in plasma temperature as it passed through the cold wall channel. Microscopic examination of the slag layer at this location showed a large population of metal globules. The metal is presumed to be iron produced by the electro-chemical reduction of the slag. This will be confirmed by further analysis.

Insulating Walls

As was the case for the inlet transition section, considerable slag erosion/corrosion damage of the insulating walls resulted from the high temperature conditions encountered in WESTF Test 41-Run 2. For the top insulating wall, no definitive statements can be made since this structure was severely damaged and essentially destroyed during disassembly of the test section. The bottom insulating wall was very heavily eroded/corroded. The material loss was approximately one-half of the thickness at the upstream end and tapered to a region of minimal loss at the downstream end.

Electrical Analysis

WESTF Test 41-Run 2 was completed during August, 1979. The top and bottom insulating walls of the channel used in this run were modified for this test as discussed in the prior quarterly report and shown in Figure 28. This change in design was made to improve the ability of the channel to withstand axial electric fields and at the same time improve the insulation between the cathode and anode electrodes. The 18 anode and 9 cathode channel was electrically connected as shown in Figure 29. The circuit used 15 of the 16 available power supplied, permitting the remaining power supply to be used for impressing axial electric fields during the early part of the test. As indicated in the circuit diagram, anode electrodes A1 and A2, and cathode electrode C9 were allowed to float electrically. The potentials and currents were recorded automatically by the Data Acquisition System.

Seed was first injected into the system in Test 41-Run 2 at 0135 on August 7, 1979. A characteristic voltage vs electrode-pair curve of the channel taken

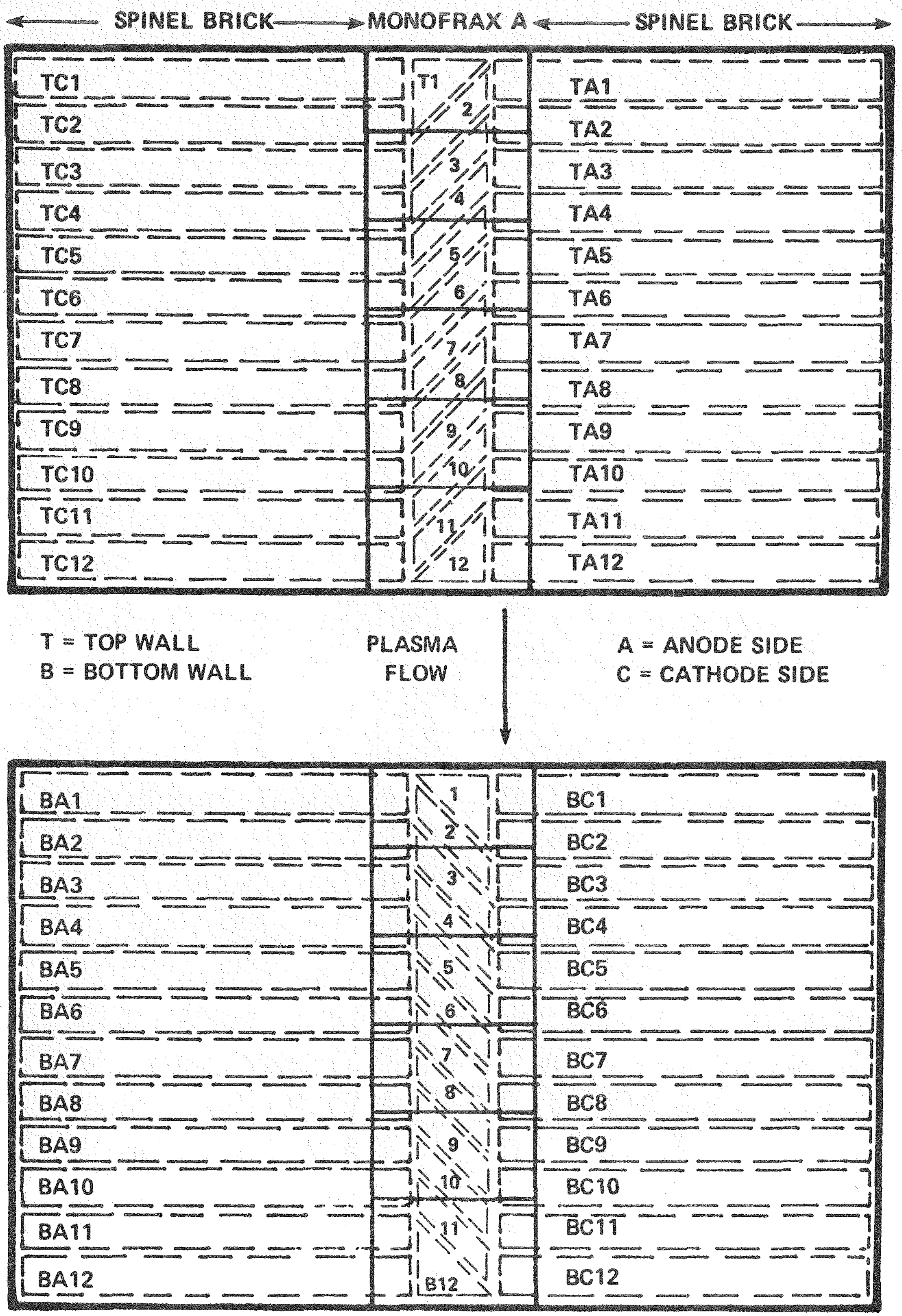

Figure 28. Schematic of Insulating Walls WESTF 41 - Run 2

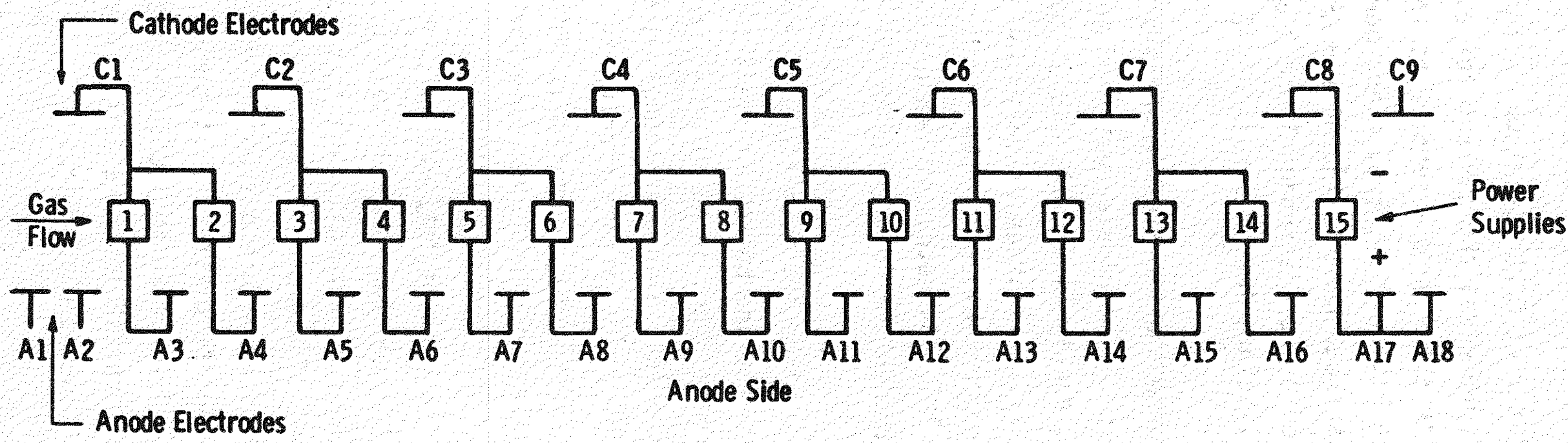

Figure 29. Electrical Circuit Used for WESTF Test 41 - Run 2

three quarters of an hour later at 0220, is shown in the top curve of Figure 30. The middle curve of this figure gives the current for each electrode-pair. The electrode-pairs are listed in the figure according to the anode number of the electrode-pair as defined in Figure 29. Thus, electrode-pairs C_1A_3, C_1A_4 and C_2A_5 are associated with electrode numbers A3, A4 and A5, respectively, in Figure 30. The potentials of anode electrodes 1 and 2 and cathode electrode 9 correspond to the Abscissa listings for electrodes 1, 2 and 19-20, respectively.

Provisions were made to measure the floating potentials of all of the water-cooled support blocks mounted in the middle region of the top and bottom insulating walls of the channel, namely T1 to T12, and B1 to B12, see Figure 28. Due to limitations in the available number of measuring circuits only the potentials of the even-numbered support blocks in the top insulating walls were measured; namely, TA2, TC2, TA4, TC4, etc. No measurements were made at the corresponding locations of the bottom insulating walls.

The bottom curve of Figure 30 gives the potentials of the water-cooled insulated support blocks mounted in the top and bottom insulating walls of the channel which were selected as described above. As can be observed in the figure, there are 12 insulating blocks along the length of the channel as compared with, for example, the 18 anode electrodes and 9 cathode electrodes. The potential profile of the cathode and anode electrodes are superimposed onto the curves giving the potentials of the insulating support blocks for reference purposes.

From the absence of significant current in Figure 30, it is evident that the three quarter hour interval between the start of seed injection and the time the data was taken was not long enough to permit deposition of a slag layer thick enough for voltage "breakdown" of the slag layer to occur. Apparently, arcing across this slag layer is required before a transfer of charges can take place between the cold electrodes and the plasma. This theses is confirmed by amperes vs volts measurements described later which indicate that the applied voltage must be greater than a minimum threshold value before current conduction can take place between cathode and anode electrodes.

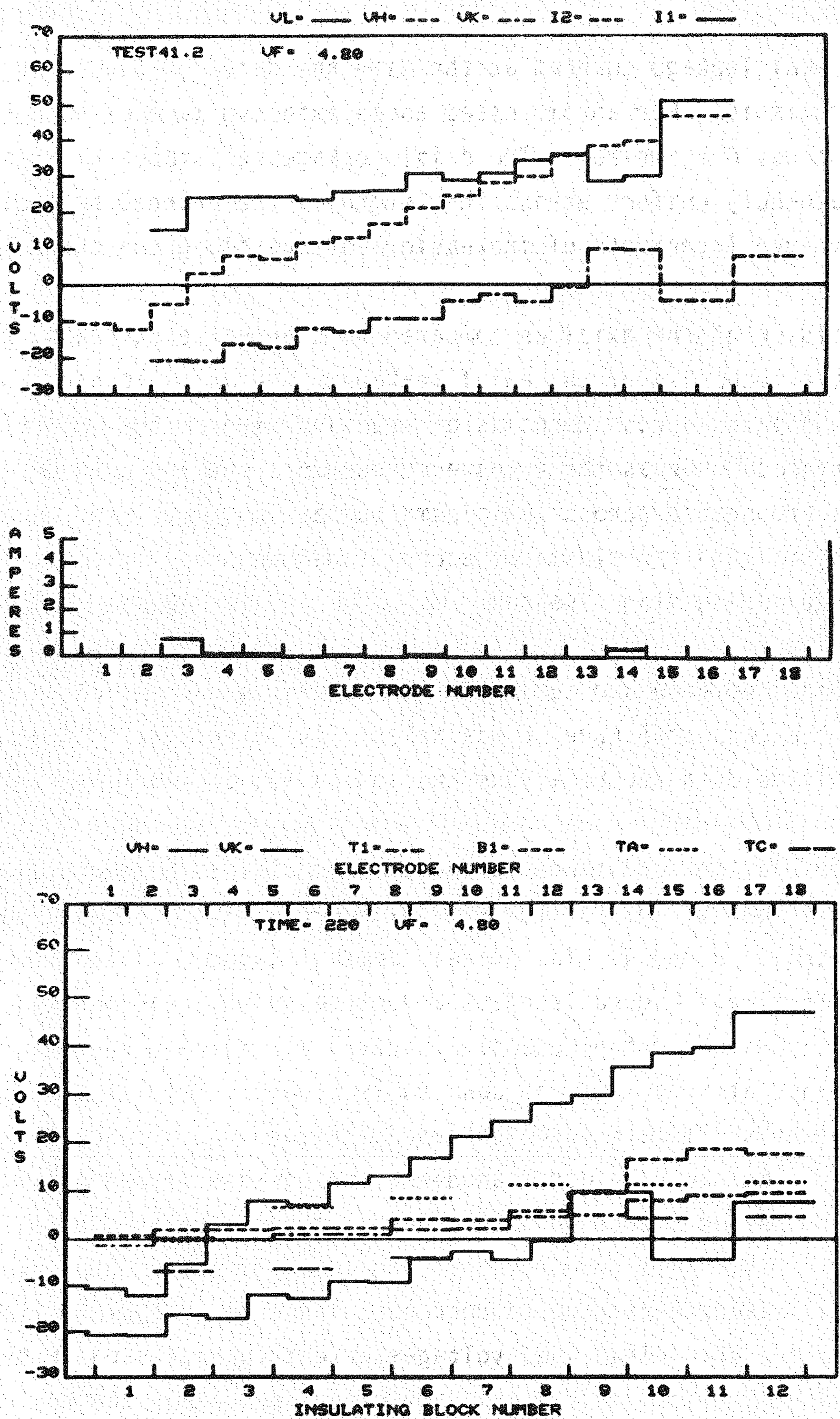

Figure 30. Applied Electrode Voltages, Currents and Floating Potentials of Insulating Wall Heat Sinks, WESTF Test 41-2, Anode Axial Voltage 48.8V, Approximately 0.7 Amperes, 8/7/79

However, the axial leakage current at the time the data for Figure 30 were taken was appreciable. For an impressed anode axial voltage of 48.8 volts, the leakage current was 0.7 amperes. The axial leakage resistance at this time was apparently reasonably uniform across the length of the channel as indicated by the relatively even increments of increasing voltage along the channel.

The faster build-up of the axial as compared to transverse currents, probably results from the mechanism of the axial leakage. The axial leakage apparently occurs by way of paths across deposits of seed and slag on the interelectrode insulating surfaces, whereas the transverse currents between cathode and anode electrodes are propagated across the plasma but are not initiated until proper electrical contact with the plasma is accomplished by means of electrical breakdown of the intervening slag layers.

Figure 31 provides voltage and current profiles of the channel taken some 40 minutes after the data of Figure 30 was taken. It is evident that most of the anode axial voltage drop occurs across the insulation between anodes 3 and 4.

The total anode leakage resistance decreased from 69.4 to 59.5 ohms during this time interval. Clearly, most of the axial leakage resistance occurred between anode and electrodes 3 and 4. The overall anode leakage resistance continued to decrease with time. Figure 32 gives a voltage and current profile taken at 0340, some 1.7 hours after the data of Figure 31 was taken. The overall anode leakage resistance at this time was down to 29.5 ohms. From Figure 32, the leakage resistance was still mainly concentrated between anodes 3 and 4. The electrical resistance between the other anodes of the channel apparently was very low compared to the resistance between anodes 3 and 4.

The anode axial leakage continued to decrease with time; at 0425, it was down to the order of one ohm. The axial voltages were then impressed on the cathode side of the channel. The same pattern of increasing leakage current with time was repeated. The initially relatively high value of leakage resistance gradually decreased with time.

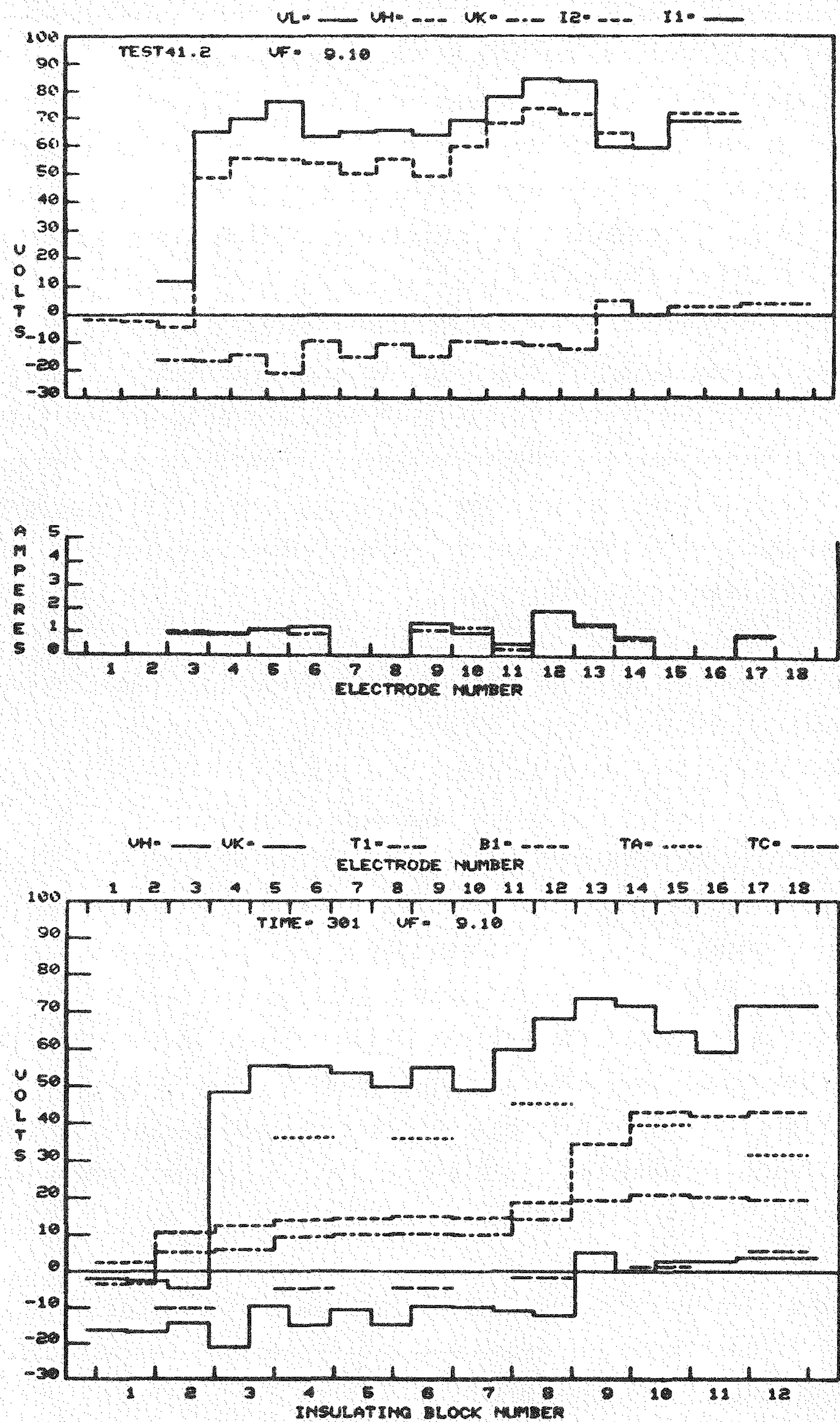

Figure 31. Applied Electrode Voltages, Currents and Floating Potentials of Insulating Wall Heat Sinks, WESTF Test 41-2, Anode Axial Voltage 71.4V, 1.2 Amperes, 8/7/79

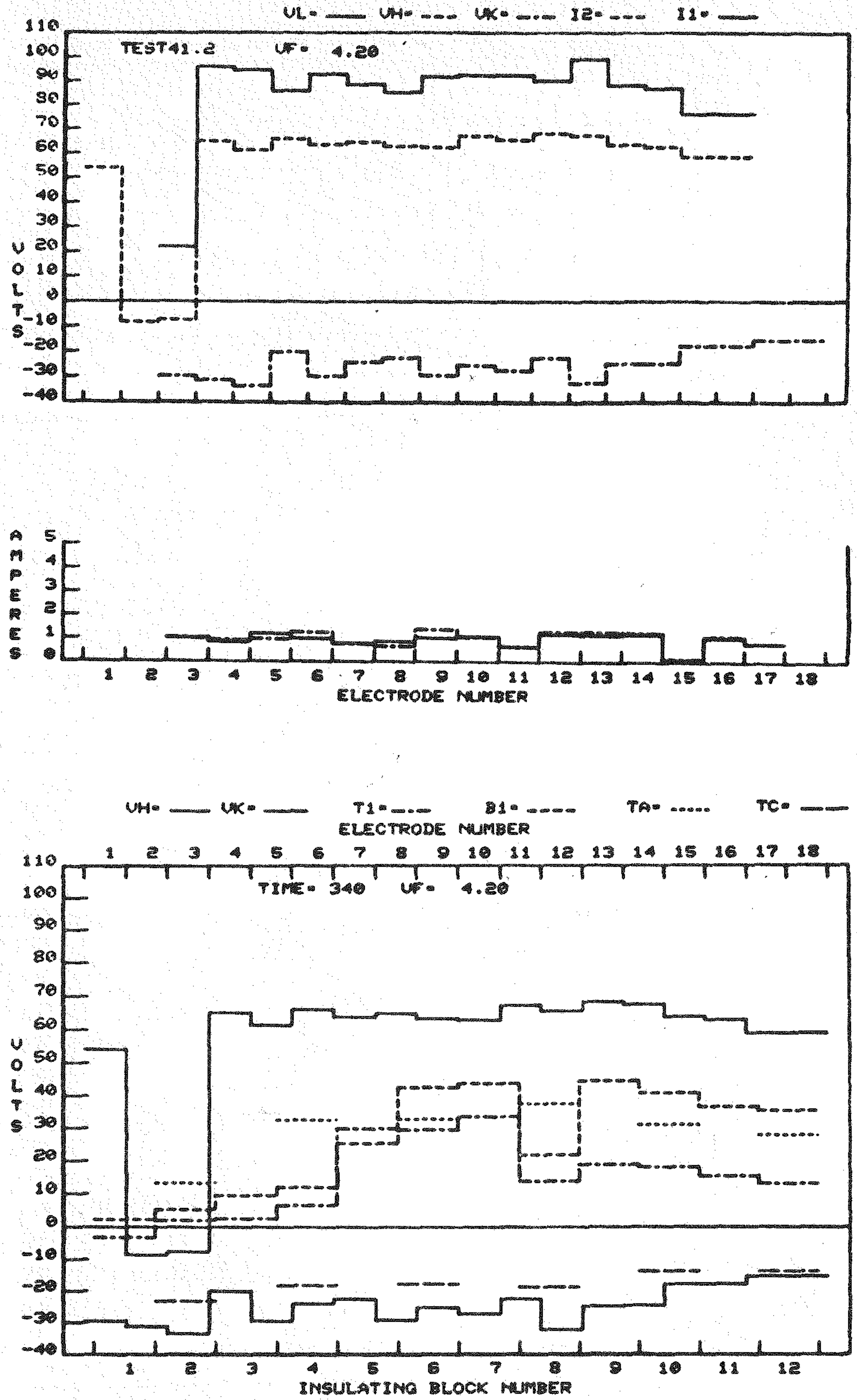

Figure 32. Applied Electrode Voltages, Currents and Floating Potentials of Insulating Wall Heat Sinks, WESTF Test 41-2, Anode Axial Voltage 70.9V, 2.4 Amperes, 8/7/79

Figure 33 gives the voltage and current profile along the length of the channel at 0500. The total cathode leakage resistance was 28.1 ohms during this time. The use of axial voltage was discontinued after an additional hour of operation. During this period of time, the cathode axial leakage resistance fluctuated from 1 ohm to 18 ohms. As in the case of the anode axial field, the voltage tended to build up across one particular interelectrode insulating section of the channel. As can be seen in Figure 33 for cathode axial fields, the segment having relatively high leakage resistance was between cathode electrodes 8 and 9.

Figures 34, 35, and 36 are representative curves giving channel potentials and current as a function of time for the duration of the time voltage was impressed on the electrodes during WESTF Test 41-Run 2. Expect for a short time at the beginning of the test, the power supplies were adjusted to operate in the constant current modes. Thus, the potential across given electrode pairs varied as the properties of the plasma and the electrode-plasma interface changed.

The current in the channel was brought up to 4 amperes by 0630 and the current kept at this level, test conditions permitting, for the remainder of the test. Operation at 4 amperes corresponds to a loading of 0.9 amperes/cm^2 if the exposed anode and insulator surface is defined as the anode area and a loading of 1.0 amperes/cm^2 if the anode surface exposed to the plasma is considered to be the anode area only.

WESTF Test 41-Run 2 was characterized by a substantial variation in the voltage required to maintain the current requirements which apparently was due to a fluctuation in the rate of injection of seed.

While the voltage required to impress the 4 ampere loading required was generally between 50 and 100 volts, on occasions of low seed flow or when the seed feed lines were clogged, impressed voltages as high as 240 volts were observed. At other time intervals, apparently when the flow of seed was excessive, extremely low cathode-anode drops were observed. As a result of difficulties noted during this run with fluctuations in seed flow, an improved method of measuring and maintaining seed flow will be put into effect.

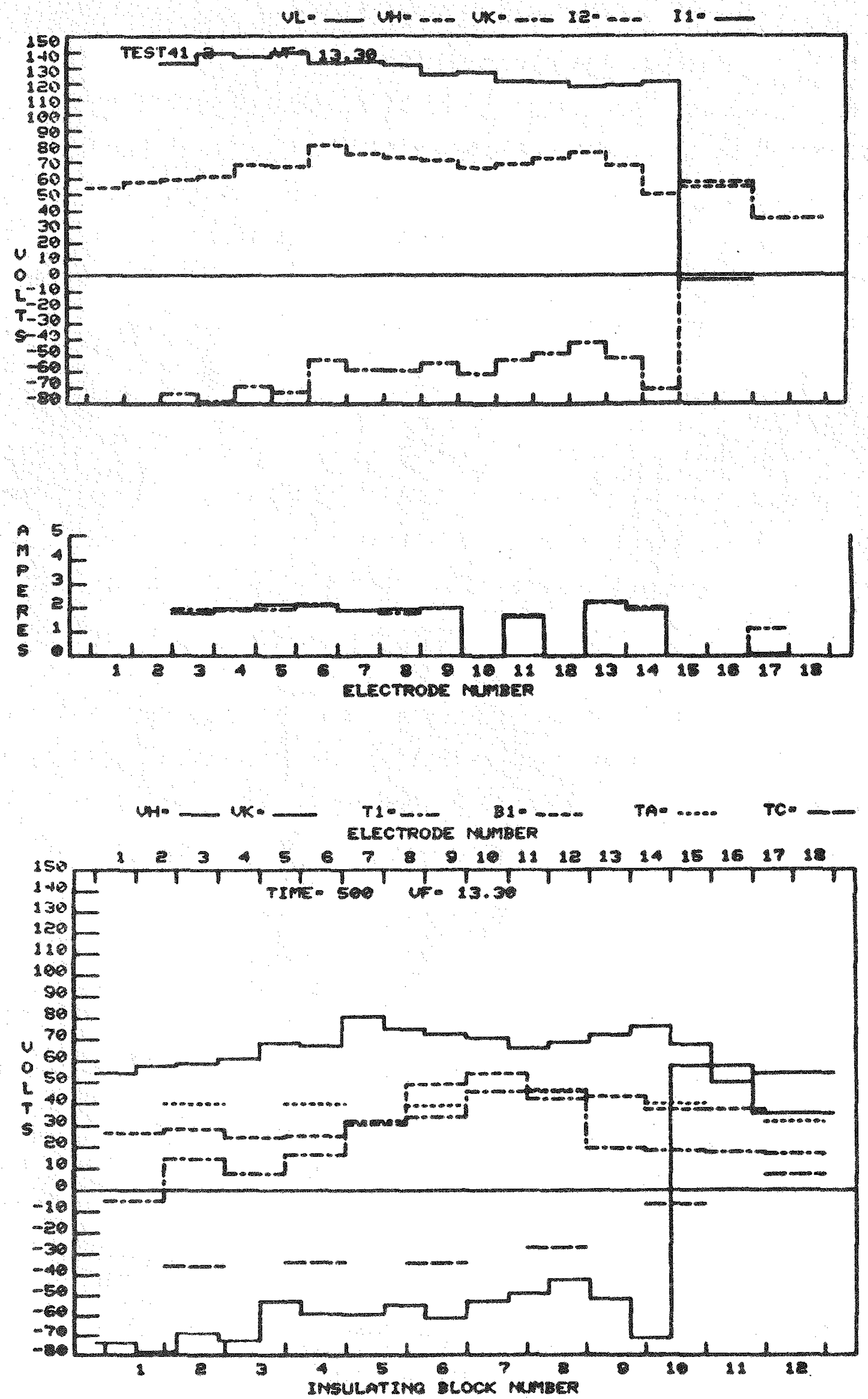

Figure 33. Applied Electrode Voltages, Currents and Floating Potentials of Insulating Wall Heat Sinks, WESTF Test 41-2, Cathode Axial Voltage 137.9V, 4.9 Amperes, 8/7/79

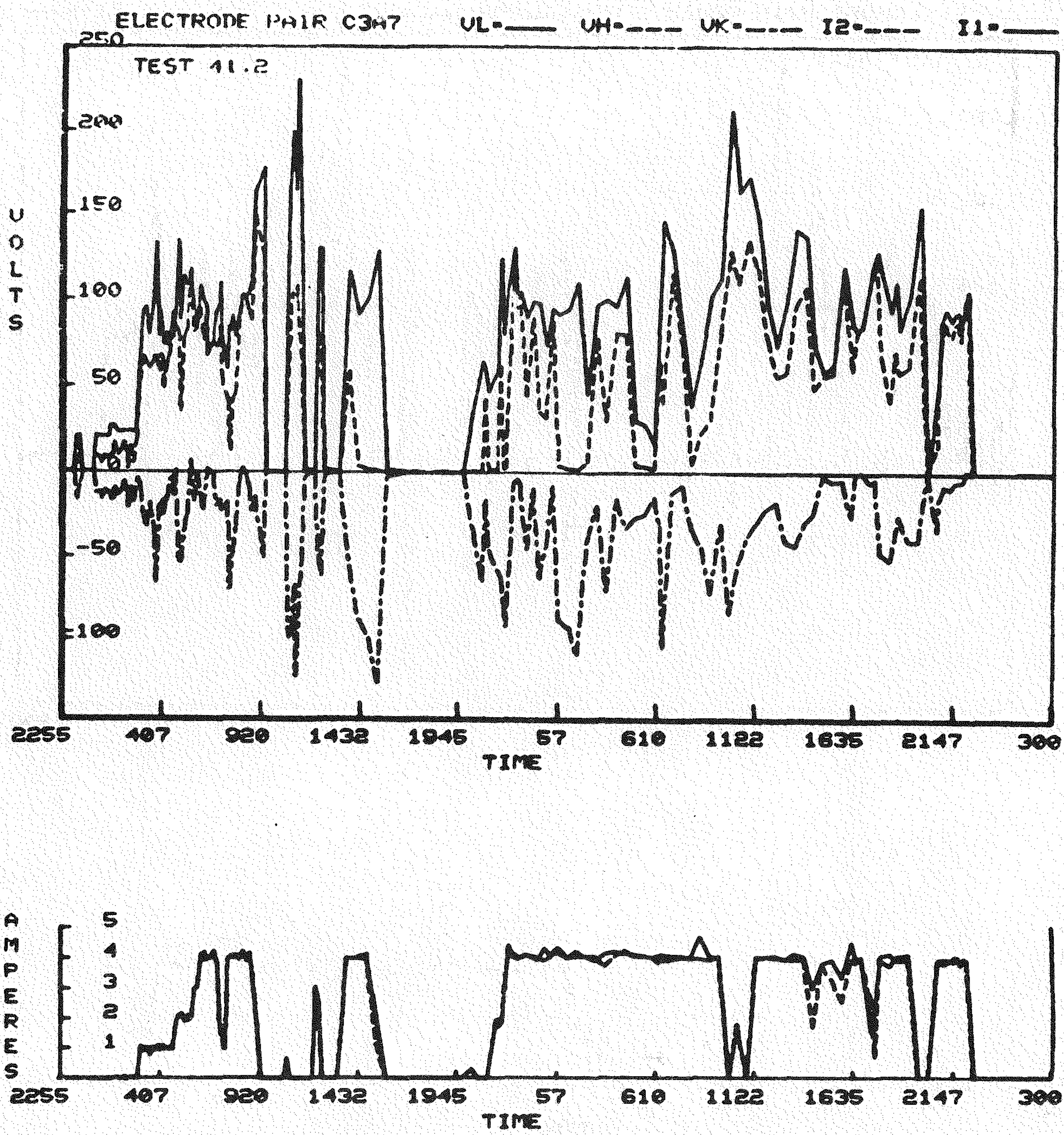

Figure 34. Impressed Voltage and Current, WESTF Test 41-2, 8/8/79

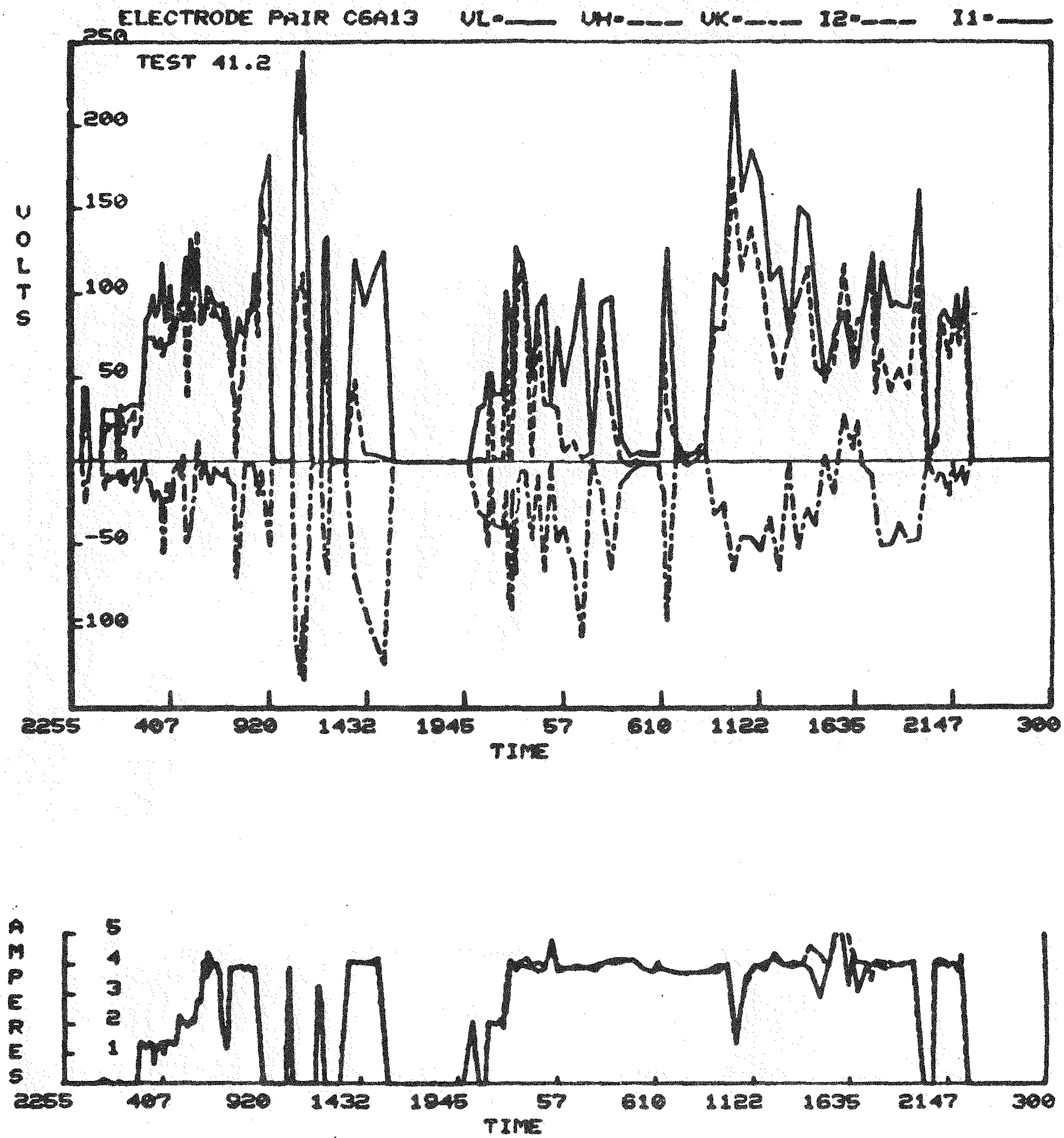

Figure 35. Impressed Voltage and Current, WESTF Test 41-2, 8/8/79

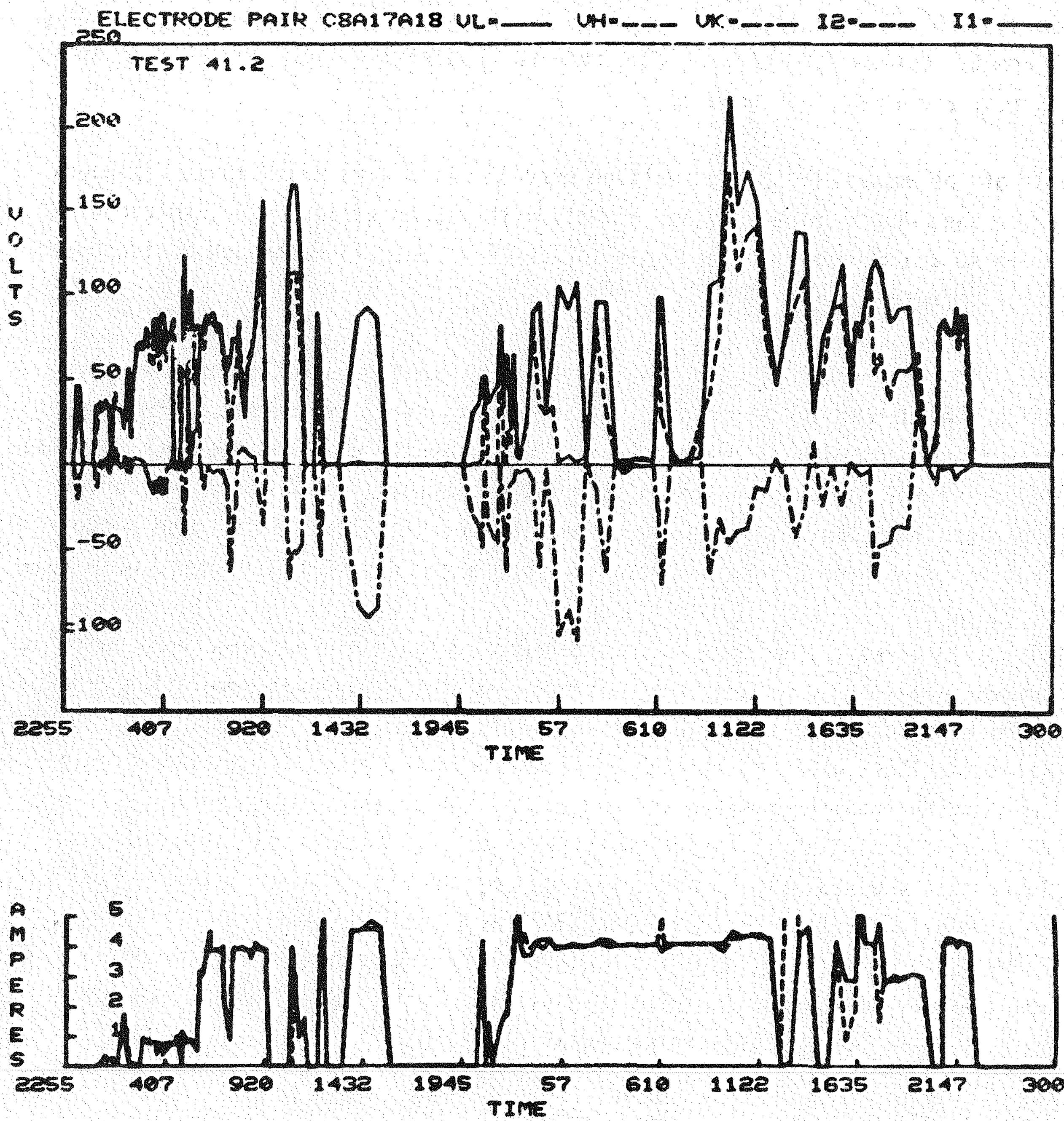

Figure 36. Impressed Voltage and Current, WESTF Test 41-2, 8/7 & 8/8/79

Characteristic ampere vs voltage curves for different representative electrode-pairs in WESTF Test 41-Run 2 are shown in Figure 37 for the case of decreasing current. Curves for the same electrode-pair under the condition of increasing current are shown in Figure 38.

All of the ampere vs applied voltage curves, which were taken about six hours after seed was introduced, show a voltage threshold effect, i.e., voltages between 40 and 60 volts are required for current conduction through a given electrode-pair to occur.

The main differences between the curves of increasing current and those for which the current was decreasing was in the slopes of the curves. The rate of rise of current with increase of voltage was significantly greater when the magnitude of the current was increased. The difference in slopes of the curves under the two conditions may have been the result of changes in seed concentration, and hence plasma conductivity, while the data for the curves were taken.

Figure 39 gives the integrated ampere-hours of the different electrode pairs as summed up by the computer. The electrode-pairs having lower cumulative ampere-hours were connected to power supplies having relatively low maximum voltage ratings. Thus, when the threshold voltage required for current conduction became higher than the maximum voltage capability of the power supply, conduction of current ceased until the voltage threshold for current conduction dropped lower than the maximum voltage capability of the power supply. This situation held for electrode-pairs 15 and 16 (C7A15 and C7A16) of Figure 39. Failure of other low voltage power supplies towards the end of the test was responsible for the lower ampere-hours accumulated at electrodes 5, 6 and 8, i.e., electrode pairs C_2A_5, C_2A_6 and C_3A_8, respectively.

<u>Materials Test Section WESTF-Test D-9</u>

Test D-9 was run at various mass flow rates at a constant plasma temperature of 2550 K for approximately four hours. The test was terminated when both thermocouples imbedded in the $La_{.95}Mg_{.05}CrO_3$ electrodes failed to operate. Observation of the test section after disassembly revealed a thin (0.5 mm) coating of slag

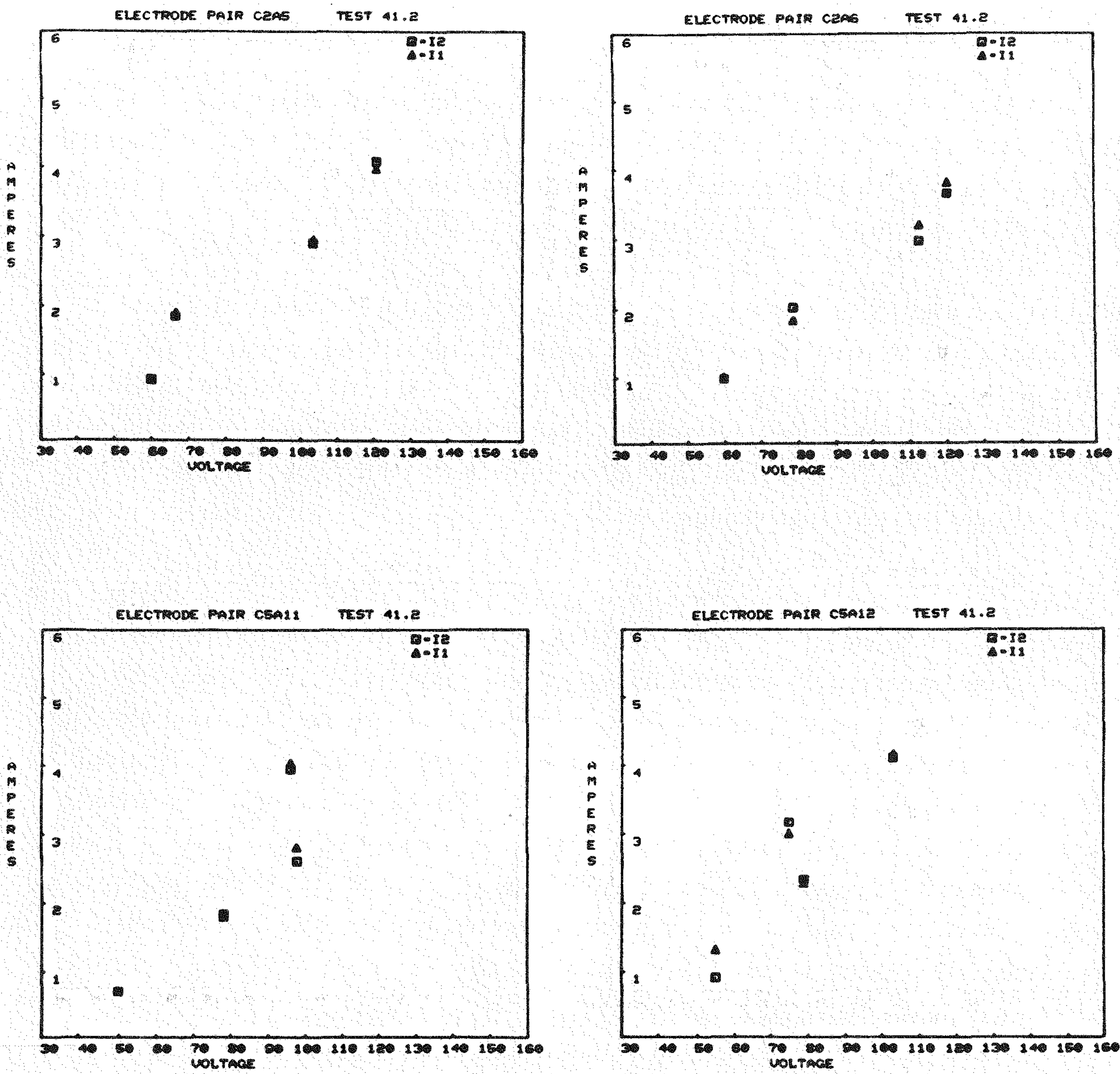

Figure 37. Currents Through Electrode-Pairs as Function of Impressed Voltages, for Decreasing Currents Between 0710 to 0732, 8/7/79

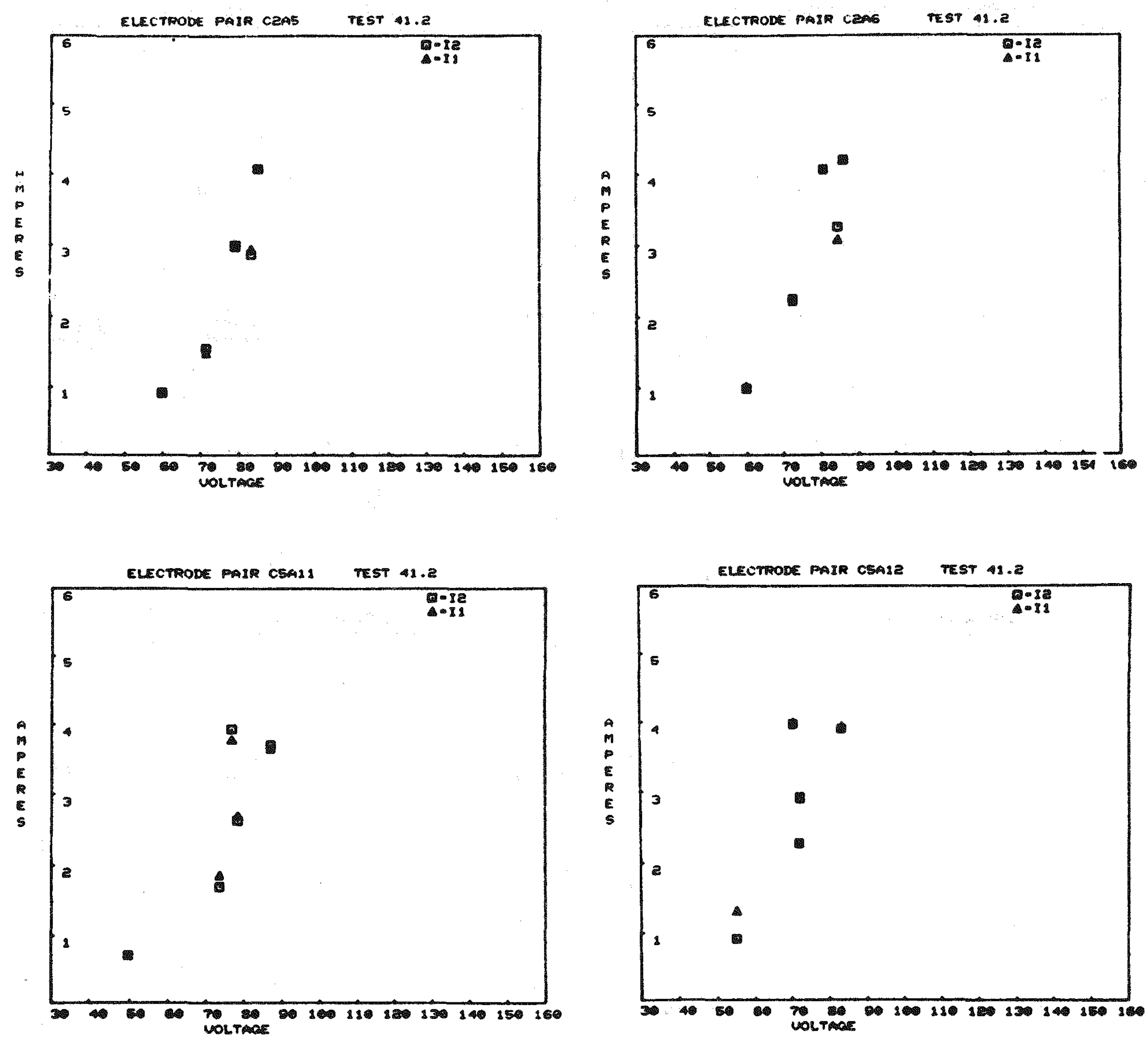

Figure 38. Current Through Electrode-Pairs as Function of Impressed Voltages for Increasing Current Between 0732 to 0750, 8/7/79

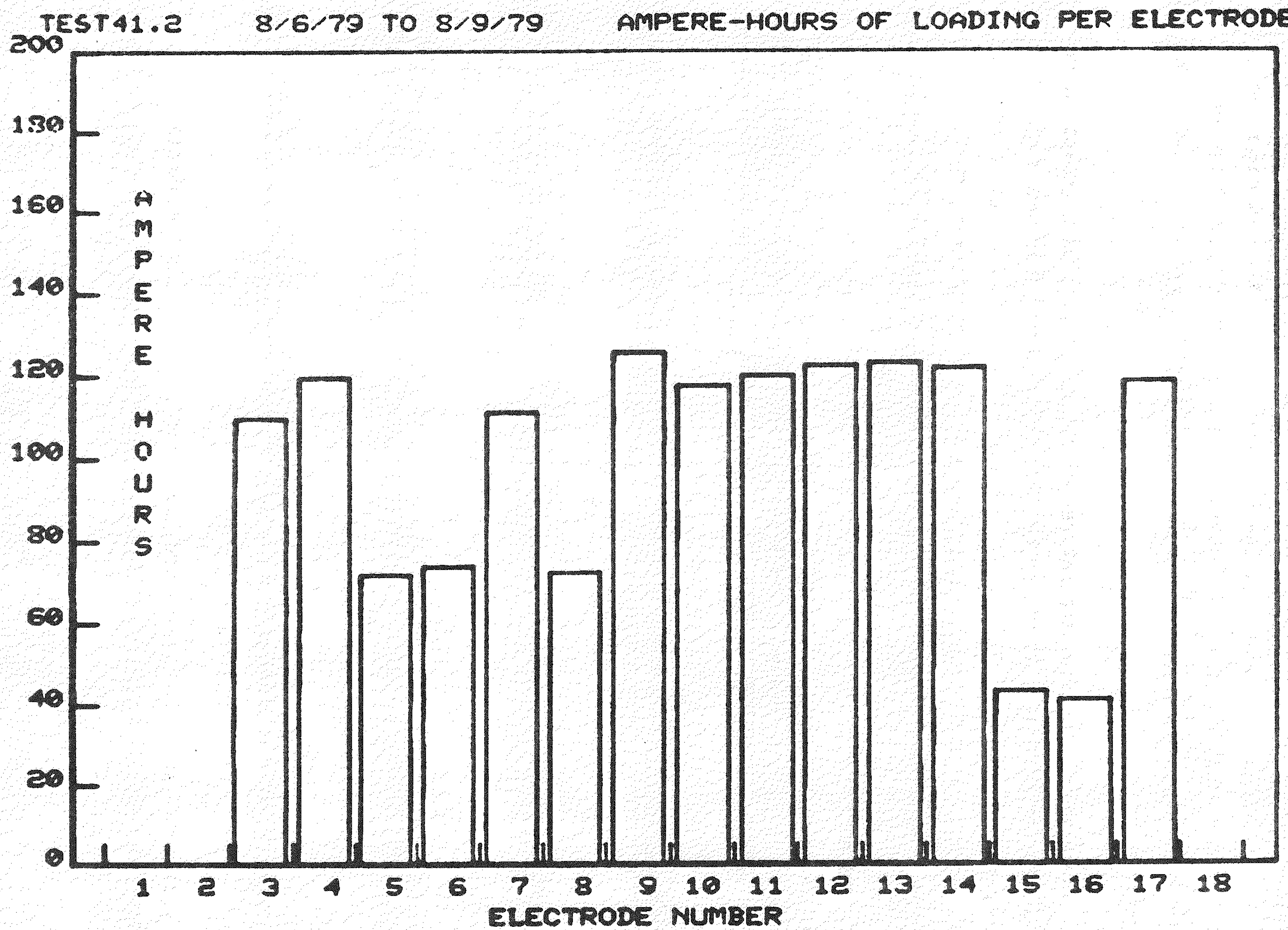

Figure 39. Ampere Hours, WESTF Test 41-2

deposited throughout. Undoubtedly, the slag deposits in the upstream mixer component from previous test runs had washed downstream into the test section. The electrodes were found to be recessed 2 mm from the slag surface, with the remains of a thermocouple exposed on the one electrode wall. From the thermocouple readings during the test, an estimate of surface temperatures was determined. These showed surface temperatures of approximately 200°C greater than predicted for the design. At the higher mass flow rates, this would mean surface temperatures exceeded 2000°C, which would cause melting of the electrodes. The MgO refractory insulation held up reasonably well considering the high temperatures, but did show some slag penetration through its open pores.

For the MTS configuration, it was shown that the surface temperature in the channel could be changed to a significant degree by varying the mass flow rate. The actual change amounted to a 10% increase in surface temperature for a 40% increase in total mass flow rate. These results will be compared to those obtained in WESTF Test D-11, where the thermal response of this test section will be investigated over a range of fuel equivalence ratios and mass flow rates.

2.2 WBS 1.2.2 - Test Assembly Fabrication

2.2.1 Materials Test Section

The initial Materials Test Section (MTS) was scheduled for use in WESTF Test D-9. Design of the MTS is described in Section 2.1.2. Fabrication of this test section was completed without difficulty. The completed test section is shown in Figure 40.

2.2.2 WESTF Test Sections

WESTF Test 42

WESTF Test 42 is a test of zirconia- and hafnia-based coupons under super-hot, non-slagging conditions. The revised layout of the WESTF Test 42 Section was presented in Section 2.1.1. This layout incorporates the hafnia-based designs, the elimination of a spinel insulator (to preclude hafnia-alumina reactions), and a rearrangement of the magnesia insulators in the channel.

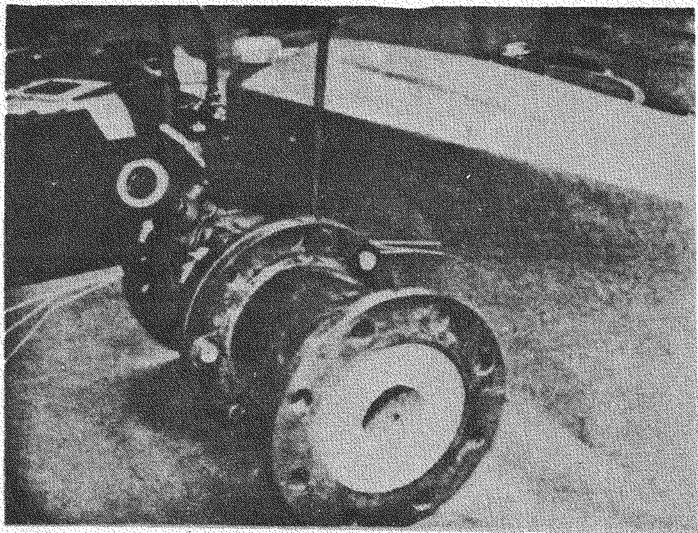

(A) DOWNSTREAM END

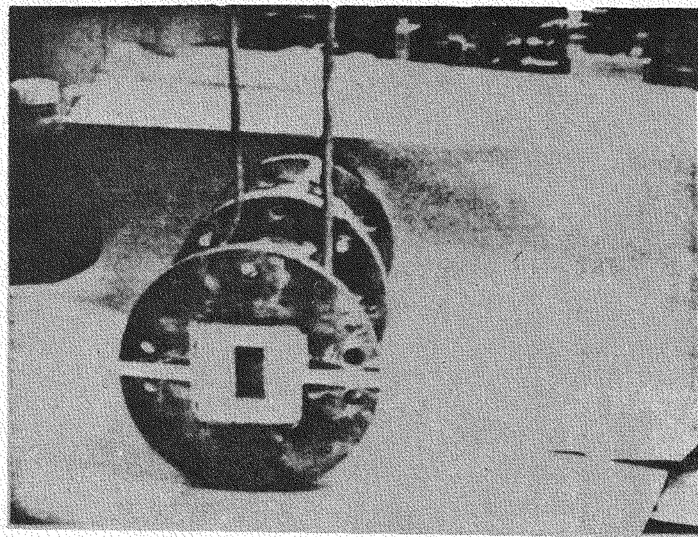

(B) UPSTREAM END

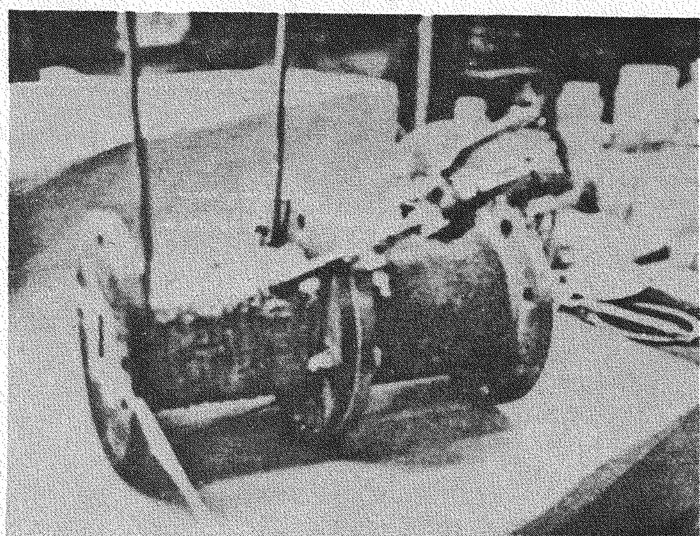

(C) SIDE VIEW

Figure 40. Materials Test Section Prior to Testing, WESTF Test D-9

The top and bottom insulating walls and the exit transition section have been assembled. Assembly of the coupon walls are in process. Design selection of the inlet transition section is dependent upon the results of a transition section test (WESTF Test D-10) intended to confirm design modifications made to correct the problem caused by loss of the transition section lining in WESTF Test 41-2. After WESTF D-10 is run and elevated, an accelerated fabrication effort will be undertaken to complete the assembly of the WESTF Test 42 test section.

WESTF Test 43

WESTF Test 43 is a test of platinum anodes and iron cathodes under hot slagging conditions. The electrode cooling blocks, alumina spacers and platinum cups for this test have been machined. The fabrication of ceramics for the insulating walls and transition sections are in process. Attachment of the platinum caps to the alumina spacers will commence shortly.

Several tests have been added to the schedule and given a higher priority than WESTF Test 43. These are WESTF Test D-10 (a prerequisite for completion of assembly of the WESTF Test 42 test section) and WESTF Test D-11 (to verify some facets of facility operation). Therefore, the assembly of the WESTF Test 43 test section has been allowed to slip.

WESTF Test D-10

The test article has been assembled to evaluate alternate thermal designs and attachments for WESTF Test 42 inlet transition sections. It is composed of inlet and outlet transition sections joined together. On the upstream transition section, two adjacent walls are lined with 0.325 in. thick Norton MgO (85% dense), TiCuSil braced to 0.1 in. thick nickel mesh, CuSil brazed to water-cooled copper. The other two walls are lined with 0.677 in. thick Norton MgO (85% dense) attached to water-cooled copper with RTV silastic. The downstream transition section is lined with 0.918 in. thick Norton MgO (85% dense) joined to two adjacent copper walls using Aremco-Coat 543 (high temperature copper base adhesive). On the other two copper walls, the attachment is made using Aremco-Bond 566 stainless steel adhesive. Design information is tabulated as follows:

	Design/Attachment No.			
	1	2	3	4
Magnesia thickness (in.)	.325	.677	.918	.918
Attachment	braze	RTV	Cu Adhesive	SS Adhesive
Nickel Mesh thickness (in.)	0.1	0	0	0
Water Flow (gph)	70-100	70-100	70-100	70-100
Surface Temperature (°C) *1	1450-1650	1450-1650	1600-1800	1600-1800
Heat Flux (W/cm^2)	70-90	70-90	55-75	55-75
Thermocouple Locations and type *2	.14(B)		.20(B)	-.125 (Pt-Ir) *3

*1 Predicted

*2 Distance from surface (in.)

*3 Gas stream

WESTF Test D-11

The test article for WESTF Test D-11 is being assembled to investigate facility and test section thermal response to operation over a range of fuel equivalence ratios. It is composed of inlet and outlet transition sections.

The upstream transition section is the primary test article; the downstream transition section functions as a spacer.

The upstream transition section will be lined with 0.325 inch thick Norton MgO (85% dense) TiCuSil brazed to 0.1 inch thick nickel mesh which is CuSil brazed to copper. The two opposing side walls will each contain 2 iridium-rhodium gas stream T/C's and 2 type R MgO T/C's, located 0.22 inch below the hot surface. A sight port will also be included for optical pyrometry. Existing inlet transition section walls have been modified to accommodate the additional instrumentation and component parts have been machined and are ready for brazing.

2.3 WBS 1.2.3 - WESTF Operations

2.3.1 Pre-Test Activity

Prior to initiating WESTF Test 41, Run 2, a general updating of the facilty operating procedures was completed. Several facility start-up runs were performed to train personnel in system operation under the new procedures.

2.3.2 Test Operations

WESTF Test 41, Run 2

This test was a continuation of WESTF Test 41, and was a test of electrodes designed and fabricated by AVCO, equivalent to CDIF Reference channel #2 electrodes. Number 2 diesel oil was used as fuel with injected potassium carbonate seed and eastern fly ash. The average conditions achieved during the test as well as the test chronology are shown in Table 21.

The test ran for 48.58 hours between initial seed on and final seed off. Difficulties were encountered during the test with seed line clogging and pressure buildup in the test passage which necessitated shutting the seed off and restarting it again several times during the test.

The total time of operation with seed was 35.62 hours. Since the electrodes had been operated for 14.1 hours during Run 1, a total of 49.62 hours were logged on these electrodes with seed and 62.7 hours at temperature.

The test was terminated because of an electrode water leak. Upon disassembly it was determined that significant transition section insulating material erosion/corrosion had occurred allowing the plasma to impinge on the upstream face of the electrode.

Data scans were output by the computer on the graphics terminal which permitted quick analysis of channel conditions. The only limitations of the system was the characteristic loss of thermocouples as the test progressed. Electrical loading data was also instantly retrieved in tabulated and graphic form permitting the analysis of a large number of varied loading conditions.

TABLE 21

WESTF TEST 41-RUN 2 OPERATING CONDITIONS AND CHRONOLOGY

Gas Temperature, K	~2480
Static Pressure, atm	2
Plasma Velocity, m/sec	550
Plasma Mass Flow, kg/sec	0.20
K_2CO_3 Seed Concentration, %K	0.9
Flyash Concentration	0.0016
Heating and Cooling Rates, $^oC/min$	30
Electrode Cooling Water:	
Anodes, gal/hr	50
Cathodes, gal/hr	30

Condition	Date	Time	Elapsed Time, Hours
Air Preheat On	8/6/79	2030	0
Combustor On	8/6/79	2200	1.50
Seed On	8/7/79	0115	4.75
Seed Off	8/8/79	2245	50.25
Combustor Off	8/8/79	2245	50.25
Combustor On	8/9/79	0055	52.83
Seed On	8/9/79	0140	53.17
Seed Off	8/9/79	0150	53.33
Combustor Off	8/9/79	0245	54.25
Air Preheat Off	8/9/79	0300	54.50

WESTF Test D-9 (MTS Run)

WESTF Test D-9 was completed on September 21, 1979. This test was run to accomplish the following:

- to transition from operation with eastern ash to western ash,
- to check-out operation of the Materials Test Section (MTS), and
- to evaluate lanthanum chromite electrode material for its general resistance to the MHD environment.

Table 22 presents the average conditions achieved during the test as well as the test chronology. During this short duration test the facility was operated at three different mass flow rates to investigate test section thermal response. Preliminary discussions of the post-test analysis data are presented in Section 2.1.3.

3.0 WBS 1.3 - WESTF MODIFICATIONS

3.1 MINI-COMPUTER/DAS

Plasma temperature tables for fuel oil #2 derived from a Westinghouse proprietary combustion simulation program have been included in the files of the mini-computer. Now an instantaneous estimate of the plasma temperature can be obtained based on the mass flow rates of fuel, air, oxygen, seed, and preheat temperature. Analysis of previous tests are also being presented in different forms in an attempt to more fully understand the operation of the channels under operating conditions.

Additional operating memory of 32K words and a magnetic tape for storage memory have been placed on order. The data acquisition and display systems utilizes the present operating memory to the maximum. The additional 32K of memory will speed the introduction of operating instructions. The magnetic tape will permit unlimited permanent storage of data and greatly increase the range of possible programming.

Delivery of the equipment was anticipated during September 1979, however, the order was not received by the supplier when issued in July. The procurement has been replaced and delivery is now projected for December 1979.

TABLE 22

OPERATING CONDITIONS AND CHRONOLOGY FOR MTS TEST

Gas Temperature		$2480^{o}K$	
Static Pressure		2 atm	
Plasma Mass Flow	0.20	0.14	0.10 kg/sec
Plasma Velocity	550	380	270

Condition	Date	Time	Elapsed Time
Air Pre Heat On	9/21/79	0900	0
Combustor On	9/21/79	1100	2
Combustor Off	9/21/79	1530	6.5
Air Preheat Off	9/21/79	1545	6.75

3.2 MAGNET INSTALLATION

Progress has been achieved in a number of areas in support of installation of the conventional 3 Tesla magnet in WESTF.

The magnet has been removed from the Waltz Mill WESO site and delivered to the Glassport plant for modification. Magnet disassembly has been completed. Coil rework fixture design activities have been completed and the future is being fabricated. Engineering drawings covering the balance of the magnet modification effort have been completed and are currently being reviewed. No significant areas of change have been noted to date although the review is not yet completed. A work plan has been prepared by the Glassport personnel covering the actual coil rework and magnet modification effort.

The status of primary long lead procurements which support the addition of the magnet to WESTF are as follows:

- Load Interrupter Switches - placed August - delivery December 1979.
- Power Supply - placed July - delivery slipped to February 1980.
- 5 KV Feeder Cable - placed August - delivery complete.
- PS to Magnet Cable - to be placed.
- Sub-Station Breaker - placed.

Vendor drawings of the magnet power supply have been reviewed and approved.

Based on the desire to minimize WESTF downtime to permit continued testing, it currently appears that the best time frame for magnet installation in February 1980. Detailed planning activities, including preparation of a detailed schedule, are continuing. A summary schedule is presented in Figure 41. This schedule is based on currently identified delivery dates for the major pieces of equipment. The schedule is also compatible with the building addition which is necessary to house a number of non-MHD facilities which were displaced as a result of the WESTF magnet addition. It is expected that construction of the building addition will start in mid-October.

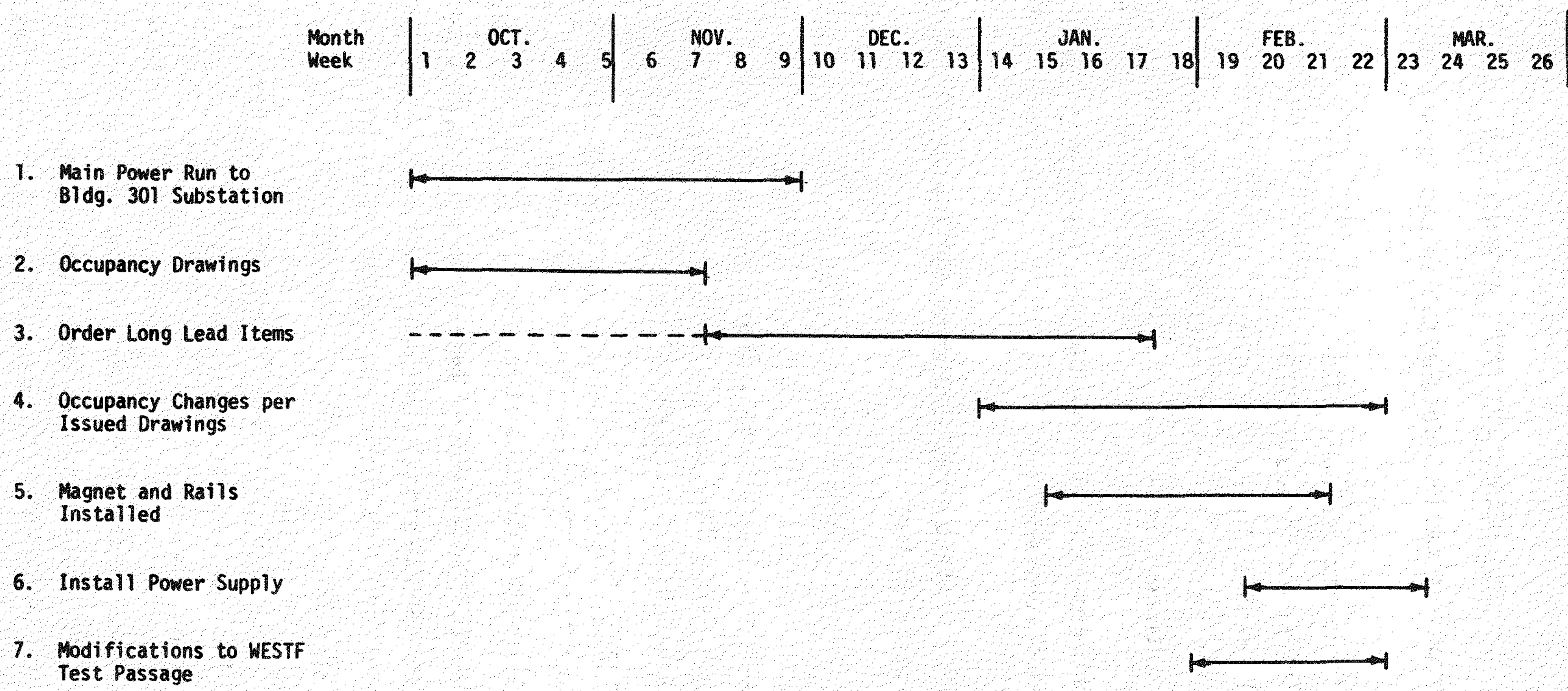

Figure 41. Summary Schedule for MHD Facility Modifications

4.0 WBS 1.4 - PROJECT MANAGEMENT AND DOCUMENTATION

The following required project documentation was issued during the reporting period:

- Monthly Report for June 1979
- Monthly Report for July 1979
- Monthly Report for August 1979
- Quarterly Report for the Period April-June 1979
- Project Management Summary Baseline Report, FY 80 Revision - For Approval.

Based on DOE comments received, the Project Management Summary Report, FY 80 Revision, is being revised.

The project review meeting scheduled with DOE for October 1979, has been postponed at the request of DOE.

5.0 REFERENCES

1. BNWL-2004-7, "Development, Characterization and Evaluation of Materials for Open Cycle MHD, Quarterly Report, April-June 1978," DOE Contract E(45-1)-1830, Battelle Pacific Northwest Laboratories, September 1978.
2. FE-15529-1, "MHD Electrode Development, Quarterly Report, October-December 1978," DOE Contract DE-AC-01-79-ET-15529, Westinghouse Electric Corporation, January 1979.
3. FE-2248-18, "Development, Testing and Evaluation of MHD Materials and Component Designs, Quarterly Report, October-December 1977," DOE Contract EX-76-C-01-2248, Westinghouse Electric Corporation, March 1978.
4. FE-15529-2, "MHD Electrode Development, Quarterly Report, January-March 1979," DOE Contract DE-AC-01-79-ET-15529, Westinghouse Electric Corporation, May 1979.
5. FE-2248-20, "Development, Testing and Evaluation of MHD Materials and Component Designs, Quarterly Report, April-June 1978," DOE Contract EX-76-C-01-2248, Westinghouse Electric Corporation, August 1978.

6. FE-15529-3, "MHD Electrode Development, Quarterly Report, April-June 1979," DOE Contract DE-AC-01-79-ET-15529, Westinghouse Electric Corporation, August 1979.

7. FE-2248-22, "Development, Testing and Evaluation of MHD Materials and Component Designs, Quarterly Report, July-September 1978," DOE Contract EX-76-C-01-2248, Westinghouse Electric Corporation, December 1978.

8. J. B. Heywood and G. J. Womack, "Open Cycle MHD Power Generation," Pergammon Press, Oxford, 1979.

9. U-02 Phase I Test, Measurements by B. R. Rossing on Test Articles, Unpublished.

10. Prof. H. K. Bowen, MIT Private Communication, August 1979.

11. S. Petty, AVCO Everett Research Laboratories, Private Communication, June 1979.

12. Estimate from March 1978 250 Hour Test Conducted at AVCO (Mark VI).

13. L. H. Cadoff, et al, 17th Symposium on Engineering Aspects of MHD, Stanford, California, March 1978.

14. D. Marchant, et al, 18th Symposium Engineering Aspects of MHD, Butte, Montana, June 1979.

15. D. Marchant, Battelle PNL, Private Communication, June 1979.

16. Hosler, et al, 15th Symposium Engineering Aspects of MHD, Philadelphia, Pennsylvania, May 1976, Estimate from Recession on AVCO 100-Hour Test, March 1976.

17. "Development, Testing and Evaluation of MHD Materials and Components, Quarterly Reports, January-December 1978," DOE Contract EX-76-C-01-2248, Westinghouse Electric Corporation.

18. FE-2248-14, "Development, Testing and Evaluation of MHD Materials and Component Designs, Quarterly Report, January-March 1977," Westinghouse Electric Corporation, April 1977.

V. SUMMARY PLANS NEXT REPORTING PERIOD

Summary plans covering significant activities in the next reporting period are presented below according to the Work Breakdown Structure primary tasks.

WBS 1.1 - ELECTRODE AND INSULATOR MATERIALS

- Evaluate various interelectrode insulator and insulating wall materials in the presence of Western slag and K_2CO_3 seed at 1500°C (prior tests were run at 1400°C).
- Prepare electrode materials for WESTF Test 45 and insulator materials for WESTF Test 46. These materials will be used in the Materials Test Section.
- Complete polarization measurements of ZrO_2 and Fe/Pt in the new electrochemical cell.
- Complete post-test characterization of WESTF Test 42 (ZrO_2/HfO_2) and evaluate correlation with prior laboratory tests.

WBS 1.2 - ENGINEERING TESTS

- Issue Test Specifications for the following WESTF Tests:
  - Single phase yttria stabilized zirconia - WESTF Test 45 (MTS)
  - Insulator Materials - WESTF Test 46 (MTS)
  - SiC electrode/Si_3N_4 insulator - WESTF Test 1D TBD
  - $MgCr_2O_4$ electrode/$MgAl_2O_4$ and Al_2O_3 insulator - WESTF Test 1D TBD
- Complete design of WESTF II Test Section, including incorporating WESTF Test 44 electrodes (HfO_2 with indium oxide current leadout).
- Complete design of electrode/insulating wall elements for test of SiC/Si_3N_4.
- Initiate fabrication for WESTF Test 44.
- Complete fabrication and assembly of test sections for WESTF Tests D-11, 42, 45, 43 and 46.
- Complete WESTF Tests D-10, D-11, 42, 45, 43 and 46.

WBS 1.3 - WESTF MODIFICATION

- Receive and install additional mini-computer components.
- Complete installation of new power line from main substation to Building 301.
- Complete modification of magnet.
- Complete preparation of 'occupancy drawings', including the HVAC and cooling water system additions.
- Prepare drawings for WESTF Test Passage modifications and initiate fabrication of selected items.

WBS 1.4 - PROJECT MANAGEMENT AND DOCUMENTATION

- Issue final version of Project Management Summary Baseline Report, FY80 Revision, reflecting DOE comments and FY79 actual costs.
- Issue July - September 1979 quarterly technical progress reports.
- Issue monthly progress reports.

VI. CONCLUSIONS

Non-reproducible results from electrochemical polarization studies have shown the need to modify the electrochemical cell used for these laboratory experiments. A modified electrochemical cell will be used in future polarization experiments.

The successful operation of the Materials Test Section (MTS) in WESTF Test D-9 demonstrates that this test section will be of value in testing electrode and insulator materials under MHD conditions in an expeditious manner so that more effective Mini-WESTF and full WESTF tests can be carried out. The use of MTS will make positive contributions to the material data base and will preclude the use of high risk materials in full WESTF tests.

Future WESTF tests will be directed towards providing quantitative data for operation in a western slag/K_2CO_3-K_2SO_4 test environment where the sulfur level is representative of that anticipated in future baseload plants. In this regard, it should be noted that the sulfur level, expressed in terms of m/o SO_2, should be approximately 0.3 m/o SO_2 to reflect the economics of seed regeneration. This level is a factor of 20 greater than that historically used in laboratory and generator tests.

☆U.S. GOVERNMENT PRINTING OFFICE: 1980 -640 -258/ 2130